2017

Characterizing the Role of the E3 Ligase ITCH in Gut Mucosal Homeostasis

Heather L. Mentrup
University of South Carolina

Characterizing the Role of the E3 Ligase ITCH in Gut Mucosal Homeostasis

by

Heather L. Mentrup

Bachelor of Science
University of South Carolina Aiken, 2008

Submitted in Partial Fulfillment of the Requirements

For the Degree of Doctor of Philosophy in

Biological Sciences

College of Arts and Sciences

University of South Carolina

2017

Accepted by:

Lydia E. Matesic, Major Professor

Franklin G. Berger, Committee Member

Hexin Chen, Committee Member

Kim Creek, Committee Member

Jeffery Twiss, Committee Member

Cheryl L. Addy, Vice Provost and Dean of the Graduate School

DEDICATION

This work is dedicated to my loving and supportive parents Steven J. Mentrup and Linda P. Mentrup. Their unwavering trust, support, and guidance throughout my life has taught me to trust my own judgment, have confidence in my abilities, and to always ask questions.

This working is also dedicated to my husband Dr. Steven R. Ballesteros. Your unyielding love, compassion, and support has taught me that I can overcome any obstacle.

ACKNOWLEDGEMENTS

First and foremost, I would like to thank my mentor and major advisor Dr. Lydia E. Matesic for her continuous support, academic expertise, and invaluable advice that has allowed me to developed both intellectually as well as personally. Additionally, I would like to acknowledge my former laboratory colleagues Measho Abreha, Wassim Basheer, and Elizabeth Thames for their emotional and academic support throughout my tenure as a graduate student. I would also like to sincerely acknowledge John and Matilda MacArthur for their amazing friendship. Throughout this journey, they have provided an amazing support system, and I am forever grateful. Furthermore, I would like to thank my grandmother Linda Neff for her emotional support during this process. I would also like to acknowledge the amazing faculty and graduate students at the University of South Carolina for the invaluable scientific support. Lastly, I would like to thank my dissertation committee members including Dr. Franklin G. Berger, Dr. Hexin Chen, Dr. Kim Creek, Dr. Jeffery Twiss for all their support, guidance and valuable input during my academic tenure as a graduate student at the University of South Carolina.

ABSTRACT

The mucosal barrier of the small intestine is highly dynamic, enabling the passage of nutrients that are necessary for the body's function while simultaneously preventing a breach by harmful microorganisms that are damaging to the host. The effectiveness of the mucosal barrier is dependent on the cohesive relationship established between the luminal mucosal epithelium and the underlying immune compartment in the small intestine. The epithelium provides the first line of defense against pathogens by establishing a physical barrier separating the external environment from the body's internal milieu, while the immune system secondarily responds to clear bacteria that have breached the epithelial barrier. The HECT E3 ubiquitin ligase ITCH is known to regulate immune responses, and loss of function of ITCH has been associated with gastrointestinal inflammatory disorders. However, the high level of ITCH expression within the intestinal epithelium suggests that it may have an important function(s) in that tissue for maintaining gut homeostasis. Indeed, we identified that global loss of ITCH (*Itch*$^{a18H/a18H}$) in young adult animals influenced intestinal architecture characterized by increases in both crypt and villus area that were more prominent in the distal part of the small intestine. Increased crypt area was found to result from expansion of both the proliferating transit amplifying progenitor population and terminally differentiated Paneth cells. Lack of ITCH also resulted in changes in numbers of goblet cells on the villus. Epithelial cell

turnover was also accelerated in *Itch*$^{a18h/a18H}$ animals, as evidenced by increases in both proliferation and apoptosis within the crypt, as well a more rapid cell migration of bromodeoxyuridine-labeled epithelial cells along the crypt-villus axis. Consistent with the observed enhancement of cellular migration, *Itch*$^{a18H/a18H}$ mice carrying the *Min* mutation (*Itch*$^{a18H/a18H}$; *Apc*$^{Min/+}$) displayed a 76% reduction in tumor burden as compared to *Apc*$^{Min/+}$ littermates with normal levels of ITCH. To identify which aspects of these changes were cell autonomous, intestinal organoids were generated from the crypts of ITCH sufficient and ITCH deficient animals. Interestingly, epithelial cell proliferation and differentiation were not perturbed in ITCH deficient organoids, in contrast to the *in vivo* phenotype of the *Itch*$^{a18H/a18H}$ small intestines. However, increased cell death was observed in organoids lacking ITCH, which was also consistent with increased cleaved-caspase 3 staining in the intestines of mice lacking ITCH exclusively in the intestinal epithelium. The failure to recapitulate the *Itch*$^{a18H/a18H}$ epithelial phenotype prompted us to investigate how loss of ITCH in immune cells impacts the intestinal epithelium. Animals lacking ITCH within the myeloid cell lineage have similar defects in crypt area, as well as increases goblet and Paneth cell numbers, as compared to the *Itch*$^{a18H/a18H}$ animals, albeit delayed. These finding highlight a cell autonomous as well as non-cell autonomous function for ITCH in mediating epithelial homeostasis, and emphasize the importance of ITCH in small intestinal barrier function.

TABLE OF CONTENTS

LIST OF FIGURES

LIST OF ABBREVEATIONS

3-D 3-dimensonal

AP ..... alkaline phosphatase

BrdU ..... bromodeoxyuridine

CBC ..... crypt base columnar

DMEM ..... dulbecco's modification of eagle's medium

DVL ..... dishevelled

DCs ..... dendritic cells

E ..... embryonic

EDTA ..... ethylenediaminetetraacetic acid

EE ..... enteroendocrine

EMT ..... epithelial mesenchymal transition

ESC ..... embryonic stem cell

H&E ..... hematoxylin and eosin

HCC ..... hepatocellular carcinoma

HECT ..... homeologous to the E6AP carboxyl terminus

Hh ..... hedgehog

HSC ..... hematopoietic stem cells

IBD ..... inflammatory bowel disease

IHC ..... immunohistochemistry

IL ..... interleukin

MDP ..... mumuryl dipeptide

PBS ..... phosphate buffered saline

SD ..... standard deviation

SEM ..... standard error of the mean

TA..... transit amplifying

TGF ..... transforming growth factor

Th ..... T-helper

TNF ..... tumor necrosis factor

Treg..... regulatory T-cell

WW ..... tryptophan-tryptophan

CHAPTER 1

GENERAL INTRODUCTION

Throughout an organism's life span, many tissues are in a constant state of flux, varying their cellular composition and function to reflect the internal and external stimuli that are present at that particular time. While tissues must vary their internal steady state to appropriately respond to the current environmental cues, if changes deviate outside of a tissue's predefined, normal steady state range, its integrity can be compromised. To prevent major shifts in cell composition and function from occurring, tissue homeostasis is essential. This homeostatic process is dependent on cell turnover, or the balanced regulation of cell death with cell proliferation. As cells become "worn out" or damaged over time, these functionally insufficient cells must be replaced with functionally competent cell types that will preserve the tissue's integrity. Regulation of this process is initiated by somatic stem cells that reside within a given tissue. Somatic stem cells are multipotent cells that are defined by their unlimited self-renewal properties as well by their ability to differentiate into all major cell types within a given tissue. When a somatic stem cell asymmetrically divides to produce two daughter cells with different cell fates, one cell will typically retain the unlimited self-renewal properties of the parental cell, while the other cell adopts a progenitor cell fate. Progenitor cells, which exhibit limited self-renewal capabilities, will continue to divide, and, when exposed to the appropriate signals,

will terminally differentiate into all the cell types that comprise a particular tissue. Once terminally differentiated cells are generated, these cells must be able to integrate into the tissue to replace the cell that was lost. If a breakdown in any component of this highly integrated process does occur, this can have catastrophic impacts on tissue homeostasis and promote pathologies ranging from neurological disorders to cancer.

Homeostasis within the small intestine is essential to digestion, nutrient absorption, and water balance. These processes are mainly dependent on the epithelium that lines the luminal cavity to separate the external environment from the internal milieu. The epithelium consists of a single layer of columnar cells that fold into long, finger-like structures, commonly referred to as villi, which protrude out into the lumen, and deep invaginations into the underlying submucosa known as the crypts of Lieberkühn (Fig.1.1). Within the small intestinal crypts, the rapidly dividing, multipotent crypt base columnar (CBC) stem cell population resides at the base of the crypt interspersed between the Paneth cells (van der Flier and Clevers, 2009). An additional slowly-dividing, reserve stem cell population also exists in the +4 (cell population located directly above the Paneth cell population) of the small intestinal crypt. During obligate asymmetrical cell divisions, intestinal stem cells will produce a single intestinal stem cell to replenish the existing pool of stem cells, as well as give rise to a progenitor cell, defined as being equivalent to a transit-amplifying (TA) cell, that is capable of terminally differentiating into one of the five major cell types of the small intestine (Barker, 2013).

Terminally differentiated intestinal epithelial cells arise from the highly proliferative TA cells that are generated during cellular division of the CBC stem cell population. As TA cells migrate along the crypt-villus axis, dividing approximately five-to-six times, they eventually specify into the five major epithelial cell types of the small intestinal epithlium (Potten, 1998). The function of these five cell types is dependent upon the lineage from which they are derived. Enterocytes originate from the absorptive cell lineage and are the most abundant cell type in the small intestine. They comprise approximately 75-80% of the total post-mitotic cells that are produced and are critical to nutrient absorption (van der Flier and Clevers, 2009). The secretory cell lineage is comprised of the remaining four major cells types: enteroendocrine, goblet, tuft, and Paneth cells (Barker, 2013). The enteroendocrine cells, located along the villi, produce and secrete hormones that are critical to physiological and homeostatic functions of the small intestine (Moran et al., 2008). Tuft cells, or brush cells, are also located on the villi and are hypothesized to play a role in chemosensitivity. However, emerging evidence suggests that they are also critical mediators of host defense during enteric infection and inflammation (Steele et al., 2016). Goblet cells provide a protective shield for the intestines through the secretion of mucin. Paneth cells reside in the crypt interposed between the CBC stem cells and contribute to the stem cell niche while concurrently protecting the small intestine by secreting antimicrobial agents against foreign microbes.

Epithelial self-renewal in the small intestine is very rapid, occurring approximately every four-to-five days (Barker, 2013). To maintain intestinal homeostasis throughout this rapid process, aged cells must be expeditiously replaced with newly differentiated cells that arise from the proliferative crypts (Nunes et al., 2014). Proliferation within the small intestinal crypt of mice has been established as the principle force governing homeostatic cell migration (Parker et al., 2017). Reduction or temporary suspension of proliferation in the crypts of mice directly influences cell migration velocities onto the villi. Preservation of proliferation and migration is critical to epithelial homeostasis, and dysregulation of these processes can promote a range of gastrointestinal pathologies (Fre et al., 2009; Hanahan et al., 2000; Roda et al., 2010).

Cellular adhesion complexes between adjacent small intestinal epithelial cells can also influence cell migration. Tight junctions, adherens junctions, and desmosomes line the lateral membranes of intestinal epithelial cells to ensure cell adhesion and polarity while concurrently preventing the entrance of luminal pathogens (Garcia et al., 2017). Tight junctions, located near the apical surface of the cells, prevent the passage of unwanted substrates from the luminal environment across the epithelium. Adherens junctions are located directly below tight junctions, and, in combination with tight junctions, they constitute an apical junctional complex that is directly attached to the actin cytoskeleton of the cell. Additional intracellular adhesion is provided by desmosomes, which are located directly under adherens junctions.

Adherens junctions are composed of the transmembrane glycoprotein E-cadherin that forms homophilic interactions with adjacent cells to mediate cellular adhesion as well as cell signaling (Bondow et al., 2012; Etienne-Manneville, 2012). To ensure cellular adhesion, E-cadherin proteins are attached to the catenin family of proteins (β-catenin, p120, and plakoglobin), which secures the entire junctional complex to the actin cytoskeleton of the cell via its association with α-catenin (Hartsock and Nelson, 2008). The epithelial-specific loss of E-cadherin in the adult intestine enhances cellular migration along the crypt-villus axis (Schneider et al., 2010). Further, disruption of cadherins in mice mediated by overexpression of dominant-negative N-cadherin under the *Fabp1* promoter resulted in accelerated migration (Hermiston et al., 1996). In contrast to loss of E-cadherin, forced expression of E-cadherin in the intestinal epithelium of mice slowed cellular migration along the crypt-villus axis (Hermiston et al., 1996).

As terminally differentiated cells migrate along the crypt-villus axis, they eventually reach the tip of the villus and are sloughed off into the luminal cavity. In the small intestine, this process is continuous and results in nearly 1,400 cells from a single villus being shed into the luminal cavity each day (Potten, 1990; J. M. Williams et al., 2015). A particular type of apoptosis, termed anoikis, mediates cell extrusion from the villus tip of the intestinal epithelium (Delgado et al., 2016). Detachment of a cell from the underlying extracellular matrix activates anoikis either through mitochondrial dysfunction (intrinisic) or cell death receptors (extrinsic) and converges on caspase 3 before the cell undergoes demise (Paoli et al., 2013). To ensure that the intestinal barrier is still maintained throughout

anoikis, both apoptotic cells as well as the neighboring cells redistributes tight junctions to their basolateral membrane (Guan et al., 2011; Marchiando et al., 2011). The surrounding cells then extend cytoplasmic processes underneath the apoptotic cells before the cell is extruded from the epithelium to ensure that tight junctions are able to reform instantaneously to prevent the passage of bacteria (J. M. Williams et al., 2015).

As a dividing line between the internal and external compartments, the epithelium also plays an indispensable role in preventing the entry of foreign substrates (Bischoff et al., 2014). The epithelium of the small intestine is generally regarded as the "first line of defense", hindering the penetration of bacteria into the internal environment of the host (Peterson and Artis, 2014). This mainstay barrier is typically an effective deterrent, however, the constant exposure of noxious substances, antigens, and microorganisms to the surface of the epithelium along the gastrointestinal tract makes a breach of foreign material eventually inevitable (Schenk and Mueller, 2008). During this event, the underlying immune compartment which coexists with the mucosal epithelium initiates an inflammatory response to contain and destroy the non-native substrate while concurrently attempting to ameliorate the defective epithelial barrier by influencing epithelial homeostasis. Since the integrity of the mucosa is consistently being challenged, synergy between these two compartments is paramount in providing an adequate level of protection against the external environment. If a breakdown in any component of this highly integrated mucosal system does occur, this can have catastrophic impacts on mucosal homeostasis,

promoting a wide-range of gastrointestinal enteropathies (Catalioto et al., 2011; Huang and Chen, 2016; Maloy and Powrie, 2011; Nunes et al., 2014).

The subepithelial immune compartment of the intestinal mucosa resides in the lamina propria, a layer of loose connective tissue that is rich in immune cells that reside in parallel with an extensive vascular network, lymphatic vessels, extracellular matrix proteins, and the mesenchyme. Immune cells are in close proximity to the intestinal epithelium and support the intestinal epithelial barrier by initiating a targeted response toward a pathogenic substrate that has circumvented the epithelial mucosal barrier (Okumura and Takeda, 2016). Intestinal immunity is orchestrated by a heterogonous population of immune cell types, derived from both the myeloid and lymphoid cell lineages, that are present in the lamina propria. Dendritic cells (DCs), macrophages, and intraepithelial lymphocytes are in direct contact with the epithelium and immediately respond to antigenic material that has permeated the epithelial barrier, while regulatory T-cells (Treg) cells in the subepithelial immune compartment precisely regulate the inflammatory response and prevent hyper-activation of the immune system to the pathogen (Okumura and Takeda, 2016). Lastly, naïve $CD4^+$ T-cells present within the lamina propria differentiate into either memory or effector T cells in response to a bacterial substrate and exhibit rapid and potent cytotoxic activity if the same substrate is encountered subsequently. The cell types work in unison to regulate intestinal immunity by mounting an appropriate inflammatory response to clear pathogenic material while simultaneously exhibiting tolerance to macromolecules and to the host's microbiota (Vindigni et al., 2016).

The innate immune system contributes to mucosal function and homeostasis by continuously surveying the gut's microbiotic landscape (Gross et al., 2015). Harmful and innocuous bacteria that have breached the epithelium are first identified by macrophages and DCs that reside in close proximity to the epithelium, and, as such, mediate immune tolerance within the intestine. Derived from a common myeloid progenitor in the bone-marrow, macrophages and DCs exhibit overlapping functions, but also display unique properties that are specific to each cell type. Traditionally, macrophages and DCs are both potent antigen-presenting cells, presenting antigens from ingested pathogens for recognition by T-cells to induce acquired immunity (Geissmann et al., 2010). While a potent inflammatory response is typically initiated by this interaction, resident intestinal macrophages and DCs have adapted to enteric commensal bacteria by dampening the inflammatory response to promote immune tolerance over inflammation (Bain and Mowat, 2014; Smythies et al., 2005).

Macrophages are dispersed throughout the lamina propria of the gut and are strategically placed to intercept invading microorganisms (Schenk and Mueller, 2008). Bacteria that have penetrated the epithelial barrier are phagocytosed and destroyed by macrophages to effectively clear the bacteria. Unlike monocytes and macrophages from other tissues, intestinal macrophages respond differently to pathogenic substrates and effectively expunge the bacteria without inducing a potent inflammatory response (Macpherson and Harris, 2004; Schenk and Mueller, 2008). Binding of the bacteria to toll-like receptors or intracellular NOD receptors does not cause the secretion of proinflammatory

cytokines, such as TNF (Tumor necrosis factor)-α , IL (Interleukin)-1, or IL-6 (Bain and Mowat, 2014; Smythies et al., 2005). However, intestinal macrophages constitutively secrete IL-10, and low amounts of TNF-α, to contribute to intestinal homeostasis and barrier function (Gross et al., 2015). IL-10 is an anti-inflammatory cytokine that mediates intestinal tolerance to bacteria by inhibiting pro-inflammatory cytokine secretion from macrophages and T-cell inflammatory responses, as well as modulating Treg (Mantovani and Marchesi, 2014). Consistent with this assertion, IL-10 deficient mice develop spontaneous colitis characterized by hyperproliferation of the epithelium and hyperactivation of the immune system in response to commensal bacteria (Kühn et al., 1993).

DCs are specialized cells that can effectively communicating with T-cells to induce their activation and differentiation (Stockwin et al., 2000). Similar to macrophages, they are located in close proximity to the epithelium, which allows them to expeditiously detect pathogenic bacteria that have gained entry into the host. Upon bacterial ingestion, DCs will migrate to other secondary lymphoid tissues to partner with naïve $CD4^+$ T-cells and induce T-cell polarization into effector cells that will propagate an inflammatory response (Gross et al., 2015). In the small intestine, DCs also display signs of tolerogenicity. DCs that are present in mesentery lymph nodes and in the lamina propria secrete retinoic acid and transforming growth factor (TGF)-β to promote the generation of Treg, which increase the inhibitory function of other immune cell types to reign in inflammation (Okumura and Takeda, 2016; Sun et al., 2007).

The chronic, low-grade inflammatory state within the small intestine is delicately balanced by the regulatory action of Treg and pro-inflammatory T-helper (Th) 17 cells within the lamina propria (Omenetti and Pizarro, 2015). Treg and Th17 cells both derive from naïve T-cells that are exposed to the key mediator TGF-β, but have distinctly opposite biological functions in the immune system (Eisenstein and Williams, 2009). While Treg potently suppress the function of other immune cells by secreting inhibitory cytokines, such as IL-10, TGF-β, and IL-35, that limit the activation and differentiation of immune cells, Th17 cells promote a robust inflammatory response to the local microbiota, which, if not restrained, will results in pathogenic inflammation (Omenetti and Pizarro, 2015). In the small intestine, the secretion of these key mediators by innate immune cells is critical for establishing a balance between Treg and Th17 to promote an environment that is tolerant to the microbiota. Retinoic acid, which is produced by DCs in the lamina propria, promotes T-cell specification toward the Treg lineage, while IL-6 and the transcription factor ROR-λt, promote Th17 development (Mucida et al., 2007). Intestinal macrophages further contribute to Treg specification by failing to secrete IL-6 upon pathogen binding. If this balance becomes disrupted, this can promote an inflammatory state that is difficult to restrain.

The pro-inflammatory Th17 cell type normally resides in the lamina propria of the small intestine during homeostatic conditions to mediate host defense extracellular bacteria and fungi that have penetrated the barrier. Secretion of the cytokine IL-23 from macrophages and dendritic cells activates Th17 cells to

mount an immune response to pathogenic substrates by secreting the cytokines IL-17, IL-21, and IL-22 (Symons et al., 2012). However, if IL-23-mediated activation of Th17 cells is not precisely regulated, their protective function can become pathological, as is seen in a spectrum of autoimmune diseases (Langrish et al., 2005; Omenetti and Pizarro, 2015). The transcription factor ROR-λt induces the secretion of IL-17, an indispensible component of Th17 mediated inflammation. Thus, understanding the regulation of ROR-λt in IL-17-mediated colitis is of therapeutic interest.

The highly variable environment within the lumen consistently challenges the mucosal barrier of the small intestine. In response to this continual flux, specific and rapid changes within the cellular architecture of the mucosa must occur to promote barrier integrity and function (Pastorelli et al., 2013). Post-translational modifications, such as ubiquitylation, regulate cellular responses to generate appropriate signals by influencing the stability, localization, or function of a protein substrate (Rotin and Kumar, 2009). Attachment of ubiquitin to a target protein requires the sequential action of the E1 ubiquitin activating enzyme, the E2 ubiquitin conjugating enzyme, and the E3 ubiquitin ligase, the latter of which confers substrate specificity (Popovic et al., 2014). Activation of ubiquitin, a 76 amino-acid polypeptide, is an ATP dependent process that is initiated by the E1 enzyme and allows the carboxy terminus of ubiquitin to attach to an active cysteine residue on the E1 via a thioester bond (Metzger et al., 2012). The activated ubiquitin is transferred to one of nearly 40 E2s, forming a similar thioester linkage with a cysteine residue on the E2. The E3 ligase-protein

complex partners with an ubiquitin-primed E2 enzyme to transfer the ubiquitin to an ε-amino group of a lysine residue on the protein target (Rotin and Kumar, 2009). With over 600 E3 ligases present within the mammalian genomes, the diverse repertoire of protein substrates that are targeted for ubiquitylation is dependent on the E3 ligase (Li et al., 2008). Two major families of E3 ligases have been identified: the really-interesting new gene (RING)-family and the homeologous to the E6AP carboxyl terminus (HECT)-family (Metzger et al., 2012). The catalytic action of the HECT-family of E3 ligases allows ubiquitin to be transferred to a cysteine residue within the HECT domain before being directly attached to the protein target. Unlike HECT E3 ligases, the RING-family does not have catalytic action to accept and transfer ubiquitin to their target proteins, rather serves as linkers to place the substrate and E2 in close proximity to facilitate ubiquitylation.

The HECT domain present within this E3 ligase family is positioned at the C-terminus of the protein, providing a protein-binding motif for the E2 enzyme to bind to as well as a critical cysteine residue to transfer the activated ubiquitin (Bernassola et al., 2008). Within this family, the E3 ligases are further classified into 3 subclasses based on their protein-protein binding domains that allow the E3 ligase and protein target to interact. Of the three, the Nedd4-like family of E3 ligases has been the best characterized. The structure of the 9 mammalian family members consists of a N-terminal C2 domain capable of binding Ca^{2+} and phospholipids, two to four tryptophan-tryptophan (WW) protein interacting domains, and a catalytic C-terminal HECT domain (Chen and Matesic, 2007).

The WW domains of HECT E3 ligases confer substrate specificity and show preferential binding to PPXY motifs present within proteins.

The HECT E3 ligase ITCH was first identified from a radiation- and 5-hydroxyurea- induced paracentric inversion on the distal end of mouse chromosome 2, which disrupted both the *Agouti* and *Itch* loci (W L Perry et al., 1998). Animals homozygous for this loss of function mutation ($Itch^{a18H/a18H}$) developed a spontaneous and progressive, late-onset autoimmune-like phenotype that was lethal by 6-8 months of age (C M Hustad et al., 1995). On a C57BL/6J background, $Itch^{a18H/a18H}$ displayed lymphoproliferaton in the spleen, lymph nodes, and thymus, atopic dermatitis, and pulmonary interstitial inflammation, the latter of which culminated in animal mortality. The inappropriate activation of the immune system at the mucosal surfaces of the skin and lung of ITCH deficient animals was attributed to a decrease in ITCH-mediated ubiquitylation of JunB, a transcription factor that drives Th2 polarization (Fang et al., 2002a). Interestingly, the autoimmune-like phenotype associated with loss of ITCH function in mice phenotypically recapitulates ITCH deficiency in humans. The multisystem autoimmune syndrome that humans displayed as a consequence of a truncating mutation of *ITCH* is characterized by organomegaly, failure to thrive, and autoimmune infiltration within the lungs, liver, and the gastrointestinal tract (Lohr et al., 2010). Further characterization of the homozygous null *a18H* mutation of *Itch* mice also identified an inflammatory phenotype within the mucosa of the gut (Kathania et al., 2016). Animals deficient for ITCH developed spontaneous colitis at 6-8 months of age that was

characterized by mixed inflammatory infiltrate present within that colon as well as deterioration of the colonic epithelium. The development of colitis within the *Itch*$^{a18H/a18H}$ animals was attributed to an increase in IL-17 produced from Th17 helper T-cells, innate lymphoid cells, and λδ T-cells, which was driven by decreased ITCH-mediated ubiquitylation of ROR-λt.

In addition to the inflammation that is present in the colon of *Itch*$^{a18H/a18H}$ animals, mild inflammation is also observed along the small intestinal tract in 5-7 month old *Itch*$^{a18H/a18H}$ animals. While a role for ITCH in the small intestine has yet to be defined, the mild inflammation is that is present in this organ suggests that loss of ITCH function influences small intestinal homeostasis. Consistent with this assertion, ITCH expression is relatively high within the normal epithelium of the small intestine in humans as compared to other tissue types, and its expression is increased in colorectal cancers that develop along an adenoma-to-carcinoma sequence. Further support for ITCH's role in the small intestinal homeostasis is evident from the numerous transcription factors, receptors, and signaling transducers that are identified as targets of ITCH that are reviewed below, and also play a signficant role within the small intestinal mucosa (Table 1.1).

Accumulating evidence supports a regulatory function for the E3 ligase ITCH within embryonic (ESC) (Liao et al., 2013), somatic (Rathinam et al., 2011), and cancerous stem cells (Tsui et al., 2017). In ESC, ITCH maintains stemness by directly interacting with and ubiquitylating OCT4, a transcription factor that induces pluripotency, to increase its transcriptional activity and stability (Liao et

al., 2013). Further, loss of ITCH reduced the self-renewal capacity of ESC and reduced a somatic cell's ability to be reprogrammed into pluripotent stem cells. ITCH also promotes cancer cell stemness in the hepatocellular carcinoma (HCC) cell line Huh-7 by targeting and degrading the phosphorylated form of Dishevelled-3 (DVL3) (Tsui et al., 2017). Within HCC, two forms of DVL3 exist: phosphorylated DVL3 and a non-phosphorylated DVL3, the latter of which promotes cancer cell stemness. Disruption of this balance can be achieved by ITCH-mediated ubiquitylation of phosphorylated DVL3, which increases the amount of non-phosphorylated DVL3 as compared to phosphorylated DVL3. Non-phosphorylated DVL3 promotes cancer stem renewal in HCC by increasing B-catenin transcriptional activity and increasing *LGR5* mRNA levels. In contrast, the hematopoetic stem cell (HSC) pool, self-renewal is negatively regulated by ITCH (Rathinam et al., 2011). Loss of ITCH function increased NOTCH1 signaling and resulted in increased proliferation and expansion of the HSC population within the bone marrow of $Itch^{a18H/a18H}$ animals as compared to $Itch^{+/+}$ animals. Transplantation of ITCH deficient HSCs into lethally irradiated ITCH sufficient or ITCH deficient animals demonstrated that the enhanced proliferative capacity of HSCs was intrinsically regulated. A number of studies report that increased proliferation in HSCs will compromise the regenerative capacity of stem cells (K.A. et al., 2015; Yu et al., 2006). Interestingly, ITCH deficient HSCs did not show signs of stem cell exhaustion even with enhanced proliferation and increased cell cycle entry.

WNT signaling contributes to tissue regeneration by influencing stem cell dynamics, proliferation, and specification. The influence ITCH has in modulating canonical WNT signaling is highlighted by the recent identification of two, novel WNT signaling components, DVL2 (Wei et al., 2012) and LRP6 (Vijayakumar et al., 2017), which are ubiquitylated by ITCH. DVL promotes canonical WNT signaling by interacting with the LRP5/6 co-receptor and Axin to stabilize the cytosolic β-catenin pool, which is capable of translocating to the nucleus to upregulate WNT-responsive genes. In 293T cells, the DVL family of proteins (DVL1, DVL2, DVL3) were all found to co-precipitate with ITCH. However, the most robust interaction was with DVL2 (Wei et al., 2012). Exogenous overexpression of DVL2, a catalytically active or catalytically dead ITCH E3 ligase, and ubiquitin confirmed that ITCH ubiquitylates DVL2 and leads to its destruction via the proteasome (Wei et al., 2012). This was further substantiated by the absence of DVL2 ubiquitylation when ITCH was knocked-down via siRNA treatment. Functionally, ITCH-mediated ubiquitylation of DVL2 negatively regulated WNT signaling. On the other hand, the targeting of the extracellular domain of LRP6 by ITCH also promotes WNT signaling in 293T cells (Vijayakumar et al., 2017). Interestingly, ITCH was found to bind and ubiquitylate LRP6 by mass spectrometry. Instead of promoting LRP6's degradation, ubiquitylation of LRP6 by ITCH promoted endocytosis of the receptor and increased Wnt3a-mediated canonical WNT signaling. The discrepancy in ITCH's function within the WNT signaling pathway is not without precedent. Within the WNT signaling pathway, GSK3β as well as AXIN can positively or negatively

regulate WNT signaling in a context-dependent manner (Vijayakumar et al., 2017). Thus, ITCH could be an additional player within the regulatory network of the WNT signaling pathway that has a dual function.

In addition to WNT signaling, the NOTCH signaling pathway also mediates stem cell decisions and lineage commitment in the intestine and hematopoietic system (Fre et al., 2009; VanDussen et al., 2012; Vooijs et al., 2011). ITCH negatively regulates the HSC population by intrinsically down regulating NOTCH1 signaling in HSCs (Rathinam et al., 2011). Dampening of NOTCH1 signaling by ITCH likely maintains the HSCs in a quiescent state to conserve this population until mature cell lineages need replenishing. Consistent with this assertion, ITCH interacts with the intracellular domain of the NOTCH1 receptor to catalytically attach ubiquitin to NOTCH and target it for degradation (Chastagner et al., 2008). The interaction between NOTCH and ITCH appears to be highly conserved. In *Drosophila melanogaster*, genetic loss of the ITCH ortholog *Suppressor of Deltex* rescues Notch signaling (Cornell et al., 1999). Further evidence that NOTCH and ITCH genetically interact is supported by an accelerated *itchy* phenotype that develops in $Itch^{a18H/a18H}$ mice with an activating mutation of a *Notch1* transgene in T-cells (Matesic et al., 2006).

On another note, moribund $Itch^{a18H/a18H}$ animals exhibit signs of barrier dysfunction (Kathania et al., 2016). When fluorescently conjugated dextran, a macromolecule that is able to passively diffuse through the intestinal epithelium, was administered by oral gavage to $Itch^{+/+}$ or $Itch^{a18H/a18H}$ animals, increased levels of FITC-dextran were present within the serum of $Itch^{a18H/a18H}$ animals as

compared to *Itch*$^{+/+}$ control animals (Kathania et al., 2016). In contrast, young adult ITCH deficient animals do not appear to have a compromised intestinal barrier, suggesting that barrier dysfunction is likely exacerbated by an inappropriate inflammatory response within these animals (Marino et al., 2014). On another note, a potential role for ITCH in altering tight junction is highlighted by the ITCH-mediated degradation of OCCLUDIN (Traweger et al., 2002). Endogenous ITCH and OCCLUDIN co-immuoprecipitated in embryonic tissue from a mouse at day 13 of gestation. Further, ITCH was confirmed to polyubiquitylate OCCLUDIN in 293T cells and alter its stability.

Accumulating evidence highlights a specific role for ITCH in apoptosis. Among ITCH's numerous targets are p63 (Rossi et al., 2006) and p73 (Rossi et al., 2005), essential transcription factors involved in cell cycle regulation and apoptosis. Both full-length (TA) p63 and p73 are transcriptionally active and can induce cell cycle arrest that results in apoptosis (Murray-Zmijewski et al., 2006). Alternatively, dominant-negative (ΔN) isoforms can also be generated from an alternative promoter within the *p63* or *p73* genes. The ratio between the TA and the ΔN isoforms influences the biological outcome. The E3 ligase ITCH has been demonstrated to target both isoforms of p63 and p73. In HEK293 cells, ITCH was shown to bind and ubiquitylate both TAp63 and ΔNp63 that consequently lead to their destruction (Rossi et al., 2006). Additionally, the primary culture of keratinocytes derived from *Itch*$^{a18H/a18H}$ animals retained the expression of ΔNp63 longer during keratinocyte differentiation as compared to *Itch*$^{+/+}$ keratinocytes. As with p63, ITCH also binds, ubquitylates, and degrades

TAp73 and ΔNp73 (Rossi et al., 2005). In response to DNA damage, ITCH expression is reduced, which likely leads to the accumulation of TAp73 to induce cycle arrest and apoptosis.

ITCH also targets and promotes the degradation of other molecules involved in apoptosis, including TXNIP (Zhang et al., 2010), LATS1 (Ho et al., 2011), and c-FLIP (Chang et al., 2006). TXNIP is a modulator of cell redox homeostasis and is induced in response to cell stress, which allows reactive-oxygen species to accumulate and initiate cell death. *In vitro* and *in vivo* ubiquitylation assays confirmed that ITCH can bind, ubiquitylate, and degrade TXNIP (Zhang et al., 2010). Consequently, loss of ITCH promoted accumulation of reactive-oxygen species and apoptosis in response to the chemotherapeutic agent etoposide. Additionally, the targeting of the tumor suppressor LATS1 by ITCH promotes cell survival by increasing proliferation and decreasing apoptosis (Ho et al., 2011). Knockdown of endogenous ITCH via shRNA treatment in MDA-MB231 cells (derived from a human breast adenocarcinoma) decreased proliferation and increased apoptosis. More importantly, this phenotype can be reversed by shRNA knockdown of endogenous LATS1 effectively demonstrating that ITCH is a negative regulator of LATS1.

The presence of ITCH within Tregs controls the inflammatory response of Th2 cells. Loss of ITCH expression under the control of a Treg specific (*Foxp3*) promoter ($Itch^{fl/fl}$; $Foxp3^{Cre/Cre}$) resulted in massive lymphocytic infiltrate in the lung, skin, stomach, and liver, skin lesions, and chronic T-cell activation (H. S. Jin et al., 2013). Furthermore, severe inflammation was localized to the lungs of

Itch$^{fl/fl}$*; Foxp3*$^{Cre/Cre}$ animals as compared to ITCH sufficient control animals when subjected to an antigen-induced airway inflammation model of asthma (H. Jin et al., 2013). Interestingly, *Itch*$^{fl/fl}$*; Foxp3*$^{Cre/Cre}$ Tregs adopted a Th2 phenotype, secreting IL4-, IL-5, IL-10, and IL-13, while still retaining their suppressive capacity in an adoptive T-cell transfer model of colitis. Furthermore, IL-4, IL-5, and IL-10 cytokine levels were also increased in $CD4^+$ T-cells derived from *Itch*$^{fl/fl}$*; Foxp3*$^{Cre/Cre}$ animals as compared to control animals, suggesting that a Th2-mediated inflammatory response was initiated in *Itch*$^{fl/fl}$*; Foxp3*$^{Cre/Cre}$ animals.

In addition to regulating T-cell differentation, ITCH has been found to influence macrophage signaling. ITCH regulates p38, JNK, and NFκB signaling within macrophages via its interaction with NOD2 and RIP2 (M. F. Tao et al., 2009). NOD2 is an intracellular pattern recognition receptor that binds to fragments of a peptidoglycan that have invaded epithelial cells of the small intestine. Subsequently, a cytokine response is initiated by NOD2 that precisely controls the type, amount, and duration of cytokines that are necessary to effectively clear the bacterial pathogen while, at the same time, limiting this reaction to prevent an aberrant inflammatory response that could lead to tissue destruction (Caruso et al., 2014). Generation of the cytokine response hinges on the interaction of NOD2 with ubiquitylated RIP2 to activate p38, JNK, and NFκB signaling. In response to a *Listeria monocytogenes* infection in HT-29 cells, K63-linked polyubiquitylaton of RIP2 was mediated by the E3 ligase ITCH, which facilitated binding with NOD2 (M. F. Tao et al., 2009). Interestingly, ITCH-mediated ubiquitylation of RIP2 selectively promoted p38-induced JNK activation

while compromising NFκB signaling. Further, this interaction was also confirmed in bone marrow-derived macrophages from *Itch*$^{a18H/a18H}$ animals that were stimulated with mumuryl dipeptide (MDP), a peptidoglycan fragment that binds to NOD2 to initiate cytokine responses. MDP stimulation resulting in increased expression of NFκB gene targets in the *Itch*$^{a118H/18H}$ animals as compared to *Itch*$^{+/+}$ bone marrow-derived macrophages. In addition to ITCH's ability to downregulate NFκB signaling in response to MDP, ITCH also attenuates NFκB signaling induced by TNFα (Shembade et al., 2008). Mechanistically, the binding of ITCH to PPXY consensus sequences of A20, an ubiquitin-editing enzyme, modifies RIP2 ubiquitylation to inhibit NFκB activation. Further evidence supporting the importance of ITCH-mediated TNF-α -induced NFκB signaling is highlighted by phosphorylation of ITCH by the IKK kinase family, an essential component that is required for NFκB activation, which inhibits its regulation over NFκB to prolong NFκB duration (Perez et al., 2015).

Expanding on this current body of literature, our studies aim to elucidate the role of the E3 ligase ITCH in the small intestine. Here we provide evidence that loss of ITCH function in the small intestine influences epithelial homeostasis in a cell autonomous and non-cell autonomous manner.

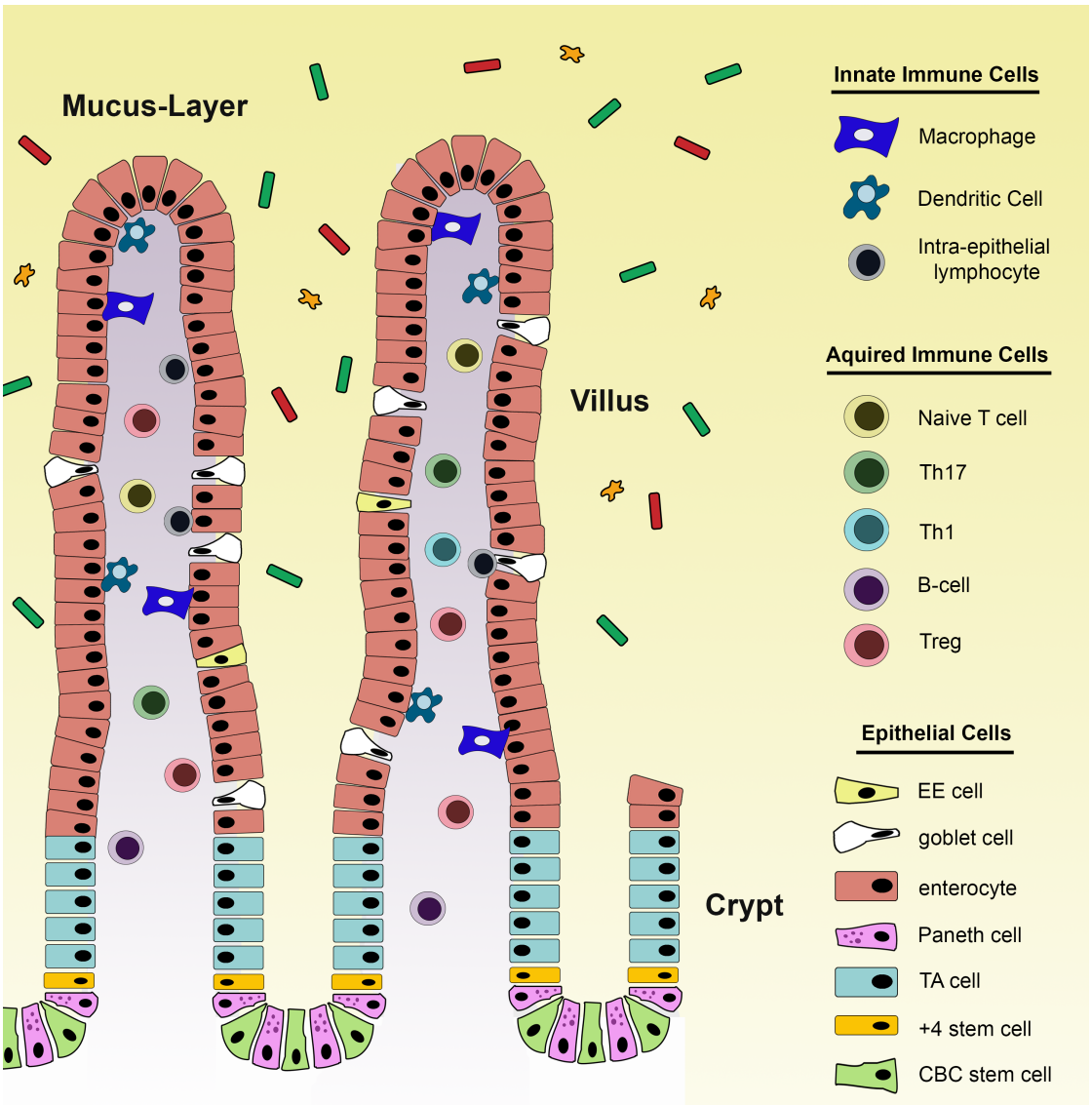

Figure 1.1. Cell types that comprise the small intestinal mucosa. The mucosa of the small intestine is composed of the epithelial barrier that separates the external environment from the body's internal milieu and the immune compartment. The epithelium is composed of CBC stem cell and +4 stem cells that reside at the base of the crypt interspersed between Paneth cells. Enterocytes, goblet cells, and enteroendocrine (EE) cells line the villi of the small intestine. The immune compartment, which underlies the epithelium, is composed of immune cells that mediate innate and acquired immune responses.

Table 1.1. List of previously described targets of ITCH.

Substrate	Function	Biological Outcome	References
c-Jun	Transcription factor	Regulation of Th2 cell differentation/anergy	Chen and Matesic, 2007
Jun-B	Transcription factor	Regulation of Th2 cell differentation/anergy	Fang et al., 2002; Chen and Matesic, 2007
Notch	Transcription factor	Regulation of autoimmunity/HSC function	Rathinam et al., 2011; Matesic et al., 2006
Gli1	Transcription factor	Repressor of Hedgehog signaling	Marcotullio et al. 2006
Deltex	Regulator of Notch signals	Regulation of autoimmunity	Cornell et al., 1999
p73	Transcription factor	Regulation of apoptosis, cancer	Rossi et al., 2005
p63	Transcription factor	Regulation of apoptosis, epithelial development, cancer	Rossi et al., 2006
DVL2	Regulator of Wnt signals	Postive regulation of Wnt signaling	Wei et al., 2012
TXNIP	Regulator of Cell-Redox Signaling	Regulation of apoptosis	Zhang et al., 2010
c-FLIP	Apoptosis inhibitory protein	Regulation of apoptosis	Chang et al., 2006
ROR-λt	Transcription factor	Regulator of IL-17 production	Kathania et al., 2016
LRP6	Regulator of Wnt signals	Negative regulation of Wnt signaling	Vijayakumar et al., 2017
Oct4	Transcription factor	Regulator of ESC self-renewal and cell reprogramming	Liao et al., 2013
Occludin	Intergral Plasma Membrane	Regulator of epithelial intercellular junctions	Traweger et al., 2002
Rip2	Protein Kinase	Regulator of NFκB signaling	Tao et al., 2009
p-DVL3	Regulator of Wnt signals	Regulator of cancer stem cells	Tsui et al., 2017
LATS1	Regulator of Hippo Signaling	Regulation of apoptosis	Ho et al., 2011

CHAPTER 2

THE UBIQUITIN LIGASE ITCH COORDINATES SMALL INTESTINAL EPITHELIAL HOMEOSTASIS BY MODULATING CELL PROLIFERATION, DIFFERENTIATION, AND MIGRATION[1]

[1] Heather L. Mentrup, Amanda Hartman, Elizabeth L. Thames, Wassim A. Basheer, and Lydia E. Matesic. Submitted to *Differentation*, August 7, 2017.

2.1 Abstract

Maintenance of the intestinal mucosa is driven by local signals that coordinate epithelial proliferation, differentiation, and turnover in order to separate antigenic luminal contents from the host's immune system. Breaches in this barrier promote gastrointestinal pathologies ranging from inflammatory bowel disease to cancer. The ubiquitin ligase ITCH is known to regulate immune responses, and loss of function of ITCH has been associated with gastrointestinal inflammatory disorders, particularly in the colon. However, the small intestine appears to be spared from this pathology. Here we explored the physiological mechanism that underlies the preservation of mucosal homeostasis in the small intestine in mice lacking ITCH (*Itch*$^{a18H/a18H}$). Histological analysis of the small intestines from young adult mice revealed architectural changes in animals deficient for ITCH, including villus blunting with cell crowding, crypt expansion, and thickening of the muscularis propria relative to age-matched mice sufficient for ITCH. These differences were more prominent in the distal part of the small intestine and were not dependent upon lymphoid cells. Underlying the observed changes in the epithelium were expansion of the Ki67^{+} proliferating transit amplifying progenitor population and increased numbers of terminally differentiated mucus-secreting goblet and anti-microbial producing Paneth cells, which are both important in controlling local inflammation in the small intestine and are known to be dysregulated in inflammatory bowel disease. Homeostasis in the small intestine of *Itch*$^{a18H/a18H}$ animals was maintained by increased cell turnover, including accelerated migration of epithelial cells along the crypt-villus

axis and increased apoptosis of epithelial cells at the crypt-villus junction. Consistent with this enhanced turnover, *Itch*$^{a18H/a18H}$ mice carrying the *Min* mutation (*Itch*$^{a18H/a18H}$; *Apc*$^{Min/+}$) displayed a 76% reduction in tumor burden as compared to *Apc*$^{Min/+}$ littermates with normal levels of ITCH. These findings highlight the role of ITCH as an important modulator of intestinal epithelial homeostasis.

2.2 Introduction

In the small intestine, the mucosal epithelium is a folded monolayer of columnar cells that is organized into crypts, which invaginate into the underlying mesenchyme, and villi, which project into the lumen. This structure is ideally suited to provide an essential, physical barrier between the host and its environment that must facilitate the absorption of nutrients while simultaneously preventing the loss of fluids and electrolytes as well as the entry of microorganisms into the body (van der Flier and Clevers, 2009). When the intestinal epithelium is disrupted, commensal and pathogenic microbes gain access to the host organism, prompting an inflammatory response, which can itself cause further tissue damage if not appropriately regulated (Turner, 2009). Thus, communication between mucosal immune cells (particularly those of the myeloid lineage) and the overlying epithelium is essential in maintaining gut homeostasis and in controlling intestinal inflammation (Van Der Gracht et al., 2016). Preservation of barrier function is dependent, in part, upon the continuous renewal of intestinal epithelial cells (Bischoff et al., 2014). Regeneration of the small intestinal epithelial architecture is a highly complex process that relies on

the balanced coordination of cellular proliferation within the crypts of Lieberkühn, preservation of epithelial function through cellular differentiation, and homeostatic cell migration along the crypt-villus axis (Pellettieri and Alvarado, 2007). Dysregulation of any one of these aspects of epithelial maintenance can drive a diverse collection of pathologies, ranging from improper nutrient absorption to inflammatory bowel disease (IBD) to intestinal carcinogenesis (J. M. Williams et al., 2015).

The rapid and constant renewal of the intestinal epithelium is initiated by the multipotent crypt base columnar (CBC) stem cells that reside at the bottom of the crypts (Barker et al., 2007a). Upon cellular division, the CBC stem cells give rise to a rapidly dividing transit-amplifying (TA) population that will commit and differentiate into the five major post-mitotic cells of the small intestinal epithelium (Barker, 2013). The most abundant of these is the absorptive enterocyte. The remaining four post-mitotic cell types originate from the secretory cell lineage and include the mucus secreting goblet cells, anti-microbial secreting Paneth cells, hormone producing enteroendocrine cells, and tuft cells (Barker, 2013). With the exception of Paneth cells, which migrate deeper into the crypt, the other four post-mitotic cell types normally move onto the villus where they continue to travel upward along this axis, eventually being sloughed off at the tip into the lumen. Because of the rapid turnover of the small intestinal epithelium, both spatial and temporal timing of signals are paramount. Accumulating evidence suggests that post-translational modifications such as ubiquitylation are essential in the

regulation of these signals to promote tissue homeostasis (Strikoudis et al., 2014).

Protein ubiquitylation is a highly conserved process characterized by the attachment of an ubiquitin molecule to a lysine residue within a target protein via the sequential action of three enzymatic/scaffolding proteins: the ubiquitin-activating enzyme (E1), the ubiquitin-conjugating enzyme (E2), and the ubiquitin ligase (E3). Ubiquitylation of a target substrate can lead to its degradation in the proteasome or lysosome, to its altered function, or to a change in its subcellular localization (Popovic et al., 2014). The E3 ubiquitin ligase ITCH was originally identified when the molecular etiology of the radiation- and 5-hydroxyurea-induced *a18H* mutation was elucidated, revealing a paracentric inversion on the distal end of mouse chromosome two, the breakpoints of which disrupted both the *Itch* and *Agouti* loci (William L. Perry et al., 1998). Animals homozygous for this null mutation of *Itch* (*Itch*$^{a18H/a18H}$) display lymphoproliferation in the spleen, lymph nodes, and thymus, atopic dermatitis, and pulmonary interstitial inflammation with alveolar proteinosis which culminates in death around 6-8 months of age on a C57BL/6J background (C. M. Hustad et al., 1995) whereas animals heterozygous for this mutation appear relatively unaffected with a normal lifespan (C. M. Hustad et al., 1995; Parravicini et al., 2008). The skin and lung inflammation in these animals occurs in the absence of known pathogen exposure, implying that immune activation may result from inappropriate inflammatory responses to environmental antigens at mucosal surfaces. Consistent with this assertion, loss of ITCH function has also been associated

with a gastrointestinal inflammatory phenotype in both mice and humans (Kathania et al., 2016; Lohr et al., 2010; Ramon et al., 2011; M. Tao et al., 2009). In mice, this appears to be more severe in the colon with moribund *Itch*$^{a18H/a18H}$ mice developing spontaneous colitis characterized by an increase in mixed inflammatory infiltrate and colonic epithelial destruction that was not observed in their age- and gender- matched wild type counterparts and has been hypothesized to be lymphoid-driven (Kathania et al., 2016). However, only mild inflammation has been observed in the small intestine of similarly aged (*i.e.*, 5-7 month old) animals lacking ITCH (Kathania et al., 2016; Ramon et al., 2011). This led us to hypothesize that, owing to differences in architecture, function, and microbiota composition, additional compensatory pathways may be activated in animals lacking ITCH in order to better maintain homeostasis in the small intestine as compared to what has already been described for the colon. Using the previously characterized *Itch*$^{a18H/a18H}$ mouse model, we found that, in the distal small intestines of *Itch*$^{a18H/a18H}$ animals, there were increased numbers of goblet and Paneth cells which correlated with increased proliferation of progenitor cells and expansion of the crypts. However, overall, homeostasis and cell number was maintained in these animals by accelerated migration and increased apoptosis of epithelial cells as compared to wild type animals. Furthermore, these changes in epithelial cell dynamics were associated with a 76% reduction in small intestinal tumor burden in animals lacking *Itch* expression on an *Apc*$^{Min/+}$ background as compared to ITCH-sufficient *Apc*$^{Min/+}$ littermates. Collectively, these data demonstrate a previously unappreciated role for ITCH in

the regulation of intestinal epithelial homeostasis, and provide further insight into regional differences in this process along the intestines.

2.3 Materials and Methods

Animals

Animals homozygous for a null allele of *Itch* (*Itch*$^{a18H/a18H}$) have been previously described (C. M. Hustad et al., 1995). For this line, the *a*^{18H} allele was backcrossed to C57BL/6J for 27 generations. Therefore, age-matched male and female C57BL/6J mice were used as referent controls (*Itch*$^{+/+}$) in the indicated experiments. To study the effect of this mutation on APC-induced tumorigenesis, a two generation intercross was performed. Specifically, *Itch*$^{a18H/a18H}$ mice were bred to *Apc*$^{Min/+}$ animals (JAX stock #002020) to produce *Itch*$^{a18H/+;}$ *Apc*$^{Min/+}$ and *Itch*$^{a18H/+}$; *Apc*$^{+/+}$ offspring, which were interbred to generate *Itch*$^{+/+}$*; Apc*$^{+/+}$, *Itch*$^{a18H/a18H}$*; Apc*$^{+/+}$, *Itch*$^{a18H/a18H}$; *Apc*$^{Min/+}$, and *Itch*$^{+/+}$; *Apc*$^{Min/+}$ animals for analysis. To assess the contribution of lymphocytes to the loss of function ITCH phenotype, *Itch*$^{a18H/a18H}$ animals were bred to B6.129S7-*Rag1*^{tm1Mom}/J (*Rag1*$^{-/-}$) mice (Jackson Laboratories stock number #002216) as previously described (Shembade et al., 2008). Since the *Rag1*$^{-/-}$ mice are severely immunocompromised, all animals from this cross were reared and maintained under high barrier conditions, following the recommendations of Jackson Laboratories. For all experiments, both genders were represented in each genotype in all experiments. All experiments were conducted in full compliance with the Institutional Animal Care and Use Committee of the University of South Carolina.

Histology and Staining

Small intestines derived from young adult animals were flushed with phosphate-buffered saline (PBS) after being cut into three equally sized segments (designated proximal, middle and distal), opened longitudinally, and fixed overnight with either 4% paraformaldehyde or with 10% neutral buffered formalin. Swiss-rolled intestinal tissues or were paraffin-embedded and sectioned at 5μm. Hematoxylin and eosin (H&E) staining was performed to assess tissue morphology. Alcian blue and nuclear fast red staining was performed by applying alcian blue, pH 2.5 for 30 minutes at 25°C followed by 0.1% nuclear fast red for 5 minutes. The Grimelius stain was performed according to previously published methodology (Grimelius, 2004). Briefly, tissue sections were treated with a 0.03% silver nitrate staining solution (Fisher Scientific, S181) for 3 hours at 60°C followed by a 2 minute treatment with a silver reducing solution (5% Sodium Sulfite/1% Hydroquione) that was pre-warmed to 58°C. Alkaline phosphatase (AP) staining was carried as previously described (Burstone, 1958). Specifically, a 2% naphthol AS-MX phosphate solution diluted in N,N-dimethyformamide was added to a 50%/50% mixture of Tris buffer, pH 8.74 and distilled water to create a final solution containing 0.5% napththol AS-MX phosphate in Tris buffer. This was then filtered through a 0.45μm filter. Slides were placed in the solution for 45 minutes at 37°C and washed before counterstaining with hematoxylin.

Immunohistochemistry and Immunofluorescence

For immunohistochemistry (IHC), antigen unmasking was performed using target retrieval solution for Ki67 (Dako # S1699) or 10 mM Tris-HCl/ 1 mM ethylenediaminetetraacetic acid (EDTA), pH=9 for 30 minutes at 95°C for cleaved-caspase 3. Sections were blocked in a solution containing 10% normal goat serum, 2% bovine serum albumin, and 0.2% Triton X-100 in Tris buffered saline (10mM Tris-HCL, pH 7.6, 150mM NaCl). An additional hydrogen peroxidase block was performed for 20 minutes at 25°C. The primary antibodies recognizing either Ki67 (B56, BD Pharmingen, 1:100) or cleaved-caspase 3 (Cell Signaling Technologies, #9664, 1:100) were diluted in Tris buffered saline containing 1% normal goat serum and 0.1% Triton X-100 and incubated on sections in a humidified chamber overnight at 4°C. The antibody was visualized using the EnVision+ system-HRP per the manufacturer's instructions (Dako # K4006). Brightfield images were acquired on a Zeiss Axio Imager A1 equipped with an AxioCam MRc5 camera.

Tissue immunofluorescence for lysozyme was performed as previously described (Basheer et al., 2015) with the following modifications: 5 µm paraffin sections were blocked for 1 hour before applying an anti-lysozyme antibody (RP028, Diagnostic BioSystems, 1:100) overnight at 4ºC. AlexaFluor659-conjugated goat anti-rabbit secondary (Jackson ImmunoResearch) was applied at a 1:500 dilution for 1 hour before mounting sections in Fluoro-gel II with DAPI (17985-51, Electron Microscopy Sciences). Phase contrast-coupled fluorescent images were acquired on a Leica DMI6000B epifluorescence microscope equipped with a Hamamatsu ORCA-R^2 CCD camera.

Quantitative Measurements: Histological Measurements, Cell Proliferation, and Post-Mitotic Cell Differentiation

All parameters quantified by histological examination were assessed in the distal segment from four or five 8-10 week old animals of each genotype (*i.e.*, *Itch*$^{+/+}$, n=4 or 5 and *Itch*$^{a18H/18H}$, n=4 or 5). Crypt and villus areas were quantified using a minimum of 25 well-oriented crypt or villus structures from at least seven different 10x fields per animal. The crypt or villus unit was outlined using the polygon tool in ImageJ, and the areas were quantified in μm^2. Cell proliferation was measured by first manually counting the total number of Ki67$^+$ cells stained by IHC in 25 well-oriented crypts from a minimum of nine 20x fields per animal. Then, the total number of cells in those same crypts was determined by enumerating the nuclei stained with Ki67 and/or hematoxylin. To calculate the average percentage of Ki67$^+$ cells in a crypt, the number of Ki67$^+$ cells was normalized to total cell number for that crypt and expressed as a percentage.

Phase contrast-coupled fluorescence images immunostained with an anti-lysozyme antibody were used to determine average Paneth cell number. In particular, individual Paneth cells were delineated using the cell membrane highlighted by phase-contrast microscopy, the DAPI-stained nucleus, as well as reactivity with the anti-lysozyme antibody. Paneth cells were counted in 30 crypts from a minimum of twelve 20x fields per animal. Average goblet cell and enterocyte number was determined by staining sections with alcian blue and a nuclear fast red counterstain. Goblet cells were recognized on the basis of the reactivity of their cytoplasm with alcian blue and by their characteristic shape,

while enterocytes were not reactive with alcian blue and were instead identified by their typical columnar appearance. Both types of cells were counted on 30 villi in at least eight different 10x fields per animal. Similarly, enteroendocrine cells identified through Grimelius stain were counted from 30 villi in eight different 10x fields per animal.

Bromodeoxyuridine (BrdU) Migration Assay

Twelve young adult *Itch*$^{+/+}$ and twelve young adult *Itch*$^{a18H/a18H}$ animals were intraperitoneally injected with 100 mg/kg BrdU (B5002, Sigma) dissolved in sterile PBS. Three animals of each genotype were randomly assigned to one of three cohorts and euthanized at 2, 24, 48, or 72 hours post-injection. The small intestines from these animals were cut into equally sized proximal, middle, and distal segments and flushed with PBS prior to 4% paraformaldehyde fixation, paraffin-embedding, and sectioning at 5 μm. IHC was performed as described above using anti-BrdU (3D4, BD Pharmingen, 1:8000). Images were acquired by bright field microscopy on a Zeiss Axio Imager A1 equipped with an AxioCam MRc5 camera and subsequently analyzed using ImageJ to determine migration and villus lengths. Percent cell migration was assessed from 25 villi in at least five different 10x fields per animal and calculated by normalizing the length of the furthest migrated epithelial BrdU^{+} cell from the base of the villus to the entire length of the villus from BrdU immunostained sections and converting to a percentage.

For figure presentation, brightfield images of sections immunostained with an anti-BrdU antibody were transformed to a spectral image using ImageJ. This

was accomplished by first inverting the images and then converting them to 8-bit gray scale. In order to specifically highlight cells that had taken up the BrdU label, the pixel intensity for those nuclei staining only for hematoxylin was subtracted out by calculating their background values. Specifically, for each converted image, a minimum of six different $BrdU^-$ nuclei were identified throughout the image and the pixel value for each was determined using a constant, ImageJ pre-defined area for the cursor. These values were averaged and considered the background level for each image. A similar background level was calculated in all the images except the 72 hour *Itch*$^{a18H/18H}$ image, which was higher. To account for this discrepancy, 55 pixels were subtracted from all the images except the 72 hour image captured from the *Itch*$^{a18H/a18H}$ animal in which 67 pixels were subtracted due to high background. Finally, the royal look-up table was applied to all images to re-colorize them.

Transmission Electron Microscopy

The small intestine from four young adult animals of each genotype was cut into three equally sized segments, flushed with PBS, and then opened longitudinally. The proximal segment was dissected into 4mm^2 pieces which were fixed in 2% glutaraldehyde/2% paraformaldehyde and secondarily post-fixed in buffered 1% osmium tetroxide/1.5% potassium ferricyanide. After dehydrating in ethanol, the samples were infiltrated and embedded in PolyBed 812 epoxy and allowed to polymerize for at least 48 hours at 60°C. At that time, blocks were sectioned at approximately 90 nm on a Leica UltraCut R and post

stained with 2% uranyl acetate (aq) and Hanaichi's calcined lead citrate. Images were obtained on a JEM 1400+ with an AMT mid-mount camera.

Polyp counts

The small intestines from 15 week-old male and female *Itch*$^{+/+}$; *Apc*$^{+/+}$, *Itch*$^{a18H/a18H}$; *Apc*$^{+/+}$, *Itch*$^{a18H/a18H}$; *Apc*$^{Min/+}$, and *Itch*$^{+/+}$; *Apc*$^{Min/+}$ animals were cut into 4 equally sized segments, flushed with PBS, opened longitudinally, and fixed overnight in 10% neutral buffered formalin. The samples were stained with 0.1% methylene blue to identify tumors. Total tumor number for each animal was assessed by counting and tabulating the polyp number along the entire axis of the small intestine by an observer blinded to genotypes.

Isolation of Mouse Intestinal Villi

Isolation of the villus fraction was performed as previously described (Huang et al., 2017) with the following modifications. To isolate adequate protein levels from just the villus fraction, the proximal most 10 cm of small intestine from two age-, gender- and genotype-matched animals was pooled. The small intestines from 8-10 week old *Itch*$^{+/+}$ and *Itch*$^{a18H/a18H}$ animals were washed in PBS (containing Mg^{2+} and Ca^{2+}) before opening longitudinally to expose crypts and villi. The proximal segment was cut into 3 to 5 mm pieces and incubated in ice-cold Dulbecco's PBS (DPBS, Cellgro # 21-031-CV). The DPBS was decanted from the previous step prior to incubating the intestinal pieces in ice-cold DPBS supplemented with 1 mM EDTA for 10 minutes at 4°C on a rocking platform. The 1mM EDTA was discarded, and the intestinal pieces were resuspended in fresh DPBS before being shaken vigorously 10-15 times to

dislodge the attached cells. The cells contained in the DPBS were labeled Fraction 1. To isolate cells from the villi, the fraction was filtered through a 70-µm nylon filter (VWR, #10199-656). The cells that remained on the filter were deemed the villus fraction. This process was subsequently followed for a total of 6 fractions, replacing each solution with fresh 1mM EDTA or DPBS prior to filtration. Fractions 3-6 contained pure villi and were pooled together before protein extraction. To isolate villi from the small intestines from *Itch*$^{a18H/a18H}$ animals, the EDTA incubation time was amended to 5 minutes for Fractions 1-6. All steps were performed at 4°C.

Protein Extraction and Western Blotting

Isolated villi were lysed in ice-cold RIPA buffer (150mM NaCl, 1% Triton X -100, 0.5% sodium deoxycholate,0.1% SDS, 50mM Tris pH 8.0) supplemented with 5mM EDTA,10mM NaF, 2mM $NaVO_4$, and protease inhibitors (P8340, Sigma, 1:100). For Western blotting, 40 µg of protein per sample were separated using a 4%-15% Mini-PROTEAN TGX gel (Biorad, #456-1084) then transferred to a PVDF membrane (Biorad, # 162-0177). The membrane was blocked in 5% milk in TBST (10mM Tris-HCL, pH8, 150mM NaCl, 0.05% Tween-20) for 1 hour at 25ºC. The following primary antibodies were incubated overnight at 4°: GAPDH (Santa Cruz, 6C5, 1:2000), Itch (BD Transduction, 611198, 1:1000), N-cadherin (Cell Signaling Technology, D4R1H, 1:1000), and Vimentin (Cell Signaling Technology, D21H3, 1:1000). Following primary antibody incubation, the appropriate HRP-conjugated rabbit (Biorad, #STAR208P,1:30,000) or mouse IgG secondary (Biorad, #STAR207P,1:20,000. was incubated for 1 hour at 25°C.

Signals were visualized using ECL reagent (Millipore, Immobilon Western, WBKLS0500) and the FluorChem E Chemiluminescent Western Blot Imaging System (ProteinSimple). Normalization and quantification of band intensities was performed with AlphaView software (ProteinSimple).

Statistics

Statistical comparisons of $Ki67^+$ cells, Paneth cells, goblet cells, enteroendocrine cells, enterocytes, BrdU migration, and tumor counts (reported as mean and standard deviation (SD) or standard error of the mean (SEM), as indicated, 2-tailed unpaired t-test for mean comparisons, Mann-Whitney test for comparing non-parametric medians of non-normally distributed enteroendocrine cells, and one-way ANOVA with a *post hoc* Tukey correction for tumor counts) were performed in Microsoft Excel or Prism Software (GraphPad Software, Inc) and plotted using Prism software. A p-value < 0.05 was considered statistically significant.

2.4 Results

Itch$^{a18H/a18H}$ animals have altered small intestinal morphology

Using a previously described loss of function mouse model (C M Hustad et al., 1995), the role of ITCH in intestinal homeostasis was examined by first characterizing the impact that loss of ITCH has on the morphology of the small intestines in young adult animals. This was accomplished by harvesting the small intestines from four or five 8-10 week old mice of each genotype and separately examining the architecture of the proximal, middle, and distal thirds of

the intestine to account for known regional variations in structure. Interestingly, examination of H&E stained sections from the various segments revealed hyperplasia of the crypts which became more prominent caudally along the small intestinal tract of *Itch*$^{a18H/a18H}$ animals as compared to ITCH sufficient referent controls (Fig. 2.2.A). Additionally, villus blunting (with more disorganized epithelial cell organization) as well as thickening of the muscularis propria were observed in the distal portion of animals lacking ITCH (asterisk, Fig. 2.2.A) and was associated with occasional mild mucosal inflammation (arrow, Fig. 2.2.A). These phenotypes were also noted in *Itch*$^{a18H/a18H}$*; Rag1*$^{-/-}$ animals which lack functional lymphoid cells (Fig. 2.3 and (M. Tao et al., 2009)) indicating that these changes were dependent on cues garnered from epithelial and/or innate immune cells. To quantify the changes in size of the crypts and villi in *Itch*$^{a18H/a18H}$ animals, we measured the area of 25 crypts and 25 villi from *Itch*$^{+/+}$ and *Itch*$^{a18H/a18H}$ animals in each region of the small intestine. Consistent with the apparent crypt expansion noted microscopically, the crypt area was significantly increased in the middle and distal segments of *Itch*$^{a18H/a18H}$ intestine as compared to age-matched wild type animals (19,772.23 μm^2 vs 11,165.53.12 μm^2 and 22,653.25 μm^2 vs. 15,780.51 μm^2, respectively) as determined by 2-tailed, unpaired t-test (Fig. 2.2.B). While there was a trend toward increased villus area across the entire small intestine, only in the distal segment was a statistically significant increase noted in animals lacking ITCH relative to those that were sufficient for ITCH (62,056.18 μm^2 vs. 47,144.47 μm^2, Fig. 2.2.C). Therefore, for

our subsequent analyses, we focused on changes in the distal segment of the small intestine.

Expansion of the crypt in adult *Itch*$^{a18H/a18H}$ animals is associated with an increase in the number of proliferating cells and Paneth cells in the distal small intestine

As there was a statistically significant increase in the crypt area of *Itch*$^{a18H/a18H}$ animals relative to *Itch*$^{+/+}$ controls, we hypothesized that an increase in cell number might underlie this expansion. Indeed, when the total number of cells in the crypts was calculated in tissues derived from five young adult animals of each genotype, a statistically significant increase in cell number was found in animals lacking ITCH (Fig. 2.4). To determine which cell populations might be expanded in the crypt, we first performed IHC using an antibody that recognizes the proliferation marker Ki67 since crypts are mostly composed of rapidly proliferating progenitor TA cells (Fig. 2.5.A). Upon evaluation of 25 well-oriented crypts from a minimum of nine 20x fields per animal (n=5 for each genotype), 40.14±4.91 (SD) Ki67^{+} cells on average were found in the crypts of the *Itch*$^{a18H/a18H}$ animals whereas 29.056±2.91 (SD) Ki67^{+} cells on average were found in the crypts of *Itch*$^{+/+}$ controls, and this difference was found to be statistically significant by 2-tailed, unpaired student t-test (Fig. 2.5.B). Although there was an increase in the absolute number of Ki67^{+} cells detected in *Itch*$^{a18H/a18H}$ animals, there was no difference in the percentage of proliferating cells within the crypt when compared to *Itch*$^{+/+}$ controls (Fig. 2.5.B), suggesting that progenitors cells were not the only cell type contributing to this increase in total cell number within the crypt.

In addition to stem and progenitor cells, Paneth cells also reside in the crypt. To test whether increased numbers of Paneth cells might be contributing to the increased crypt area observed in *Itch*$^{a18H/a18H}$ mice, small intestinal sections from five animals of each genotype were immunostained with an antibody recognizing lysozyme, a mature Paneth cell maker (Fig. 2.5.C), allowing for the enumeration of Paneth cells in 30 crypts from a minimum of twelve 20x fields per animal. Interestingly, there was a significant increase in Paneth cells in the crypts of *Itch*$^{a18H/a18H}$ animals (6.82±0.64, SEM) compared to *Itch*$^{+/+}$ controls (5.17±0.19, SEM). When the means were compared by unpaired, 2-tailed student t-test, the difference was found to be statistically significant (Fig. 2.5.D). Taken together, these results indicate that increases in the number of proliferating progenitor cells and differentiated Paneth cells contributed to the crypt expansion observed in *Itch*$^{a18H/a18H}$ animals.

Itch$^{a18H/a18H}$ animals have increased numbers of goblet cells along the villi of the distal small intestine

The epithelium of the small intestine is comprised of a variety of different cell types that arise from the rapidly dividing TA progenitor population found within the crypt. Since there was an expansion of proliferating cells in the crypts of mice lacking ITCH and since Paneth cells are only one of several different kinds of differentiated cells contributing to the epithelial architecture of the small intestine, it was a distinct possibility that other classes of post-mitotic cells which localize to the villi could also be altered in *Itch*$^{a18H/a18H}$ animals. To determine if goblet and enteroendocrine cells were also affected in *Itch*$^{a18H/a18H}$ animals, we

stained small intestinal tissue sections obtained from four animals of each genotype to specifically highlight each type of post-mitotic secretory cell. In particular, goblet cells were visualized using alcian blue, a stain identifying glycosylated mucins (Fig. 2.6.A), and the cell number determined by counting positively stained cells on 25 villi in at least eight different 10x fields per animal. Interestingly, there was a 48% increase in the number of goblet cells on the villus of *Itch*$^{a18H/18H}$ animals as compared to *Itch*$^{+/+}$ animals (10.93±0.98 (SEM) vs. 7.37±0.69 (SEM)), and this difference was statistically significant by 2-tailed, unpaired t-test (Fig. 2.6.D). However, no statistically significant difference in the number of enteroendocrine cells (visualized by Grimelius stain, which reacts with the hormones in the secretory granules, and quantified in 30 villi from eight different 10x fields per animal) was observed in the distal small intestine derived from *Itch*$^{a18H/18H}$ mice as compared to those derived from age-matched ITCH sufficient controls. Because of the left-shifted distribution of enteroendocrine cells in animals of both genotypes, a Mann-Whitney comparison of non-parametric medians was performed to determine significance for this population (Fig. 2.6.B and 2.6.D).

In addition to the post-mitotic cells derived from the secretory lineage, the absorptive enterocyte (the most abundant cell type in the small intestine) is essential to the structure and function of the small intestine. For this reason, mature enterocytes were characterized by staining distal intestinal tissues derived from young adult mice of both genotypes with AP in order to visualize the brush boarder (which is critical in nutrient absorption). When examining the

sections of *Itch*$^{+/+}$ and *Itch*$^{a18H/a18H}$ derived tissues, no appreciable difference in AP staining was seen, suggesting that the overall architecture and functionality of the enterocytes was preserved even in the absence of ITCH (Fig. 2.6.C). To determine whether there was instead a difference in enterocyte number between the two genotypes, the number of enterocytes was determined using alcian blue/nuclear fast red stained distal intestinal sections from four animals of each genotype. For this analysis, enterocytes were identified on the basis of their nuclear morphology and typical columnar cell profile and were counted from 25 villi in at least eight different 10x fields per animal. Although there was a trend towards reduced enterocyte number in the ileum of *Itch*$^{a18H/a18H}$ animals (48.52±2.38, SEM) as compared to the control (54.67±3.13, SEM, Fig. 2.6.D), this difference was not statistically significant by two-tailed unpaired t-test ($p=0.07$). Additionally, there was no statistically significant difference between genotypes in the total number of epithelial cells on those same villi (Fig. 2.7). Collectively, these data suggest that proliferating progenitor cells in the *Itch*$^{a18H/a18H}$ animals still retain the ability to give rise to both the absorptive and secretory cell lineage, albeit the percentage of the cell types are altered.

Itch$^{a18H/a18H}$ animals have increased epithelial cell turnover

Because *Itch*$^{a18H/a18H}$ animals have an increase in the number of proliferating progenitor cells within the crypt compartment yet still have comparable numbers of post-mitotic cells on the villus as age-matched ITCH sufficient controls, we speculated that animals lacking ITCH might have increased apoptosis of epithelial cells. To evaluate steady-state apoptosis levels,

IHC was performed on sections derived from the distal small intestines of four young adult animals of each genotype using an antibody that recognizes cleaved-caspase 3, a critical executioner for apoptosis. As would be expected under normal conditions, very few apoptotic cells could be detected in *Itch*$^{+/+}$ intestines, except for the rare epithelial cell at the tip of a villus that was presumably in the process of being sloughed off (Fig. 2.8). In addition to the occasional cleaved-caspase 3^{+} cell at the tip of a villus, there were a number of apoptotic cells at the crypt-villus junction in *Itch*$^{a18H/a18H}$ animals that were never seen in the intestines derived from *Itch*$^{+/+}$ mice (second row of images, Fig. 2.8). Thus, there was increased apoptosis of epithelial cells in the distal small intestines derived from animals lacking ITCH, even without some sort of stress or stimulus.

Another potential mechanism for more rapid turnover of the epithelium would be enhanced homeostatic epithelial cell migration along the crypt-villus axis, particularly since this is known to be influenced by proliferation within in the small intestinal crypt, wherein an increase or reduction in cell proliferation can enhance or slow migration respectively (Parker et al., 2017). Given the observed increase of proliferative cells within the crypts of *Itch*$^{a18H/a18H}$ animals, we sought to evaluate intestinal epithelial cell migration by intraperitoneally injecting twelve young adult *Itch*$^{a18H/a18H}$ and twelve young adult *Itch*$^{+/+}$ animals with 100 mg/kg BrdU, and three animals of each genotype were euthanized 2, 24, 48 or 72 hours post injection. IHC was performed on sections from the distal small intestines of these animals using an anti-BrdU antibody in order to localize the cells that had

taken up the BrdU pulse. As illustrated in Fig. 2.9.A, at 2 hours, all labeled cells were contained within the crypts of both ITCH sufficient and ITCH deficient mice. By 24 hours following injection, there were distinct differences between the two genotypes. In particular, mice lacking ITCH showed accelerated exodus of the label from the proliferating cells in the crypt at 24 hours, increased migration up the villus at 48 hours, and nearly complete elimination by 72 hours. To quantify the difference in cell migration along the villus while simultaneously accounting for the influence of ITCH on the crypt-villus architecture, a normalized measure of cell migration was calculated by dividing the measured length of the furthest migrated $BrdU^+$ cell on the villus to the entire length of the villus from 25 well-oriented villi in at least five different 10x fields per animal and expressed as a percentage (Fig. 2.9.B). Consistent with our qualitative observations, cell migration in the $Itch^{a18H/a18H}$ animals was more than double that of the $Itch^{+/+}$ animals at the 24 hour time point (33.46±3.64%, SD, vs. 15.47±4.68%, SD), which was statistically significant. A similar trend was apparent at both the 48 and 72 hour time points, though the difference between genotypes was not as drastic due to the sloughing of cells from the villus tip. In particular, at 48 hours, the edge of the BrdU label front had migrated 58.57±1.91% (SD) up the villus in $Itch^{a18H/a18H}$ animals whereas, on average, in $Itch^{+/+}$ animals, the leading edge had not yet reached the midway point (47.15±2.02%, SD). At 72 hours post injection, the BrdU pulse was nearly completely shed in animals lacking ITCH, and those labeled cells that remained were at the very tip of the villi (97.58±0.09%, SD). In contrast, in those animals sufficient for ITCH, the vast

majority of the labeled cells were present with the farthest migration point being 90.39±4.36% the length of the villus. Collectively, our data suggest that expansion of the proliferating progenitor cell population leads to accelerated cell migration along the crypt-villus axis in *Itch*$^{a18H/a18H}$ animals.

In the small intestine, the intercellular junctions of epithelial cells have been noted to be highly dynamic in order to accommodate the rapidly dividing tissue while still maintaining tissue integrity (Peglion et al., 2014). Further, alterations in adherens junctions and desmosomes are known to influence cell migration in the small intestine (Schneider et al., 2010). Since *Itch*$^{a18H/a18H}$ animals have increased proliferation and cell migration compared to *Itch*$^{+/+}$ animals, we hypothesized the cell-cell junctions might be affected in mice lacking ITCH. To test this hypothesis, small intestinal tissues derived from four young adult *Itch*$^{a18H/a18H}$ and four age-matched *Itch*$^{+/+}$ mice were examined by transmission electron microscopy. This analysis revealed several differences in the ultrastructure of these junctions. In particular, while tight junctions could be readily identified in both *Itch*$^{a18H/a18H}$ and *Itch*$^{+/+}$ derived tissue (Fig. 10, asterisks), adherens junctions were less discernable in small intestines derived from *Itch*$^{a18H/a18H}$ animals (Fig. 10, arrow) and the associated actin cytoskeleton appeared to be less organized. In addition, there was a complete absence of desmosomes in the small intestines of *Itch*$^{a18H/a18H}$ mice (Fig. 10, arrow head). Collectively, these data are consistent with a role for ITCH in regulating intestinal epithelial turn over.

Loss of ITCH significantly decreases intestinal adenoma formation in the small intestine of *Apc*$^{Min/+}$ animals

As the epithelium of the small intestine is under rapid and continuous renewal, stringent regulation of epithelial cell turnover is essential to prevent the growth of intestinal adenomas (Wong et al., 1996). In fact, increases in homeostatic cell migration have been associated with reduced *Apc*$^{Min/+}$ -induced tumorigenesis in the small intestine (Sansom et al., 2007). Since *Itch*$^{a18H/a18H}$ animals have enhanced epithelial cell migration, we hypothesized that loss of *Itch* would decrease intestinal adenoma formation. To test this hypothesis, the *Min* mutation (*Apc*$^{Min/+}$) was moved onto the *Itch*$^{a18H/a18H}$ background via a two generation intercross. This allowed for polyp assessment in *Itch*$^{+/+}$; *Apc*$^{+/+}$ (ITCH and APC sufficient), *Itch*$^{a18H/a18H}$; *Apc*$^{+/+}$ (ITCH deficient but APC sufficient), *Itch*$^{a18H/a18H}$; *Apc*$^{Min/+}$ (ITCH deficient and carrying the mutant *Apc* allele), and *Itch*$^{+/+}$; *Apc*$^{Min/+}$ (ITCH sufficient and carrying the mutant *Apc* allele) littermates. Total polyp number in the small intestines derived from 11 animals of each genotype (with approximately equal numbers of males and females) was determined when the animals reached 15 weeks of age. Consistent with previous reports (Tucker et al., 2005, 2002) a total of 115.7±52.49 (SD) polyps were observed in *Itch*$^{+/+}$; *Apc*$^{Min/+}$ animals at this age (Fig. 11). Interestingly, the *Itch*$^{a18H/a18H}$; *Apc*$^{Min/+}$ animals examined had only 27.36±19.62 (SD) polyps (Fig. 11). This represents a 76% reduction in tumor burden as compared to the *Itch*$^{+/+}$;*Apc*$^{Min/+}$ cohort, which was statistically significant ($p<0.001$). However, the number of polyps found in *Itch*$^{a18H/a18H}$; *Apc*$^{Min/+}$ animals was not statistically

different from that of either wild type animals (*Itch*$^{+/+}$; *Apc*$^{+/+}$) or from animals lacking ITCH (*Itch*$^{a18H/a18H}$; *Apc*$^{+/+}$) as assessed by one-way ANOVA with *post hoc* Tukey correction. Further, despite the altered cell-cell junctions seen in mice lacking ITCH (Fig. 2.10), this accelerated migration appeared to be physiological and was not associated with a pathological epithelial to mesenchymal transition (EMT) process as EMT markers N-cadherin and vimentin could not be detected by western blot on villus protein extracts from either *Itch*$^{+/+}$ or *Itch*$^{a18H/a18H}$ animals but were detected in positive controls (heart tissue lysate for N-cadherin and HeLa lysate for vimentin, Fig. 2.12). Thus, as a whole, these data suggest increased cell turnover in *Itch*$^{a18H/a18H}$ mice protects from the initiation of small intestinal adenoma formation in *Apc*$^{Min/+}$ animals.

2.5 Discussion

As a dividing line between self and non-self, the mucosal surface of the intestine is essential to maintaining homeostasis, and its breach is associated with pathologies like IBD (Mankertz and Schulzke, 2007), chronic viral infections (Brenchley et al., 2006; Sandler et al., 2011), and extra-intestinal autoimmune diseases such as type 1 diabetes (Wen et al., 2008), rheumatoid arthritis (Wu et al., 2010), and multiple sclerosis (Berer et al., 2011; Lee et al., 2011). However, the intestine is far from being a single homogeneous organ; rather, it consists of a number of anatomically and functionally specialized segments, each with distinct environmental pressures (Agace and McCoy, 2017). Here, we have identified a novel role for the E3 ubiquitin ligase ITCH in the proliferation, migration, and differentiation of small intestinal epithelial cells, and, in so doing,

offer a putative physiological mechanism for the attenuated inflammatory phenotype in the small intestine vs. what has been previously reported in the large intestine of animals lacking ITCH (Kathania et al., 2016; Ramon et al., 2011). Consistent with those studies, we found little inflammation in the mucosa of the small intestine of young adult *Itch*$^{a18H/a18H}$ mice despite the chronic inflammation that is known to accumulate with age at other mucosal surfaces like the lungs and skin (C. M. Hustad et al., 1995). Even though there was a lack of inflammatory infiltrate, distinct architectural changes (including villus blunting with some cellular disarray, crypt expansion, and thickening of the muscularis propria) were present along the length of the small intestine, and these were most pronounced in the distal portion. Many of these same alterations were seen in the small intestines of *Itch*$^{a18H/a18H}$*; Rag1*$^{-/-}$ mice which lack a functional lymphoid compartment of the immune system. This suggests that these changes result from altered programs in non-hematopoietic cells, in the resident innate immune cells, or a combination thereof.

Animals lacking ITCH also displayed increased numbers of Paneth and goblet cells in the distal small intestine. Paneth cells are normally only found in the small intestinal epithelium and play an important protective role in intestinal homeostasis by secreting antimicrobial peptides (Mukherjee et al., 2008; Vaishnava et al., 2008). Further, defects in Paneth cell function have been described in IBD patients (Elphick and Mahida, 2005; Wehkamp et al., 2008) as well as in a number of mouse lines that develop spontaneous intestinal inflammation including *Casp8*$^{IEC-KO}$ (Günther et al., 2011), *FADD*$^{IEC-KO}$ (Welz et

al., 2011), *NEMO*$^{IEC\text{-}KO}$ (Nenci et al., 2007), and *IKK2ca*$^{IEC\text{-}KO}$ (Vlantis et al., 2011). While the phenotypes in these lines result from intestinal epithelial-specific loss of proteins, the effects of Paneth cell function are far from cell autonomous as they help shape the microbiome, modulate the mucosal immune response, and provide important signaling cues in the intestinal stem cell niche (Okumura and Takeda, 2017). Similarly, the mucins secreted by goblet cells in the small and large intestine offer a protective barrier against commensal and pathogenic bacterial contact with the immune system. However, the composition of the mucous layer is different in the small and large intestine. In the former, there is a loose, more porous mucus that better facilitates the absorption of nutrients and depends on peristaltic actions to propel trapped microbes down the digestive tract whereas in the large intestine, the mucus is made of two discrete layers (an upper, thinner layer and a thicker lower layer) that has more permanence and thus more resident bacteria (Johansson and Hansson, 2016). As with defects in Paneth cell function, goblet cell depletion or dysfunction is a frequent histopathological feature of IBD (Gersemann et al., 2009). Thus, increased numbers of goblet and Paneth cells in the small intestine of animals lacking ITCH may protect it from the more severe inflammation observed in the colon.

In *Itch*$^{a18H/a18H}$ mice, increases in Paneth and goblet cells were associated with increased proliferation of progenitor cells in the crypt. It is tempting to speculate that either cell intrinsic or local cues promote secretory cell specification towards these cells fates. Differentiation within the secretory cell

lineage is highly complex wherein a heterogeneous population of precursors exists to direct lineage specification toward enteroendocrine cells or a common goblet and Paneth progenitor cell (Basak et al., 2017). While loss of ITCH was associated with an increase in goblet and Paneth cell numbers, enteroendocrine lineage specification and maturation appeared unaffected since there were equivalent numbers of these cells in the distal small intestine of mice sufficient and deficient for ITCH. Thus, ITCH may influence goblet and Paneth cell differentiation downstream of this specification step, potentially through the regulation of transcription factors such as SPDEF (Gregorieff et al., 2009).

While changes in epithelial differentiation might be driven by epithelial-intrinsic factors, it is also a formal possibility that they result secondarily from signals from the surrounding stroma. In fact, both mesenchymal and immune cells that normally reside in the lamina propria also contribute to intestinal self-renewal. Secretion of Hedgehog (Hh) ligands from the epithelium activates this signaling pathway within the mesenchyme, which, in turn, can influence intestinal homeostasis by altering cell proliferation, differentiation, inflammation, and turnover (Buller et al., 2012; Powell et al., 2011). Interestingly, ITCH has also been shown to negativity influence Hh signaling by targeting the downstream transcription factor GLI1 (Di Marcotullio et al., 2011), but it remains to be determined how loss of ITCH might impact Hh signals in the mesenchyme and innate immune system. In addition to their capacity as potential targets for Hh signals, inflammatory cells within the lamina propria can influence epithelial homeostasis via the release of proinflammatory cytokines that are capable of

feeding back onto the intestinal epithelium to modulate renewal (Garrett et al., 2010). Interestingly, ITCH deficient animals have an increase in the mucosal production (particularly in the colon) of the proinflammatory cytokines TNF-α, IL-1β, IL-6, and IL- 17 (Kathania et al., 2016; M. Tao et al., 2009; Theivanthiran et al., 2015), which are similarly dysregulated during gastrointestinal inflammation and barrier dysfunction (Schenk and Mueller, 2008). In order to pinpoint the initiating signals for the altered intestinal homeostasis observed in ITCH deficient mice, future studies employing the recently generated floxed allele of *Itch* (H. Jin et al., 2013) are necessary to delineate the tissue-specific contribution of ITCH in the epithelium, immune system, and mesenchyme in isolation from the other genes potentially influenced by the a^{18H} inversion to gain important additional insight into the multifaceted role ITCH plays in mucosal barrier function.

Increased proliferation in the small intestinal crypts of animals lacking ITCH was balanced by increased apoptosis at the crypt/villus junction and by the enhanced migration and shedding of epithelial cells. Renewal of the small intestinal epithelium is very rapid, and complete epithelial turnover occurs every 4-5 days (van der Flier and Clevers, 2009). Turnover in $Itch^{a18H/a18H}$ animals is accelerated even further, with approximately 98% of cells being shed from the villus after 3 days. This increased migration correlated with the presence of altered cell-cell junctions between intestinal epithelial cells. In particular, ITCH deficient mice lacked desmosomes and had disorganized adherens junctions while the tight junctions appeared to remain intact. Interestingly, E-cadherin, a critical component of adherens junctions, has been shown to influence intestinal

homeostasis. Its loss in the intestinal epithelium was associated with altered differentiation and maturation of Paneth and goblet cells, induction of cell death, loss of adherens junctions and desmosomes, and mislocalization of Paneth cells along the crypt-villus axis of the small intestine, and this phenotype was more severe in the colonic epithelium despite the fact that more residual E-cadherin expression was retained there (Schneider et al., 2010). Further, overexpression of E-cadherin within the intestinal epithelium resulted in suppression of proliferation and a reduction in migration along the crypt-villus axis (Hermiston et al., 1996). As mice lacking ITCH still have adherens junctions (albeit disorganized ones), it is possible that there might be a slight decrease in E-cadherin within epithelial cells that is sufficient to contribute to increased proliferation, accelerated migration, and increased apoptosis of epithelial cells within the small intestine which does not affect maturation programs. Because of the reported disparity in response to loss of E-cadherin between the epithelium of the small intestine and that of the colon, it is tempting to speculate that this might contribute to the different inflammatory profiles of the small and large intestine in *Itch*$^{a18H/a18H}$ mice.

Further evidence that homeostasis is more appropriately regulated in the small intestine than in the colon of mice lacking ITCH comes from our observation that *Itch*$^{a18H/a18H}$*; Apc*$^{Min/+}$ animals had a 76% reduced tumor load as compared to *Itch*$^{+/+}$*; Apc*$^{Min/+}$ littermates (Fig. 7), whereas ITCH deficient mice have been reported to be more susceptible to the induction of colitis-associated cancer which develops in the context of chronic inflammation of the colon

(Kathania et al., 2016). This likely reflects, in part, the different initiating events in these types of tumors. Specifically, while the *Apc*$^{Min/+}$ mouse more closely parallels what occurs in sporadic colon cancers where there is a sequential accumulation of genetic mutations that promotes a progressively more malignant phenotype in what has been dubbed the "adenoma-carcinoma sequence" (Cho and Vogelstein, 1992), colitis associated cancer is driven by the activation of completely different pathways, usually without constitutive activation of the APC-β-catenin-TCF axis (Foersch and Neurath, 2014). Furthermore, the increased cell turnover in the small intestine of ITCH deficient animals potentially contributes to the decrease in adenoma initiation observed in *Itch*$^{a18H/a18H}$; *Apc*$^{Min/+}$ mice. Previous studies have shown that increased homeostatic epithelial migration was associated with reduced *Apc*$^{Min/+}$ -induced tumorigenesis in the small intestine (Sansom et al., 2007), suggesting that perturbations in the intestinal epithelial cell migration observed in *Itch*$^{a18H/a18H}$ mice potentially influence intestinal adenoma formation by limiting the anchorage of cancer-initiating cells needed for adenoma induction and growth. However, there was no evidence that animals lacking ITCH had a switch from E-cadherin to N-cadherin expression which is observed in EMT and promotes the invasive capabilities of cancer cells (Halbleib and Nelson, 2006), though this possibility needs to be more thoroughly evaluated in a more aggressive colorectal cancer model than the *Apc*$^{Min/+}$ mouse because the tumors in those animals rarely become invasive (Nalbantoglu et al., 2016).

In conclusion, the differences observed in the homeostasis of the intestinal epithelium of the small vs. the large intestines in *Itch*$^{a18H/a18H}$ animals provide physiological insight into regional specificities of these segments of the gastrointestinal tract. Further studies aimed at defining the molecular pathways downstream of ITCH and determining whether the phenotype of the *Itch*$^{a18H/a18H}$ small intestine resembles that of “mucosal healing” in IBD following the abatement of inflammation may allow for the identification of novel biomarkers associated with long-term remission and low risk of surgical treatment in IBD as well as potential new avenues for therapeutic intervention.

2.6 Figures

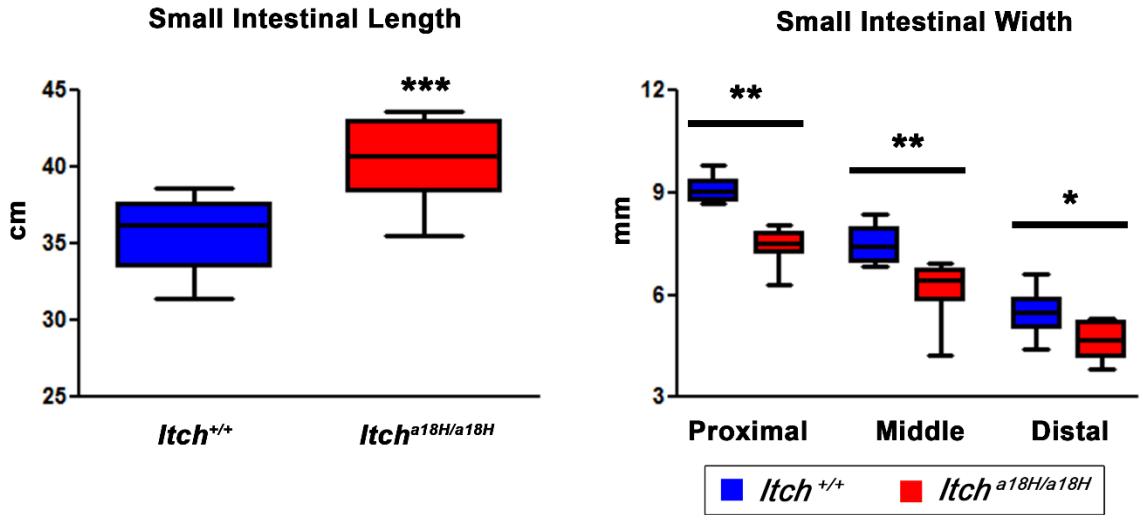

Figure 2.1. *Itch*$^{a18H/a18H}$ intestines have increased rostral-to-caudal length and decreased circumference. The entire length of the small intestine from 9 week old *Itch*$^{+/+}$ (n=12) and *Itch*$^{a18H/a18H}$ (n=12) animals were removed and the length along the x-axis was measured in cm. *Itch*$^{a18h/a18H}$ small intestines are significantly longer (***p<0.001) than *Itch*$^{+/+}$ animals. The proximal, middle, and distal segments from the small intestine of 9-week old *Itch*$^{+/+}$ (n=10) and *Itch*$^{a18H/a18H}$ (n=10) were opened longitudinally to quantify the width of the small intestine in mm. The small intestine from *Itch*$^{a18H/a18H}$ animals had a significantly shorter width proximally (**p<0.005), middle (**p<0.005), and distally (*p<0.05) when compared to *Itch*$^{+/+}$ animals.

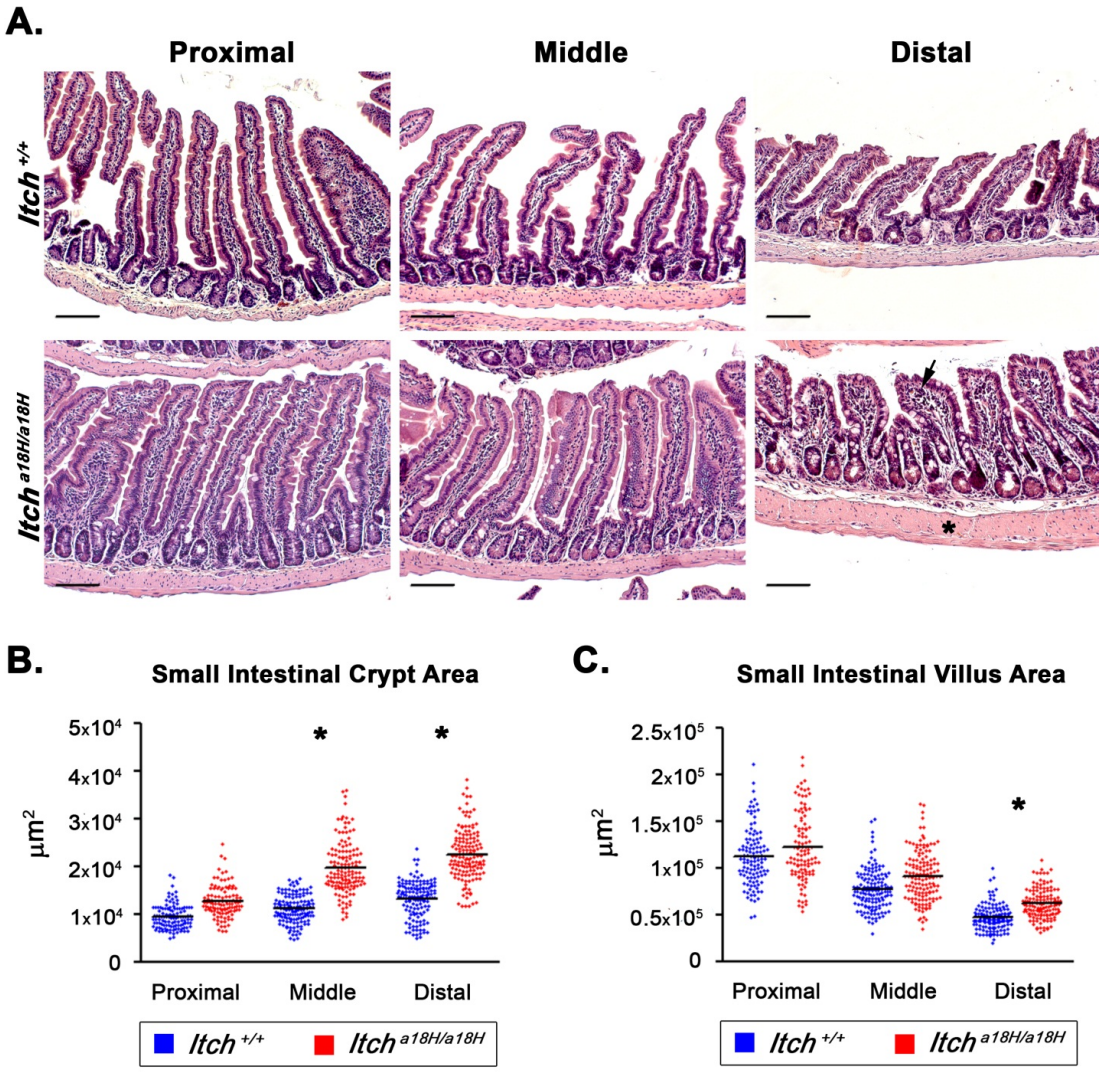

Figure 2.2. Small intestinal architecture is altered in *Itch*$^{a18H/a18H}$ animals. (**A**) Representative H&E stained paraffin-embedded small intestinal sections derived from the proximal (left most column), middle (center column), and distal (right hand column) segments of young adult *Itch*$^{+/+}$ and *Itch*$^{a18H/a18H}$ animals accentuate an enlargement of the intestinal crypt in *Itch*$^{a18H/a18H}$ animals, becoming more pronounced distally. Scale bars = 200 μm. (**B**) Small intestinal crypt and villus areas from young adult *Itch*$^{+/+}$ (n = 4 or 5) and *Itch*$^{a18H/a18H}$ (n = 5) were measured in μm^2 using ImageJ. A minimum of 25 well-orientated crypts or villi from at least seven different 10x fields were measured per animal. Average crypt area was significantly increased (*p<0.005) in the middle and distal small intestine of *Itch*$^{a18H/a18H}$ compared to *Itch*$^{+/+}$. (**C**) Average villus area was significantly increased (*p<0.05) distally in the small intestine of *Itch*$^{a18H/a18H}$ animals compared to *Itch*$^{+/+}$.

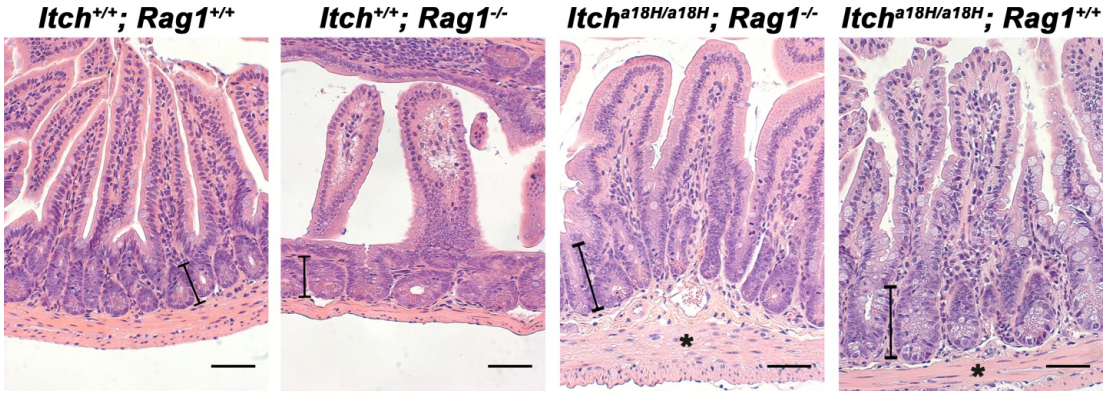

Figure 2.3. Small intestinal architectural changes observed in ITCH deficient mice are lymphoid independent. Representative H&E stained paraffin-embedded distal small intestinal sections from 12 week old *Itch*$^{+/+}$; *Rag1*$^{+/+}$ (wild type, far left), *Itch*$^{+/+}$; *Rag1*$^{-/-}$ (RAG1 deficient, middle left), *Itch*$^{a18H/a18H}$; *Rag1*$^{-/-}$ (RAG1 and ITCH deficient, middle right), and *Itch*$^{a18H/a18H}$; *Rag1*$^{+/+}$ (ITCH deficient, far right) animals are shown. Animals lacking both ITCH and RAG1 produce no functional lymphocytes, yet still develop crypt hyperplasia (height of bracketed bar), villus blunting, and expansion of the muscularis propria (asterisk), suggesting that these phenotypes arise as a consequence of signals produced by epithelial and/or resident innate immune cells. However, the cellular disorganization seen in *Itch*$^{a18H/a18H}$; *Rag1*$^{+/+}$ animals was not observed in *Itch*$^{a18H/a18H}$; *Rag1*$^{-/-}$ mice. Scale bars = 100 μm. Magnification= 20x.

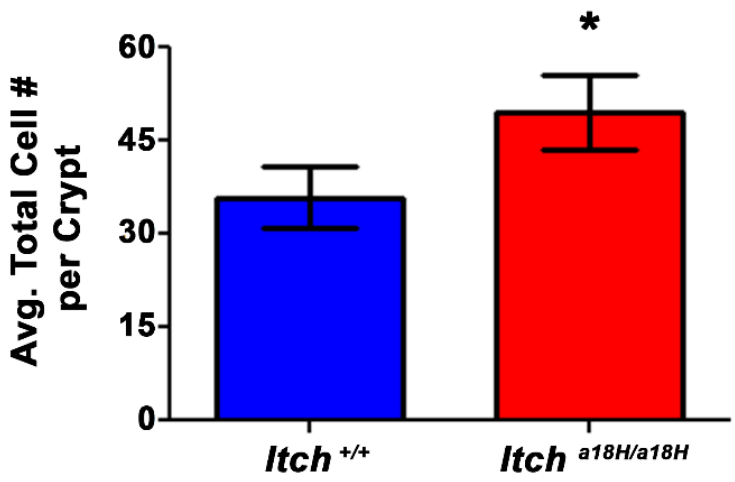

Figure 2.4. Alterations in *Itch*$^{a18H/a18H}$ crypt morphology is reflective of increased total cell numbers within the crypt. Total cell numbers within the crypt were manually counted from paraffin-embedded adult *Itch*$^{+/+}$ and *Itch*$^{a18H/a18H}$ intestinal sections immunostained for Ki67 and counterstained with hematoxylin. The average total cell number within the crypts were assessed by counting the total number of cells from 25 well-oriented crypts in a minimum of nine different 20x fields from each adult *Itch*$^{+/+}$ (n = 5) or *Itch*$^{a18H/a18H}$ (n = 5) animal. *Itch*$^{a18H/a18H}$ animals had a statistically significant increase (49.46±6.03, SD) in total cell number (*$p<0.005$) within the crypt compared to Itch$^{+/+}$ animals (35.90±34.86, SD) when analyzed by a 2-tailed, unpaired t-test. Error bars represent SD.

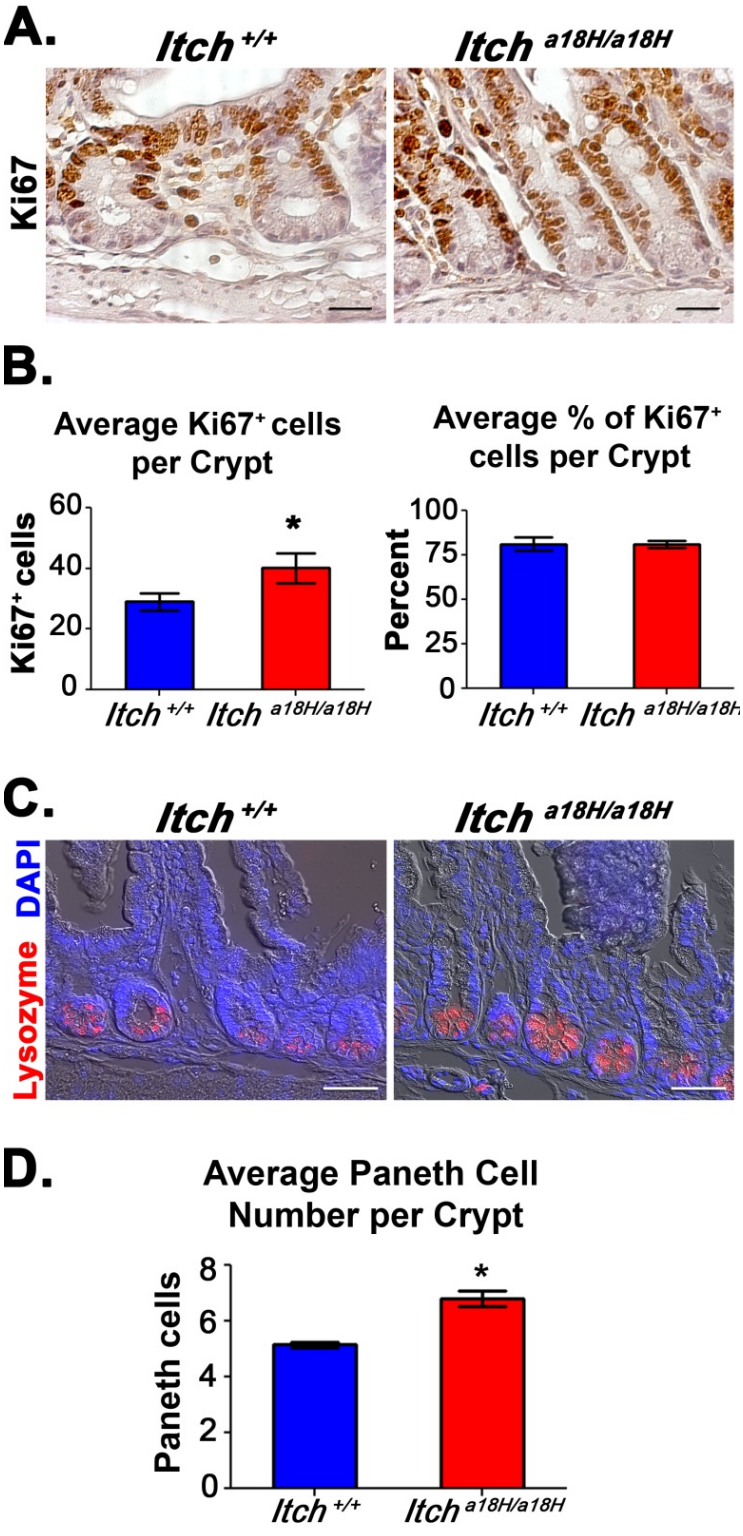
A.
Itch +/+
Itch a18H/a18H
Ki67
B.
Average Ki67+ cells per Crypt
Ki67+ cells
60
40
20
0
*
Itch +/+
Itch a18H/a18H
Average % of Ki67+ cells per Crypt
Percent
100
75
50
25
0
Itch +/+
Itch a18H/a18H
C.
Itch +/+
Itch a18H/a18H
DAPI
Lysozyme
D.
Average Paneth Cell Number per Crypt
Paneth cells
8
6
4
2
0
*
Itch +/+
Itch a18H/a18H

.

Figure 2.5. Crypt expansion in *Itch*$^{a18H/a18H}$ animals is accompanied by an increase in proliferating TA cells and differentiated Paneth cells. (**A**) Pictured are representative micrographs of IHC performed on paraffin-embedded distal intestinal sections derived from young adult *Itch*$^{+/+}$ and *Itch*$^{a18H/a18H}$ animals (n = 5 for each genotype) using an anti-Ki67 antibody and subsequently counterstained with hematoxylin. Animals lacking ITCH appear to have increased cellular proliferation in the crypt. Scale bars = 50 μm. (**B**) Average number and average percentage of Ki67^{+} cells in the crypts from adult *Itch*$^{+/+}$ (n = 5) and *Itch*$^{a18H/a18H}$ (n = 5) animals. Ki67^{+} cells and total cell numbers were counted from 25 well-oriented crypts in a minimum of nine different 20x fields per animal. *Itch*$^{a18H/a18H}$ animals had, on average, 13 more Ki67^{+} cells per crypt which was statistically significant (*$p<0.01$). No difference was observed in the percentage of proliferating cells within the crypt. Error bars represent SD. (**C**) Representative phase contrast-coupled immunofluorescent images of paraffin-embedded sections of distal intestine from five adult *Itch*$^{+/+}$ and five age-matched *Itch*$^{a18H/a18H}$ animals stained with anti-lysozyme (red) and DAPI (blue). Scale bars = 100 μm. (**D**) Average number of Paneth cells per crypt from adult *Itch*$^{+/+}$ (n = 5) and *Itch*$^{a18H/a18H}$ (n = 5) animals. Paneth cells from 30 crypts in a minimum of 12 different 20x fields were averaged to determine that *Itch*$^{a18H/a18H}$ animals have significantly more Paneth cells (*$p<0.05$) than *Itch*$^{+/+}$ animals. Error bars represent SEM.

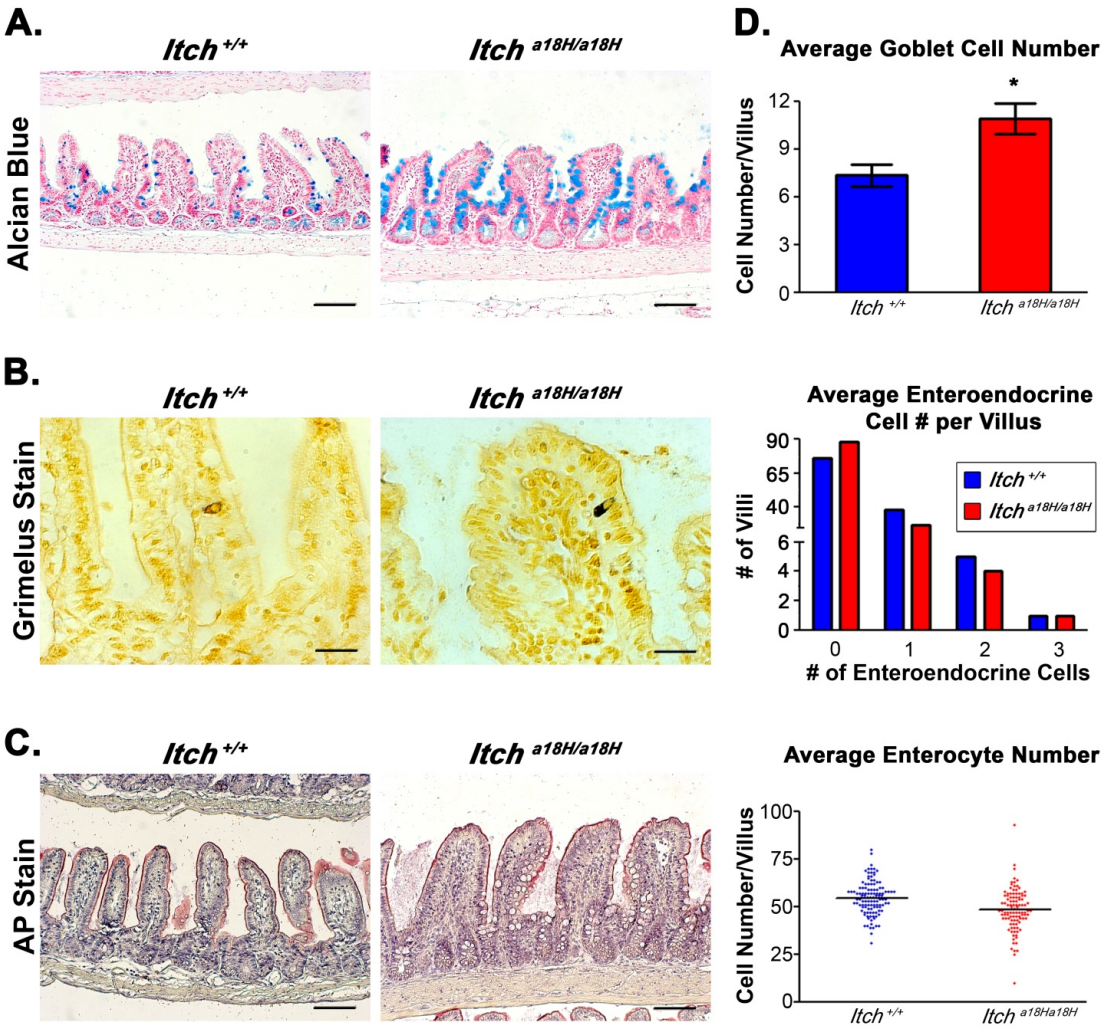
A.
Itch +/+
Itch a18H/a18H
Alcian Blue
D.
Average Goblet Cell Number
Cell Number/Villus
12
9
6
3
0
*
Itch +/+
Itch a18H/a18H
B.
Itch +/+
Itch a18H/a18H
Grimelus Stain
Average Enteroendocrine Cell # per Villus
# of Villi
90
65
40
6
4
2
0
Itch +/+
Itch a18H/a18H
0
1
2
3
# of Enteroendocrine Cells
C.
Itch +/+
Itch a18H/a18H
AP Stain
Average Enterocyte Number
Cell Number/Villus
100
75
50
25
0
Itch +/+
Itch a18Ha18H

Figure 2.6. Loss of ITCH promotes goblet cell differentiation. (**A**) Paraffin-embedded intestinal sections stained with alcian blue, pH 2.5 and counterstained with nuclear fast red distinguish goblet cells from adult *Itch*$^{+/+}$ and *Itch*$^{a18H/a18H}$ animals. Scale bars = 200 μm. (**B***)* Pictured are representative *Itch*$^{+/+}$ and *Itch*$^{a18H/a18H}$ derived paraffin-embedded sections stained with 1% silver nitrate to identify enteroendocrine cells in the small intestine. Scale bars = 200 μm. (**C**) Paraffin-embedded sections stained with AP highlights the brush boarder of enterocytes on the villi of *Itch*$^{+/+}$ and *Itch*$^{a18H/a18H}$ animals. Scale bars = 200 μm. (**D**) Average number of goblet cells, enteroendorcine cells, and enterocytes located on the villus of *Itch*$^{+/+}$ (n = 4) and *Itch*$^{a18H/a18H}$ (n = 4) animals. Indicated type of cells were counted on 30 villus structures from a minimum of eight different 10x fields per animal. Enteroendocrine cell counts are presented as a histogram of the total number of villus structures bearing no, one, two or three cells in *Itch*$^{+/+}$ (n = 4) and *Itch*$^{a18H/a18H}$ (n = 4) animals. *Itch*$^{a18H/a18H}$ animals have a statistically significant increase (*$p<0.05$) in goblet cells. There was no statistically significant difference in enteroendocrine or enterocyte cell number. Error bars represent SEM for goblet cell counts.

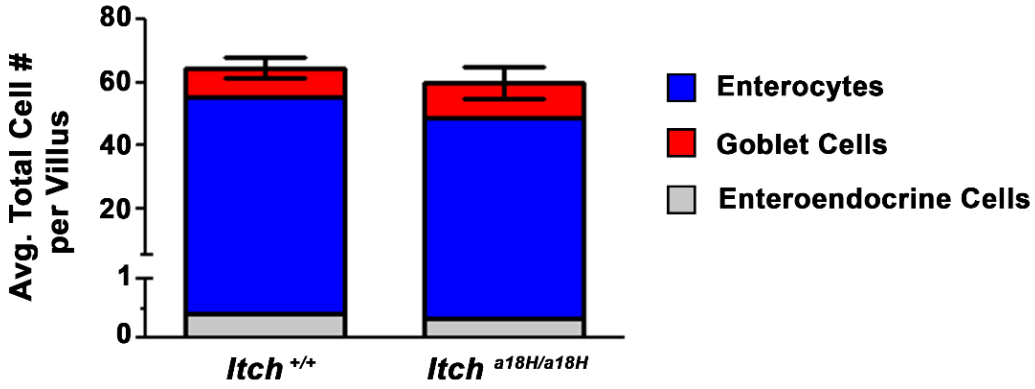

Figure 2.7. Loss of ITCH influences specification without altering total epithelial cell numbers on the villus. Average total epithelial cell number on the villus was determined by adding the means from enterocytes, goblet cells, and enteroendocrine cells that were counted on 25 to 30 separate villus structures in a minimum of eight different 10x fields from each adult *Itch*$^{+/+}$ (n = 4) or *Itch*$^{a18H/a18H}$ (n = 4) animal. To determine significance, the mean total cell villus numbers from adult *Itch*$^{+/+}$ (n = 4) or *Itch*$^{a18H/a18H}$ (n = 4) animals were compared using a 2-tailed, unpaired t-test, which showed no statically significant difference between the *Itch*$^{+/+}$ and *Itch*$^{a18H/a18H}$ groups (62.04±3.43, SD versus 59.45±5.18, SD). Error bars represent SD of total cell number.

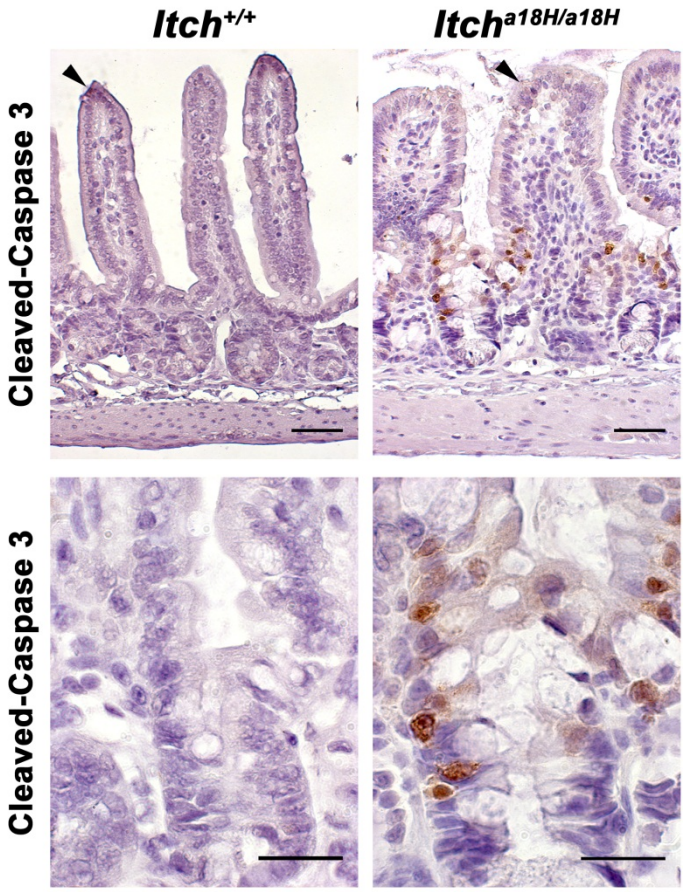

Figure 2.8. Loss of ITCH promotes epithelial apoptosis in the small intestine. Paraffin embedded sections from the distal small intestine of young adult *Itch*$^{+/+}$ and *Itch*$^{a18H/a18H}$ animals (n = 4 for each genotype) were immunostained for cleaved-caspase 3 and counterstained with hematoxylin. Representative photomicrographs are shown. While rare apoptotic cells could be found at the tips of villi in animals of both genotypes (arrowheads, top row of micrographs), increased apoptosis was seen at the crypt-villus junctions in only those animals lacking ITCH (bottom row, 63x). Scale bars = 100 μm (top row) or 50 μm (bottom row).

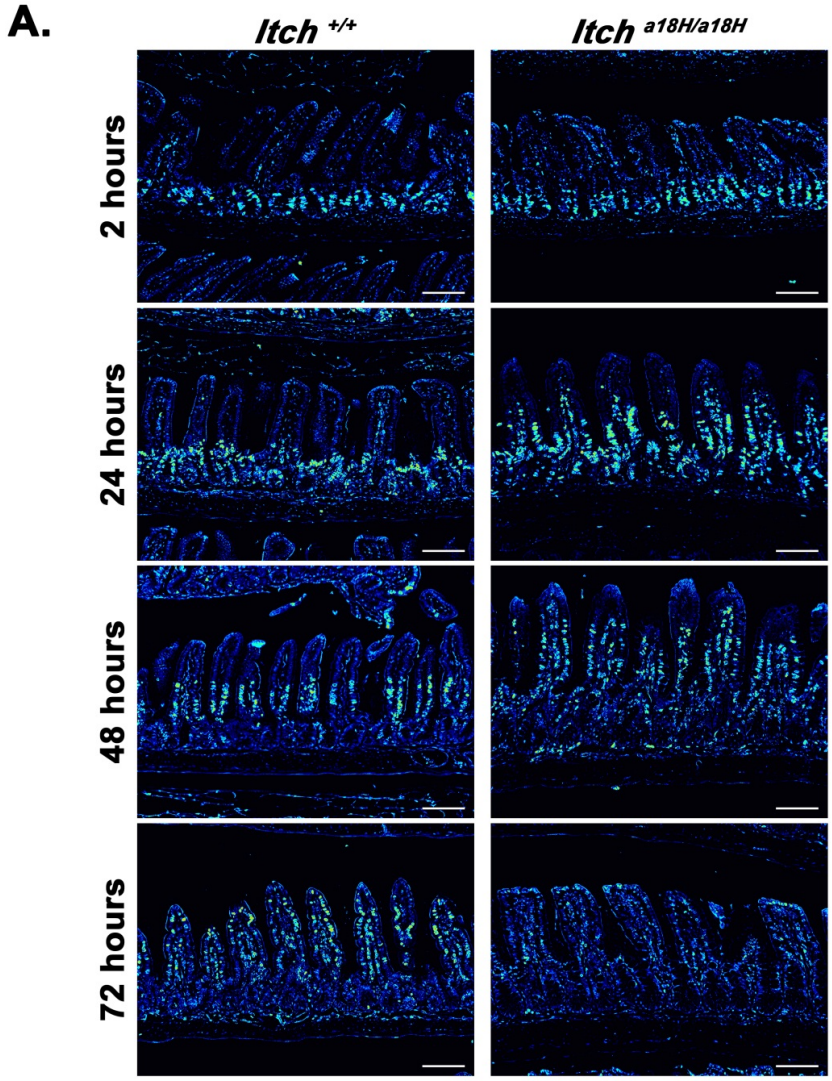
A.
Itch +/+
Itch a18H/a18H
2 hours
24 hours
48 hours
72 hours

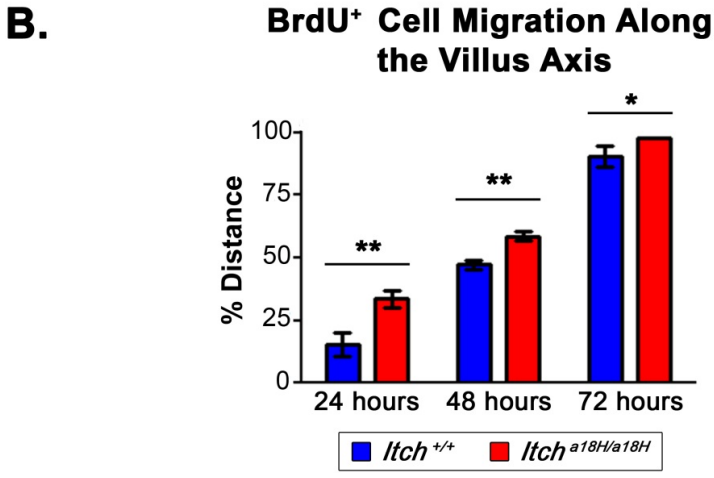
B.
BrdU+ Cell Migration Along the Villus Axis
% Distance
100
75
50
25
0
**
**
*
24 hours
48 hours
72 hours
Itch +/+
Itch a18H/a18H

Figure 2.9. Epithelial turnover is increased in animals that lack ITCH. (**A**) IHC with an anti-BrdU antibody was conducted on paraffin-embedded sections obtained from young adult *Itch*$^{+/+}$ and *Itch*$^{a18H/a18H}$ animals intraperitoneally injected with 100mg/kg of BrdU. Brightfield images were taken 2, 24, 48, and 72 hours post injection and representative examples from each genotype and time point were converted to spectral images using the lookup tables available in ImageJ as seen here. These images demonstrate enhanced migration of epithelial cells in *Itch*$^{a18H/a18H}$ animals with complete sloughing by 72 hours following the BrdU pulse. Scale bars = 200μm. (**B**) Average cell migration of BrdU-labeled cells along the villus axis in *Itch*$^{+/+}$ (n = 3) and *Itch*$^{a18H/a18H}$ (n = 3) animals at 24, 48, and 72 hours after BrdU incorporation was calculated by dividing the measured distance of the furthest migrated labeled cell from the base of the villus by the entire length of the villus from 25 villi in a minimum of five different 10x fields per animal. Since all cells were localized to the crypt in both genotypes at the 2-hour timepoint, this data point is not shown. A statistically significant increase in cell migration at was detected in *Itch*$^{a18H/a18H}$ derived tissues at 24 (**$p<0.005$), 48 (**$p<0.005$), and 72 hours (*$p<0.05$) versus tissues derived from *Itch*$^{+/+}$ animals. Error bars represent SD.

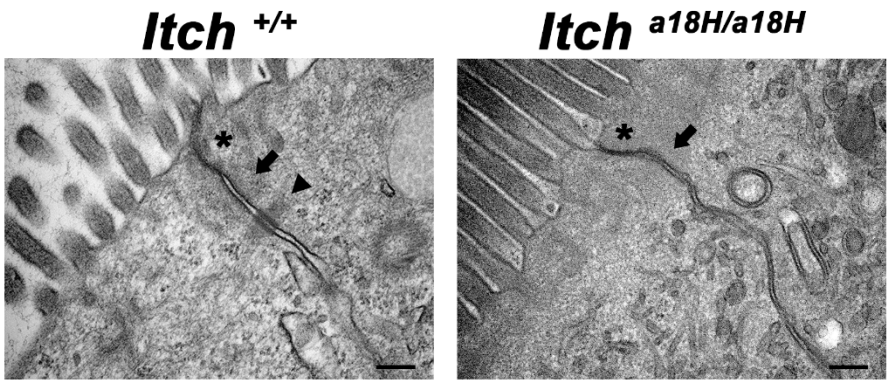

Figure 2.10. *Itch*$^{a18H/a18H}$ animals have altered cell-cell junctions. Representative transmission electron micrographs of cell-cell junctions (tight junctions marked by asterisks, adherens junctions by arrows, and desmosomes by arrow head) from the proximal small intestine of nine week-old *Itch*$^{+/+}$ and *Itch*$^{a18H/a18H}$ animals are depicted here. In total samples from 4 animals of each genotype were examined. *Itch*$^{a18H/18H}$ animals lack identifiable desmosomes and adherens junctions appeared more disorganized than the ITCH sufficient control samples. Scale bar = 200 nm.

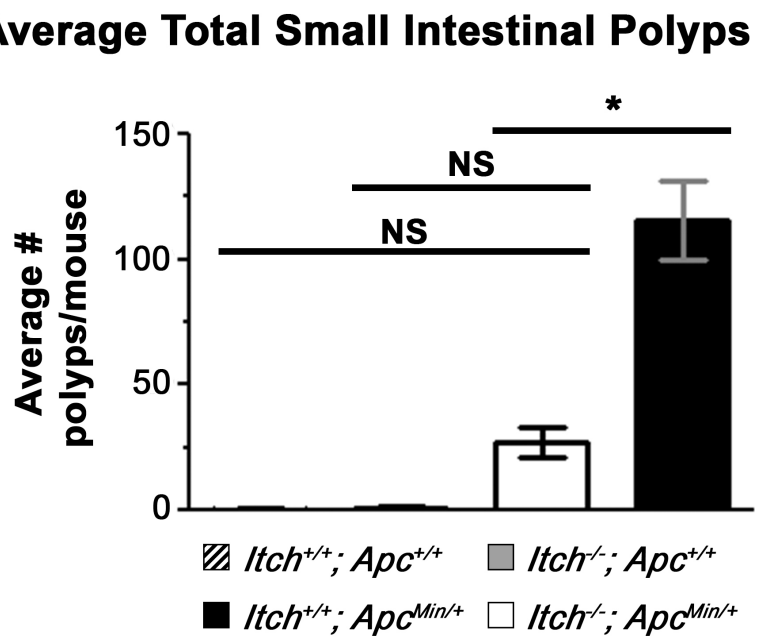

Figure 2.11. Loss of ITCH is protective in *Apc*$^{Min/+}$ tumorigenesis. Polyps from the small intestine of 15 week-old *Itch*$^{+/+}$; *Apc*$^{+/+}$ (n = 11), *Itch*$^{a18H/a18H}$; *Apc*$^{+/+}$ (n = 11), *Itch*$^{+/+}$; *Apc*$^{Min/+}$ (n = 11), and *Itch*$^{a18H/a18H}$; *Apc*$^{Min/+}$ (n = 11) animals were visualized by staining the flushed and fixed small intestine with 0.1% methylene blue. Polyps from the entire length of the intestine were counted under a dissecting scope. The graph shown here depicts the average number of small intestinal polyps per animal. *Itch*$^{a18H/a18H}$; *Apc*$^{Min/+}$ animals were observed to have a significant reduction in tumor burden compared to *Itch*$^{+/+}$; *Apc*$^{Min/+}$ littermates (*p<0.001, NS = not significant). Error bars represent SD.

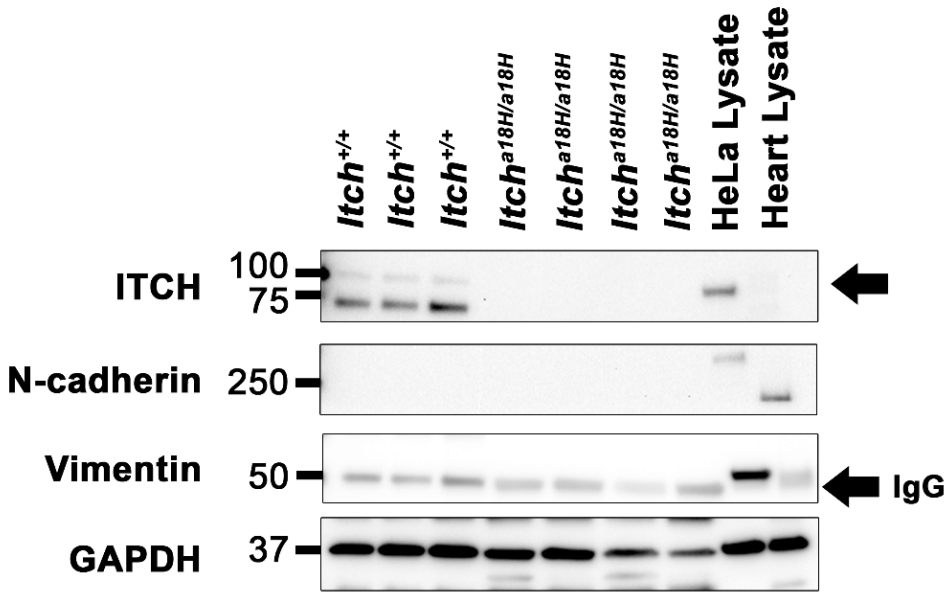

Figure 2.12. Loss of ITCH promotes epithelial migration without leading to an epithelial-to-mesenchymal transition (EMT). 40 µg of protein lysate isolated from the villi of *Itch*$^{+/+}$ (n = 6) and *Itch*$^{a18H/a18H}$ (n = 8) animals separated by SDS-PAGE was transferred to a PVDF membrane prior to immunblotting for ITCH, N-cadherin, Vimentin and GAPDH. Protein lysate from HeLa cells or murine heart was used as a positive control for markers of EMT. As expected, protein derived from ITCH deficient animals expressed no ITCH protein (arrow in top panel) while all samples expressed GAPDH. EMT markers N-cadherin or Vimentin could not be detected in either *Itch*$^{+/+}$ or in *Itch*$^{a18H/a18H}$ villus lysates, indicating that loss of ITCH in the small intestine likely does not promote EMT. Each lane represents one villus isolation from two pooled animals of the same age and genotype.

CHAPTER 3

INTESTINAL MUCOSAL HOMEOSTASIS IS DEPENDENT ON THE TISSUE SPECIFIC FUNCTIONS OF ITCH IN BOTH THE EPITHELIUM AND IMMUNE SYSTEM

3.1 Introduction

With the advent of new extracellular matrices, in combination with the identification of the $Lgr5^+$ intestinal stem cell population, the ability to culture 3-dimensonal (3D) epithelial organoids *ex vivo* without the surrounding stroma recently became an actuality (T. Sato and Clevers, 2013). Through the years, the term “organoid” has evolved from its originally meaning, which was synonymous with oncogenic teratomas, to its current form being defined as the growth of *ex vivo* structures from pluripotent stem cells or tissue-specific adult stem cells that adopt a near native 3-D architecture reminiscent of the tissue architecture *in vivo*. In the presence of growth factors and morphogens specific to the intestinal stem cell niche, single crypts isolated from the small intestine can develop and grow into small intestinal organoids. These 3-D “mini guts” form a highly stereotypical layout wherein a continuous layer of cells is organized into a central, spherical lumen surrounded by a monolayer of differentiated epithelial cells that arise from the highly proliferative budding structures that jut outward from the central lumen (T. Sato and Clevers, 2013). Consistent with the

definition of “organoid”, the intestinal organoids (or enteroids) reconstitute the intestinal epithelial architecture in the absence of the mesenchyme. The base of the budding structure in the organoid houses the $Lgr5^+$ stem cell population and differentiated Paneth cells, similar to the anatomy of the *in vivo* intestinal crypt. As the stem cells divide, the progeny migrate along the bud to give rise to the transit-amplifying population, which continue to migrate eventually differentiating into epithelial post-mitotic cells that will line the central lumen. At the end of the differentiated cell’s lifespan, the apoptotic cell will be sloughed off in to the lumen where it will remain indefinitely (Grabinger et al., 2014), in contrast to what occurs *in vivo*, wherein the continual peristaltic motion and passage of chyme eliminate the extruded epithelial cells. Thus, in the 3-D intestinal organoid system, all apoptotic cells that have been discarded from the inception of the organoid can be quantified, making it a more accurate measure of apoptosis compared to *in vivo*, which relies on capturing a “snap-shot” of a continual process via pro-apoptotic markers as a surrogate for cell death.

The continued growth and expansion of the enteroid is promoted by the enormous self-renewal capacity of the $Lgr5^+$ intestinal stem cell population that resides in the budding structures, thereby providing a proxy to assess the regenerative capacity of the intestinal organoid *ex vivo* (Kretzschmar and Clevers, 2016). Growth of the spherical organoid into a mature mini-gut is initiated by the formation of a bud, which occurs at a location where intestinal stem cells and Paneth cells are both present. The proliferative stem cell population surrounded by the WNT-producing Paneth cells propels itself outward

to initiate a bud, likely mediated by the repulsive forces established from the EphB-EphrinB gradient that is influenced by WNT signaling (Batlle et al., 2002a; T. Sato and Clevers, 2013). *In vivo*, as progenitor cells migrate down the WNT gradient, they differentiate and slowly replace EphBs with EphrinBs, which establishes the crypt-villus boundary and the proper positioning of cells (Fig.3.1). It is thought that similar signaling pathways operate *ex vivo* (T. Sato and Clevers, 2013). Once mature crypts are formed in the enteroid, the continued growth and expansion of crypts is driven by crypt fission, a process that increases crypt number through the bifurcation of a crypt into two daughter crypts (Baker et al., 2014). While this homeostatic process occurs *in vivo* at a fairly low basal rate, the destruction of the crypt by chemical, immunological, or radiological means, exponentially increases crypt fission to promote tissue regeneration (Pin et al., 2015). Postnatally, crypt fission is also increased to expand the existing population of crypts to generate the appropriate number required to preserve intestinal homeostasis in the adult. Though the mechanisms driving this process remain unclear, it has been postulated that the mechanical forces from the underlying mucosa, which establishes a buckle at the base of the crypt to promote crypt division, are influenced by the spatial orientation of both $Lgr5^{+}$ stem cells and Paneth cells in the crypt (Langlands et al., 2016; Pin et al., 2015). Thus, the importance of stem and Paneth cell numbers as well as their spatial distribution appear paramount in driving this process.

Previously, we showed that global loss of the E3 ligase ITCH ($Itch^{a18H/a18H}$) alters intestinal epithelial homeostasis by promoting intestinal epithelial cell

proliferation, secretory cell differentiation, and migration, which could be intrinsic to the epithelium (Chapter 2). However, since ITCH is known to have important functions within the immune system (Aki et al., 2015), in combination with the high level of interplay between the epithelium and the immune system in the small intestine (Vindigni et al., 2016), loss of ITCH in this compartment likely contributes the epithelial defects observed in the *Itch*$^{a18H/a18H}$ animals. Interestingly, the potential dual role of ITCH in both the epithelium and immune system is comparable to the complex role described for NFκB signaling in the small intestine (Wullaert et al., 2011). While activation of this pathway within the immune system promotes intestinal epithelial inflammation and altered intestinal homeostasis, NFκB is required in the epithelium to limit the response of the immune system (M. F. Tao et al., 2009; Wullaert et al., 2011). To this end, we hypothesize that loss of ITCH in the epithelium and immune compartment plays a dual role in promoting intestinal mucosal inflammation that leads to altered intestinal homeostasis.

To identify whether an intrinsic function for ITCH exists in the intestinal epithelium independent of the influence of the immune compartment, small intestinal organoids sufficient and deficient for ITCH were established. Surprisingly, a significant decrease in both the number of nonbudding organoids and in the average number of buds (in those colonies that do bud) was observed in ITCH deficient as compared to ITCH sufficient isolates. Despite the defects in budding observed in organoids lacking ITCH, comparable numbers of intestinal Lgr5^{+} stem cells were present in the organoids sufficient and deficient for ITCH.

Further, proliferation and cell differentiation were not perturbed in ITCH deficient enteroids, in contrast to the *in vivo* phenotype of the *Itch*$^{a18H/a18H}$ small intestines (Chapter 2). However, increased apoptosis was observed in enteroids lacking ITCH, which was also detected in mice lacking ITCH in only the intestinal epithelium, thus identifying an epithelial specific role for ITCH in the intestine. Interestingly, at six months of age, animals with a myeloid-specific loss of ITCH (*Itch*$^{fl/fl}$*; LysM*$^{Cre/Cre}$), displayed alterations in the epithelial architecture similar to those seen in two month old mice constitutively lacking ITCH (Chapter 2). Thus, the delay in the presentation of this phenotype in *Itch*$^{fl/fl}$*; LysM*$^{Cre/Cre}$ animals highlights a potential synergistic role for ITCH in the intestinal epithelium and in the immune system to fine-tune mucosal immune responses and maintain homeostasis.

3.2 Materials and Methods

Animals

Animals homozygous for a null allele of *Itch* (*Itch*$^{a18H/a18H}$) have been previously described (Hustad et al., 1995). For developmental staging, the day a copulatory plug was detected was designated E0.5 while the date of birth was considered P0.

To generate *Itch*$^{a18H/a18H}$ animals in which intestinal stem cells were labeled with eGFP (B6.129P2-*Lgr5*$^{tm1(cre/ERT2)Cle}$/J, stock #008875, hereafter referred to as *Lgr5*$^{eGFP/+}$), *Itch*$^{a18H/a18H}$ mice were bred to *Lgr5*$^{eGFP/+}$ animals to produce *Itch*$^{a18H/+}$; *Lgr5*$^{eGFP/+}$ and *Itch*$^{a18H/+}$; *Lgr5*$^{+/+}$ offspring. Subsequently, *Itch*$^{a18H/+}$; *Lgr5*$^{eGFP/+}$ mice were backcrossed to *Itch*$^{a18H/a18H}$ animals to produce *Itch*$^{a18H/a18H}$*; Lgr5*$^{eGFP/+}$ animals used for analysis. Controls animals (*Itch*$^{+/+}$*;*

Lgr5$^{eGFP/+}$*)* for age-matched male and female *Itch*$^{a18H/a18H}$*; Lgr5*$^{eGFP/+}$ mice were obtained from the original *Lgr5*$^{eGFP/+}$ line used to establish the *Itch*$^{a18H/a18H}$; *Lgr5*$^{eGFP/+}$ colony. To generate mice lacking *Itch* in the myeloid cell lineage, animals heterozygous for a floxed *Itch* allele (Fig.3.2) were bred to *LysM*$^{Cre/Cre}$ animals (JAX stock #004781). A series of intercrosses and backcrosses were performed to generate *Itch*$^{fl/fl}$*; LysM*$^{Cre/Cre}$ animals. Age-matched animals from C57BL/6J or *Itch*$^{fl/fl}$*; LysM*$^{+/+}$ animals were used as experimental controls and are designed as wild-type (WT) in the indicated experiment. A similar breeding scheme using *Villin*$^{Cre/Cre}$ animals was applied to generate animals lacking *Itch* in the intestinal epithelium (*Itch*$^{fl/fl}$*; Villin*$^{Cre/+}$). All experiments were conducted in full compliance with the Institutional Animal Care and Use Committee of the University of South Carolina or the University of Central Florida.

Establishment of Murine Small Intestinal Organoids

Small intestinal organoids were established from 9-11 week old *Itch*$^{+/+}$*; Lgr5*$^{eGFP/+}$ and *Itch*$^{a18H/a18H}$*; Lgr5*$^{eGFP/+}$ animals. To establish a single isolate of intestinal organoids, approximately 10 cm from the most proximal segment of the small intestines from two age-, gender- and genotype-matched animals were placed in a petri dish containing 10 mL of ice-cold Dulbecco's PBS (DPBS, Corning, # 21-031-CV). Before flushing the small intestine with 1 mL of DPBS, the tissue was cut into 2 equal size segments to facilitate the removal of the luminal content. Flushing of the small intestine was performed 3 times before longitudinally opening the small intestine and transferring the tissue to a new

petri dish containing 5 mL of DPBS. To remove any residual waste, the small intestinal segments were gently agitated before cutting them into 2 mm size pieces that were collected in a 50 mL conical tube containing 15 mL of fresh, ice-cold DPBS. To isolate crypts, the small intestinal pieces were placed on ice before pipetting all intestinal pieces up and down in 12 mL of fresh, ice-cold DPBS three times using a 10 mL pipet. Once the tissue settled to the bottom of the tube, the supernatant was carefully removed using a 10 mL pipet. This process was repeated 14 times with fresh, ice-cold DPBS to gently remove debris as well as villi before placing the tissue in 25 mL of Gentle Cell Dissociation Buffer (25°C) (Stem Cell Technologies # 07174) on a rocking platform at 20 rpm for 15 minutes at 25°C. The tissue was placed back on ice to allow the intestinal pieces to settle to the bottom of the tube. At that time, the Gentle Cell Dissociation Buffer was removed and the cells were resuspended in 10 mL of ice-cold DPBS supplemented with 0.1% fetal bovine serum. The intestinal tissue was pipetted up and down three times to dissociate intestinal crypts from the tissue prior to removing and filtering the supernatant through a 70 µm filter, which was labeled as Fraction 1. This process was repeated with three additional 10 mL aliquots of ice-cold DPBS plus 0.1% fetal bovine serum was to generate Fractions 2-4. Once all four fractions were collected, the supernatant was centrifuged at 290 x g for 5 minutes at 4°C. The supernatant was decanted and the pellet was resuspended in 10 mL of ice-cold DPBS supplemented with 0.1% fetal bovine serum. To assess the quality of the crypt isolation, 1 mL from each fraction was placed in an individual well of a 6-well plate and crypt

enrichment was ascertained using bright-field microscopy. The two fractions with the highest crypt-to-cell debris ratio were selected (usually fractions 3 and 4) to carry out the remaining steps. Before centrifuging the 2 selected fractions at 200 x g for 3 minutes at 4°C, the 1 mL used to assess crypt quality was returned to the appropriate fraction. After centrifugation, the supernatant was decanted and the pellets were resuspended in 10 mL of ice-cold Dulbecco's Modification of Eagle's Medium (DMEM)/Ham's F-12 50/50 media (Corning, # 21-031-CV) each. To determine total crypt number, 10 µL of each fraction was placed in a hemacytometer, and the total number of crypts was quantified. A total of 3,000 crypts were transferred to a new tube and supplemented with DMEM/Ham's F-12 50/50 media to produce a final volume of 10 mL. After centrifuging the crypts at 200 x g for 5 minutes at 4°C, the media was gently removed using a pipet and the crypts were resuspended in 150 µL of pre-warmed IntestiCult organoid growth media (Stem Cell Technologies, #06005) followed by 150 µL of matrigel (Corning #356234) that had been thawed on ice. Crypts were plated in 50 µL drops into a pre-warmed 24-well plate and placed in an incubator at 37°C/5% CO_2 for a minimum of 10 minutes to allow the matrigel to solidify before adding 750 µL of pre-warmed organoid growth media to each well. Media was changed every 2-3 days and organoid plugs were passaged every 6-9 days (as described below) to allow for optimal growth conditions. All organoids were passaged at least twice before being used in the indicated experiments to mitigate the contribution of the surrounding stroma on the epithelium. A total of 2 isolates (1 male and 1 female) from *Itch*$^{+/+}$*; Lgr5*$^{eGFP/+}$ and *Itch*$^{a18H/a18H}$*; Lgr5*$^{eGFP/+}$ animals

were used for all intestinal organoid experiments with the exception of the intestinal budding experiments in which 3 isolates (2 male, and 1 female) per genotype were used for quantification.

Passaging of Intestinal Organoids

Organoid growth media from 5-9 day old organoids was removed and 1 mL of ice-cold Gentle Cell Dissociation Buffer was placed in each well to be passaged for 1 minute at room temperature. The matrigel plug was gently pipetted up and down 20 times to disassociate the pellet before placing it in a 15 mL conical tube. Each well was washed with 1 mL of the gentle dissociation buffer and collected in the appropriate 15 mL conical tube. Disassociation of the organoids was accomplished by placing organoids on a rocking platform at 20 rpm for 10 minutes at 25°C before centrifugation at 290 x g for 5 minutes at 4°C. The supernatant was decanted and the organoids were resuspended in 10 mL of DMEM/Ham's F-12 50/50 media prior to centrifuging at 200 x g for 5 minutes at 4°C. The supernatant was gently removed using a pipet, and the organoids were resuspended at a 1:1 ratio in pre-warmed organoid growth media followed by the addition of matrigel that had been thawed on ice using a volume sufficient for the proper split according to density of the culture (*i.e.*, 1:3 to 1:6). Organoids were plated in 50 µL drops into a pre-warmed 24-well plate and placed in an incubator at 37°C/5% CO_2 for a minimum of 10 minutes to allow the matrigel to solidify before adding 750 µL of pre-warmed organoid growth media to each well. Organoids used for the experiments described here were passaged a minimum of 3 times prior to analysis but no more than eight times total.

Quantification of Intestinal Organoid Budding

Three isolates for age- and gender-matched *Itch*$^{+/+}$; *Lgr5*$^{eGFP/+}$ (n = 3, 2 male-derived and 1 female-derived isolates) and *Itch*$^{a18H/a18H}$; *Lgr5*$^{eGFP/+}$ (n = 3, 2 male-derived and 1 female-derived isolates) were seeded in triplicate, and numbers of nonbudding versus budding organoids were quantified from a minimum of eight 10x phase contrast images acquired on a Leica DMI6000B microscope equipped with a Hamamatsu ORCA-R^2 CCD camera. To assess significance, a chi-squared analysis of a 2x2 contingency table was performed and plotted using Prism software (GraphPad Software, Inc).

Intestinal Organoid Growth Characterization

Two independent age- and gender-matched isolates from each genotype (consisting of 1 male-derived and 1 female-derived isolate) were seeded in duplicate on a 4-chambered slide, and growth was monitored by phase-contrast microscopy. Specifically, images were acquired one, three and five days following plating for all 8 matrigel plugs. Day 1 images were acquired using a 40x objective while day 3 and day 5 images were acquired using a 20x objective on a Leica DMI6000B microscope equipped with a Hamamatsu ORCA-R^2 CCD camera.

Sample Prep Fluorescent Confocal Microscopy

To obtain frozen sections, organoid growth media from five to six day intestinal organoids was removed and replaced with 1 mL of ice-cold DPBS for 1 minute before gently disassociating the plug mechanically by pipetting up and down. Organoids were placed in a 1.5 mL microfuge tube and centrifuged at 100

x g for 1 minute at 4°C to pellet organoids. The intestinal organoids were resuspended in 4% PFA and fixed for 20 minutes at 25°C. To remove PFA, organoids were centrifuged at 100 x g for 1 minute at 4°C and resuspended in 1 mL of PBS. Organoids were centrifuged as above a total of three times. To facilitate visualization of the organoids, the organoids were incubated with 250 µL Alcian Blue, pH 2.5 for a minimum of 5 minutes, but not longer than 20 minutes, centrifuged (100 x g for 1 minute at 4°C), and resuspended in 1 mL PBS. Organoids were washed as previously described a total of three times before cryoprotecting the organoids by incubating them sequentially in a 15% and 30% sucrose/PBS solution at 4°C in each solution for a day. The organoids were washed once in PBS before embedding the samples in Optimal Cutting Temperature (OCT) compound and freezing in an 100% ethanol:dry ice bath. To embed organoids in OCT compound, the enteroids were resuspended in approximately 30 µL of PBS and transferred to the center of a mold before forming a circular well surrounding the organoids with OCT compound. The remaining mold was filled with OCT compound to the desired level. 40 µm thick frozen sections were brought to 25°C before being post-fixed in 4% PFA for 10 minutes. The PFA was removed and the samples were allowed to air dry for 10 minutes at 25°C before 3 sequential washes in PBS for 3 minutes each. The samples were blocked for 1 hour in a solution containing 10% normal goat serum, 2% bovine serum albumin, and 0.2% Triton X-100 in PBS. The primary antibodies Chromogranin A (C-12, Santa Cruz, 1:200) and Lysozyme (RP028, Diagnostic BioSystems, 1:100) were diluted in PBS containing 1% normal goat

serum and 0.1% Triton X-100 and incubated on sections in a humidified chamber overnight at 4°C. Before incubation with the appropriate secondary antibody, the samples were washed 3 times in PBS for 3 minutes each wash. AlexaFluor659-conjugated goat anti-mouse secondary (Jackson ImmunoResearch, 1:500) or Cy3-conjugation goat anti-rabbit secondary (1:200) was applied for an hour before mounting sections in ProLong Gold Antifade Mountant with DAPI (P36931, Molecular Probes). To identify goblet cells, 40 µm frozen sections that were post-fixed in 4% PFA for 10 minutes were mounted in ProLong Gold Antifade Mountant (P36930, Molecular Probes) and DIC images were acquired to identify goblet cells by morphology. DIC coupled fluorescent images and DIC images were acquired on a Leica SP8X confocal microscope equipped with HyD detectors and conventional photomultiplier tubes (PMTs).

Visualization of endogenous eGFP-marked $Lgr5^{+}$ stem cells was carried out using whole mount intestinal organoids fixed in 4% PFA for 20 minutes at 25°C after isolation of intestinal organoids from the matrigel as above. Samples were incubated in block containing 10% normal goat serum, 2% bovine serum albumin, and 0.2% Triton X-100 in PBS for 1 hour before mounting whole organoids in ProLong Gold Antifade Mountant with DAPI (P36931, Molecular Probes). 40x fluorescent images were acquired on a Leica SP8X confocal microscope equipped with HyD detectors and conventional PMTs.

EdU Incorporation in Intestinal Organoids

Two independent intestinal organoid isolates (1 male and 1 female) for both $Itch^{+/+}; Lgr5^{eGFP/+}$ and $Itch^{a18H/a18H}; Lgr5^{eGFP/+}$ genotypes were seeded in

triplicate in a 4-chamber slide, and, six days later, 10 μM EdU was applied to each plug for 1 hour at 37°C. Upon removal of EdU supplemented media, the organoids were washed in DPBS at 25°C for 3 minutes, which was repeated an additional 2 times. The organoids were fixed in 4% PFA for 20 minutes at 25°C and washed in DPBS at 25°C, three times for three minutes each wash. Samples were blocked for 1 hour at 25°C before applying the Click-IT reaction cocktail contained in Click-IT AlexuFluor Kit (ThermoFisher Scientific, C10337) supplemented with an AlexaFluor 594 Azide anitbody (ThermoFisher Scientific, A10270). The Click-IT reaction cocktail was applied to the organoids for 30 minutes at 25°C in the dark. The samples were washed twice for two minutes each wash in PBS before applying DAPI (Invitrogen, C10457, 1:2000) diluted in PBS for 10 minutes at 25°C. Prior to mounting (50% glycerol/50% PBS medium) the organoids contained within the 4-chambered slides, the organoids were washed once in PBS for 5 minutes. Fluorescent images were acquired on a Leica SP8X confocal microscope equipped with HyD detectors and conventional photomultiplier tubes (PMTs).

Propridum Iodide (PI) Staining

Two isolates of age- and gender- matched *Itch*$^{+/+}$*; Lgr5*$^{eGFP/+}$ (1 male and 1 female isolate) and *Itch*$^{a18H/a18H}$*; Lgr5*$^{eGFP/+}$ (1 male and 1 female isolate) intestinal organoids were seeded in duplicate in a 4-chamber slide, and, four days later, intestinal oragnoids were incubated with 100 μg/mL propridium iodide (PI) (Sigma, stock #81845) for 30 minutes at 37°C/5%CO_2. Organoids were washed three times with pre-warmed DPBS before placing 750 μL of pre-warmed

DMEM/Ham's F-12 50/50 media on the matrigel plugs. Phase contrast-coupled fluorescent images were acquired on a Leica DMI6000B epifluorescence microscope equipped with a Hamamatsu ORCA-R^2 CCD camera. Quantification of fluorescent and organoid surface area was measured using ImageJ software from eight 10x images from each matrigel plug. A total of 94 and 84 organoids were counted for ITCH sufficient and deficient organoids, respectively. An unpaired, two-tailed student t-test was used to assess significance.

Immunohistochemistry

Paraffin sections (4-6 μm) from the distal small intestine of *Itch*$^{fl/fl}$; *Villin*$^{Cre/+}$ and WT controls were subjected to IHC. In particular, antigen unmasking was performed using 10 mM Tris-HCl/ 1 mM EDTA, pH=9 for 30 minutes at 95°C. Subsequently, slides were cooled for 1 hour at 25°C in the antigen unmasking solution before being washed three times in PBS for three minutes each. Sections were blocked in a solution containing 10% normal goat serum, 2% bovine serum albumin, and 0.2% Triton X-100 in PBS. An additional hydrogen peroxidase block (50% hydrogen peroxide of a 3% solution) / 50% methanol) was performed for 20 minutes at 25°C. The primary antibody cleaved-caspase 3 (Cell Signaling Technology #9664, 1:100) was diluted in PBS containing 1% normal goat serum and 0.1% Triton X-100 and incubated on sections in a humidified chamber overnight at 4°C. The antibody was visualized using the EnVision+ system-HRP (Dako # K4006) with the following modifications: the samples were incubated with the HRP-conjugated anti-rabbit secondary for 1 hour before being washed three times three minutes.

Localization of antibody staining was visualized by incubating the samples for five minutes in 37.5 μM DAB chromagen diluted in 1 mL of DAB substrate. Brightfield images were acquired on a Zeiss Axio Imager A1 equipped with an AxioCam MRc5 camera.

Histology

Decapitated embryos were fixed whole in 4% paraformaldehyde/2% glutaraldehyde. Postnatal day 7 (P7) and adult small intestines were flushed with PBS after being cut into three equally sized segments (designated proximal, middle and distal), opened longitudinally, and fixed overnight with either 4% paraformaldehyde or with 10% neutral buffered formalin. Whole embryos or Swiss-rolled intestinal tissues were paraffin-embedded and sectioned at 5μm. Hematoxylin and eosin staining was performed to assess tissue morphology.

3.3 Results

Intestinal organoids lacking ITCH have more viable, nonbudding organoid structures and less intricate growth patterns

To investigate the epithelial-specific contribution of ITCH in the small intestine, 3-D enteroid cultures were established *ex vivo* from the intestinal crypts of 9-11 week old $Itch^{+/+}; Lgr5^{eGFP/+}$ and $Itch^{a18H/a18H}; Lgr5^{eGFP/+}$ animals. After passaging these cultures a minimum of three times to mitigate the signaling contributions of the mesenchyme, the 3-D structures of the enteroid cultures were assessed using phase contrast microscopy. This analysis revealed that ITCH deficient organoids, though viable, were not as intricate, and there seemed to be a greater number of nonbudding enteroids present in the $Itch^{a18H/a18H};$

Lgr5$^{eGFP/+}$ culture as compared to the *Itch*$^{+/+}$*; Lgr5*$^{eGFP/+}$ culture (Fig.3.3.A). To determine if this shift toward a nonbudding phenotype was statistically significant, the number of nonbudding organoids versus budding organoids was quantified from three independent isolates (independent culture preps) from each genotype. Out of a total of 184 ITCH sufficient and 199 ITCH deficient enteroids assessed, 13 ITCH sufficient organoids versus *29* ITCH deficient organoids lacked buds (Fig. 3.3.B). This difference was determined to be statistically significant using a chi-squared analysis with a 2x2 contingency table wherein the null hypothesis stated that no difference in the number of nonbudding versus budding organoids existed between the ITCH sufficient and ITCH deficient organoids (chi-square = 5.519, df = 1, and p = 0.0188).

Even though lack of ITCH compromised the initiation of crypt regeneration in enteroid culture, there were a considerable number of colonies lacking ITCH that did develop buds. Since it is thought that the continued growth and expansion of crypts/buds is driven by crypt fission in organoids (Baker et al., 2014), we sought to determine whether ITCH had any impact on this process. To that end, we reanalyzed the budding data after removing the counts for nonbudding colonies for each genotype. This revealed that while *Itch*$^{+/+}$*; Lgr5*$^{eGFP/+}$-derived budding enteroids (n=167) displayed a median of 7 buds with an interquartile range (IQR) of 6, budding enteroids derived from *Itch*$^{a18H/a18H}$*; Lgr5*$^{eGFP/+}$ animals (n=160) had a median of 6 buds with an IQR of 5 (n=160), and this difference was statistically significant ($p < 0.05$) by Mann-Whitney U-test (Fig. 3.3.C). This result suggested that ITCH may influence crypt fission to

promote branching of buds in organoid culture. Thus, it would be predicted that organoids lacking ITCH should have less intricate, branching structures. To test this hypothesis, organoid growth and morphology were qualitatively assessed in ITCH deficient and ITCH sufficient enteroids (n=2 independent isolates per genotype) using phase contrast microscopy at day 1, day 3, and day 5 after plating (Fig. 3.4). The general trend that was noted was that at day 1 no budding was observed in cultures of either genotype, whereas at day 3 and day 5, buds were present and continuing to increase in number in both ITCH sufficient and deficient organoids. However, when comparing the morphology of the organoids at day 5, the ITCH deficient cultures appeared more compact and less intricate with regards to branching as compared to the ITCH sufficient cultures (Fig 3.4.). Collectively, these data emphasize that while loss of ITCH does not impact the growth kinetics of the organoids, it does influence the intricacy of the budding structures of the organoids.

Lack of ITCH does not grossly alter epithelial cell differentiation in enteroid culture

The subtleties in growth dynamics of those organoid cultures deficient for ITCH relative to those sufficient for ITCH prompted us to examine the $Lgr5^{+}$ CBC stem cell population, which is known to promote the expansion of budding structures within enteroids (Sato et al., 2009). Because, in our enteroid system, Lgr5-expressing intestinal stem cells are endogenously labeled with eGFP, green fluorescence can be utilized as a proxy to assess intestinal stem cell dynamics. However, only 17% of CBC stem cells are expected to be labeled because of the

mosaic nature of this construct (Dehmer et al., 2011). This, coupled with the loss of organoids during processing, resulted in the examination of only 3 GFP^+ organoids from two independent isolates of each genotype. If these particular samples are viewed as representative of budding organoids at day 6, no difference in location of the eGFP signal, eGFP intensity, or number of $eGFP^+$ cells was readily discernable within the budding structures of ITCH sufficient and ITCH deficient organoids (Fig. 3.5.A), though this certainly warrants further investigation.

Even though a robust cell intrinsic role for ITCH does not seem apparent in intestinal stem cells, global loss of ITCH in the small intestine does impact both intestinal epithelial progenitors as well as cell differentiation (Chapter 2). Thus, we hypothesized that epithelial-specific loss of ITCH would result in similar defects observed in the *Itch*$^{a18H/a18H}$ animals, skewing cell specification toward the goblet and Paneth cell lineages. To investigate this hypothesis, confocal fluorescence images coupled with phase-contrast microscopy were captured from day 6, *Itch*$^{+/+}$*; Lgr5*$^{eGFP/+}$ and *Itch*$^{a18H/a18H}$*; Lgr5*$^{eGFP/+}$ intestinal organoids immunostained for chromagranin A and lysozyme to identify enteroenocrine cells and Paneth cells, respectively. Surprisingly, no gross difference in number of Paneth or enteroendocrine cells was detected in *Itch* deficient organoids compared to *Itch* sufficient organoids (Fig. 3.5.B). To assess goblet cell differentiation, the distinctive cell shape of goblet cells was identified using phase-contrast microscopy revealing no marked defects in goblet cell differentiation between the two genotypes (Fig. 3.5.B). Collectively, these data

demonstrate that loss of ITCH in organoid culture does not recapitulate the observed phenotype associated with global loss of ITCH in the *Itch*$^{a18H/a18H}$ animal, suggesting that the role of ITCH in epithelial cell specification is cell non-autonomous and is likely influenced by ITCH deficient signals from other tissue types (most likely the immune system) in the small intestine *in vivo*.

Itch$^{a18H/a18H}$*; Lgr5*$^{eGFP/+}$ intestinal organoids have increased apoptosis

Despite not observing a change in intestinal homeostasis with regards to intestinal stem cell dynamics and cell fate specification within the ITCH deficient organoids, it is possible that ITCH may influence the integrity of the intestinal mucosal by regulating the turnover of the epithelium in the small intestine. Within the *Itch*$^{a18H/a18H}$ small intestine, an increase in the proliferating progenitor population within the crypt leads to an acceleration of intestinal epithelial migration along the crypt-villus axis, thus, making it tempting to speculate that *Itch*$^{a18H/a18H}$*; Lgr5*$^{eGFP/+}$ intestinal organoids might display an increase in proliferation compared to *Itch*$^{+/+}$*; Lgr5*$^{eGFP/+}$ intestinal organoids. To investigate this possibility, we assessed EdU incorporation from three replicates of whole mount intestinal organoids that were derived from 2 independent isolates of sufficient and deficient for ITCH. Organoids plated for six days were pulsed with 10 μM EdU for 1 hour before evaluating EdU incorporation by click chemistry. Upon the acquisition of fluorescent images captured by confocal microscopy, no difference in proliferation was observed between the two genotypes (Fig. 3.6.A).

While the continued replacement of differentiated cells is an important component of intestinal cell turnover, proliferation must be balanced with the

extrusion of cells via the apoptotic process of anoikis in order to maintain intestinal epithelial function (J. M. Williams et al., 2015). Since an increase in cleaved-caspase 3 staining was observed in the small intestine of young adult *Itch*$^{a18H/a18H}$ animals (Chapter 2), we hypothesized that lack of ITCH in just the intestinal epithelium would result in an increase in apoptosis. Therefore, ITCH sufficient and ITCH deficient intestinal organoids were incubated with PI for 30 minutes and then evaluated by epifluorescence microscopy. Micrographs were taken from a minimum of eight 20x fields and the ratio of the surface area of the PI fluorescence to the total organoid surface area was measured from two age- and gender- matched isolates from each genotype using Image J. Consistent with what was observed in whole animal studies, a significant increase ($p<0.05$) in percent surface area of PI staining was observed in the *Itch*$^{a18H/a18H}$*; Lgr5*$^{eGFP/+}$ intestinal organoids (30.9% ± 3.53%, SEM) compared to *Itch*$^{+/+}$*; Lgr5*^{eGFP} intestinal organoids (20.9% ± 2.42%, SEM) (Fig. 3.6.B). This suggests a cell autonomous role for ITCH in intestinal epithelial apoptosis.

To corroborate the results obtained from the intestinal organoid assay, apoptosis was also assessed *in vivo* using animals deficient for ITCH within the intestinal epithelium (*Itch*$^{fl/fl}$*; Villin*$^{Cre/+}$). For this analysis, cellular apoptosis was assessed by immunohistochemistry via the pro-apoptotic marker cleaved-caspase 3. Cleaved-caspase 3 staining was assessed from paraffin-embedded tissues that were derived from the distal small intestines of one *Itch*$^{fl/fl}$*; Villin*$^{Cre/+}$and WT animal at 3 months of age. Consistent with the *ex vivo* results, *Itch*$^{fl/fl}$*; Villin*$^{Cre/+}$ animals had an increase in cleaved-caspase 3 staining, which

was most prevalent on the villi, compared to WT animals where a minimal amount of apoptosis was observed (Fig. 3.7). Since global loss of ITCH results in altered differentiation programs on the villi (Chapter 2), images were acquired at a higher power magnification (63x) to determine if apoptosis in the small intestines from *Itch*$^{fl/fl}$*; Villin*$^{Cre/+}$ animals was specific to enterocytes. Interestingly, cleaved caspase 3 staining was observed in both enterocytes and goblet cells present on the villi (Fig. 3.7), emphasizing that ITCH's role in apoptosis is not cell type specific, but seems to act in differentiated cells of both the absorptive and secretory lineages.

Myeloid-derived cells lacking ITCH influence epithelial cell specification within the small intestine in a time dependent manner

Contrary to the described role for ITCH we observed in intestinal epithelial homeostasis *in vivo*, no difference in cell proliferation (Fig. 3.6.A) or specification (Fig. 3.5.B) was observed between ITCH sufficient and deficient organoids. Further support for this phenotype is evidenced from histological evaluation of *Itch*$^{fl/fl}$*; Villin*$^{Cre/+}$ and WT small intestines. In particular, no marked deviation in cell type specification (*i.e*., comparable numbers of goblet and Paneth cells), as well as crypt and villus size were present in *Itch*$^{fl/fl}$*; Villin*$^{Cre/+}$ intestines when compared to the WT controls histologically at 2 months of age (Fig. 3.7). Thus, the global loss of ITCH function phenotype likely results from the combined actions of cell types outside of just the epithelium. The most likely suspect for non-cell autonomous function of ITCH influencing epithelial homeostasis would be the immune system due to its immunosurveillance function within the small

intestine. Recently, ITCH was determined to attenuate NOD2:RIP2 induced NFκB signaling in primary macrophages derived from *Itch*$^{a18H/a18H}$ animals (M. F. Tao et al., 2009). Thus, in combination with the presence of neutrophils (Ramon et al., 2011) and eosinophils (Ramon et al., 2011) within the lamina propria of the small intestine in 5-6 month old *Itch*$^{a18H/a18H}$ animals, we hypothesized that loss of ITCH within the myeloid cell lineage could contribute to the altered epithelial homeostasis in the small intestine.

To analyze the contribution of ITCH in the innate immune system, animals lacking ITCH within the myeloid cell lineage (*Itch*$^{fl/fl}$*; LysM*$^{Cre/Cre}$) , *Itch*$^{a18H/a18H}$ and WT animals were compared at 2 and 6 months of age. Formalin-fixed, paraffin-embedded sections dervived from all three genotypes were stained with H&E to assess tissue morphology (Fig. 3.8). At two months of age, the *Itch*$^{fl/fl}$*; LysM*$^{Cre/Cre}$-derived small intestines looked comparable to the small intestines of the WT controls. However, this was in stark contrast to the small intestines from *Itch*$^{a18H/a18H}$ animals, which displayed signs of crypt hyperplasia that was accompanied by an increase in goblet and Paneth cells. Interestingly, the intestine from 6-month-old *Itch*$^{fl/fl}$*; LysM*$^{Cre/Cre}$ animals more closely resembled the intestines of the *Itch*$^{a18H/a18H}$ at 2 months of age in that crypt area was increased, as well as goblet and Paneth cell numbers. Furthermore, the *Itch*$^{a18H/a18H}$ intestines from 6-month-old animals appeared progressively worse with regards to goblet cell differentiation. Collectively, these data highlight the fact that loss of ITCH in the small intestine, whether ubiquitous or myeloid-specific, drives a progressive shift in epithelial homeostasis.

3.4 Discussion

Here, we have delineated epithelial- and myeloid-specific roles for ITCH that collectively contribute to the preservation of adult intestinal epithelial homeostasis and mucosal function by regulating crypt formation, cellular differentiation, and apoptosis. When mature intestinal organoids sufficient and deficient for ITCH were established, loss of ITCH had no impact on temporal cell growth (Fig. 3.4), proliferation (Fig. 3.6.A), or cell fate specification (Fig. 3.5.B). However, an increase in apoptosis was observed in ITCH deficient organoids compared to ITCH sufficient organoids (Fig. 3.6.B), which was further substantiated by an increase in cleaved-caspase 3 staining within the small intestine of *Itch*$^{fl/fl}$ *; Villin*$^{Cre/+}$ animals (Fig. 3.7). Among ITCH's numerous substrates, c-FLIP, the p53 family members, p63 and p73, LATS1, and TXNIP, have been implicated in cell apoptosis (Aki et al., 2015). With the exception of the anti-apoptotic protein c-FLIP, loss of ITCH stabilizes these protein substrates to promote apoptosis. Thus, we anticipate that *Itch*$^{a18H/a18H}$ and *Itch*$^{fl/fl}$*; Villin*$^{Cre/+}$ would have increased expression in one or more of these pro-apoptotic targets. With the limited expression of p73 in the small intestine, and complete absence of p63, the likelihood of this family that one of these proteins is driving the observed apoptosis in the small intestine. In contrast, the tumor suppressor, LATS1 (Ho et al., 2011), and the cellular redox inhibitor, TXNIP (Zhang et al., 2010) are both expressed in the small intestine, offering a potentially mechanism by which cell demise could be mediated in both ITCH deficient organoids as well as *Itch*$^{fl/fl}$*; LysM*$^{Cre/Cre}$ animals.

In the highly proliferative small intestine, the Lgr5^{+} CBC stem cell population is a critical driver of self-renewal. There is mounting evidence to support a cell-autonomous contribution for ITCH in the cellular dynamics of embryonic (ESC) and hematopoietic (HSC) stem cells. Specifically, ITCH has been shown to downregulate the transcription factor OCT4 in ESCs, compromising ESC renewal capacity as well as somatic cell reprogramming (Liao et al., 2013). Furthermore, ITCH deficient HSCs were shown to have a hyperproliferative phenotype, which was attributed to accelerated cell cycle entry, as compared to ITCH sufficient HSCs (Rathinam et al., 2011). When intestinal organoids deficient for ITCH were cultured, a significant decrease in the average number of buds per organoid was observed in *Itch*$^{a18H/a18H}$*; Lgr5*$^{eGFP/+}$ organoids versus *Itch*$^{+/+}$ *; Lgr5*$^{eGFP/+}$ organoids (Fig. 3.3.A), suggesting that a cell-autonomous role for ITCH in the epithelium likely influences the stem cell niche. Though a decrease in the average number of buds in mature ITCH deficient organoids was noted, a reduction in eGFP-labeled Lgr5^{+} intestinal stem cells was not readily apparent, indicating that a depletion of the rapidly cycling stem cell population is not necessarily the driving factor of this phenotype. However, due to the mosaic nature of this construct (Dehmer et al., 2011) and the limited number of samples assessed, a decrease in Lgr5^{+} stem cells within ITCH deficient organoids still remains a formal possibility. Due to the similarities in EdU incorporation between the ITCH sufficient and ITCH deficient organoid cultures, it seems unlikely that a decrease in proliferation underlies the observed decrease in average budding number associated with ITCH deficiency.

Alternatively, p53-independent spontaneous apoptosis of epithelial cells within the crypts of the small intestine has been suggested to influence homeostatic stem cell dynamics (Renehan et al., 2001), and provides a potential mechanistic link between increased epithelial cell apoptosis associated with loss of ITCH and the defects observed in crypt fission within mature, budding ITCH deficient organoids.

While loss of ITCH alters crypt fission in mature, budding intestinal organoids, an additional role for ITCH upstream of this process is suggested by the significant expansion of the nonbudding population in the *Itch*$^{a18H/a18H}$*; Lgr5*$^{eGFP/+}$ organoid cultures as compared to *Itch*$^{+/+}$*; Lgr5*$^{eGFP/+}$ organoid cultures (Fig 3.3.B). Interestingly, the nonbudding *Itch*$^{a18H/a18H}$*; Lgr5*$^{eGFP/+}$ organoids did not adopt a hyperproliferative, cyst-like phenotype that typically appears either with organoids disrupted for APC (Germann et al., 2014) or those with constitutive β-catenin signaling (T. Sato and Clevers, 2013), minimizing the possibility that an expansion in stem and/or progenitor cell populations, at the expense of differentiation, is the impetus behind this phenotype. A failure to bud in the ITCH deficient organoids could result from improperly integrating signals necessary for the initiation budding. Normally the Lgr5^{+} stem cell population and the surrounding WNT-producing Paneth cells propel themselves outward, likely mediated by the repulsive force established from the EphB-EphrinB gradient along the budding structure (Toshiro Sato and Clevers, 2013), similar to what has been described *in vivo* (Batlle et al., 2002b). Establishment of the EphB-EphrinB gradient is dependent on β-catenin and TCF, a transcription factor that mediates

canonical WNT signaling (Fig. 3.1) (Batlle et al., 2002b). In the small intestine of *Itch*$^{a18H/a18H}$ animals, we observed a decrease in β-catenin levels within the crypt of the small intestine (Fig.3.9). Thus, we speculate that a decrease in β-catenin within the budding structure of the organoid could disrupt the gradients of WNT and EphB-EphrinB to compromise bud initiation. While defects in bud initiation and budding numbers are observed *ex vivo* in *Itch*$^{a18H/a18H}$*; Lgr5*$^{eGFP/+}$ organoids, accelerated crypt formation is observed in *Itch*$^{a18H/a18H}$ intestines at E18.5 and P7 (Fig. 3.10), suggesting loss of ITCH function in additional cell types could influence crypt development. Thus, identifying the molecular signatures associated with loss of ITCH within the crypts of *Itch*$^{a18H/a18H}$ animals and budding defects in ITCH deficient organoids will provide insight into the contribution of ITCH to mucosal homeostasis.

The failure of ITCH deficient intestinal organoids and *Itch*$^{fl/fl}$ *; Villin*$^{Cre/+}$ animals to completely recapitulate the altered intestinal epithelial phenotype in *Itch*$^{a18H/a18H}$ animals emphasizes the contribution of ITCH within the immune compartment of mucosa. Support for this crosstalk between the immune system and epithelium is derived from the comparable intestinal phenotype between 6-month-old *Itch*$^{fl/fl}$*; LysM*$^{Cre/Cre}$ and *Itch*$^{a18H/a18H}$ animals at 2 months of age (Figure 3.8). Within the innate immune system, ITCH influences the proinflammatory response of macrophages by regulating NOD2-dependent NFκB (M. F. Tao et al., 2009). We anticipate that the macrophage population within the lamina propria drives alterations in intestinal epithelial homeostasis within the small intestine of *Itch*$^{fl/fl}$*; LysM*$^{Cre/Cre}$ animals. Interestingly, tissue-resident intestinal

macrophages are highly tolerogenic of the external environment and are capable of employing a variety of mechanisms that effectively clear pathogens while tempering the immunological response (Bain and Mowat, 2014). Thus, it is tempting to speculate that ITCH deficient macrophages within the small intestine generate an inappropriate immunological response to the local environment, which likely promotes intestinal inflammation and altered epithelial homeostasis.

While a novel myeloid-specific role for ITCH in intestinal epithelial homeostasis is highlighted by an expansion in crypt area, and goblet and Paneth cell hyperplasia, a delay in the presentation of the phenotype in *Itch*$^{fl/fl}$*; LysM*$^{Cre/Cre}$ compared to *Itch*$^{a18H/a18H}$ animals emphasizes the multifaceted role ITCH plays in the integration of intestinal mucosal functionality and integrity. Thus, it is tempting to speculate that an increase in apoptosis associated with loss of ITCH in the epithelium could contribute to the inflammatory response by allowing bacteria to more easily interact with the immune compartment. Since apoptosis of intact intestinal epithelium alone does not increase intestinal inflammation (Hausmann, 2010), the altered inflammatory response in ITCH deficient immune cells, both within the myeloid and lymphoid compartments, is likely required to drive the altered intestinal epithelial phenotype. However, a formal possibility remains wherein additional tissue types, such as surrounding mesenchyme, could influence intestinal homeostasis. Thus, the continued examination of the tissue-specific functions for ITCH as well as the synergistic roles of ITCH within the epithelium and the immune system in the intestinal mucosa is vital to

identifying novel therapeutic avenues to explore in the treatment of mucosal enteropathies.

3.5 Figures

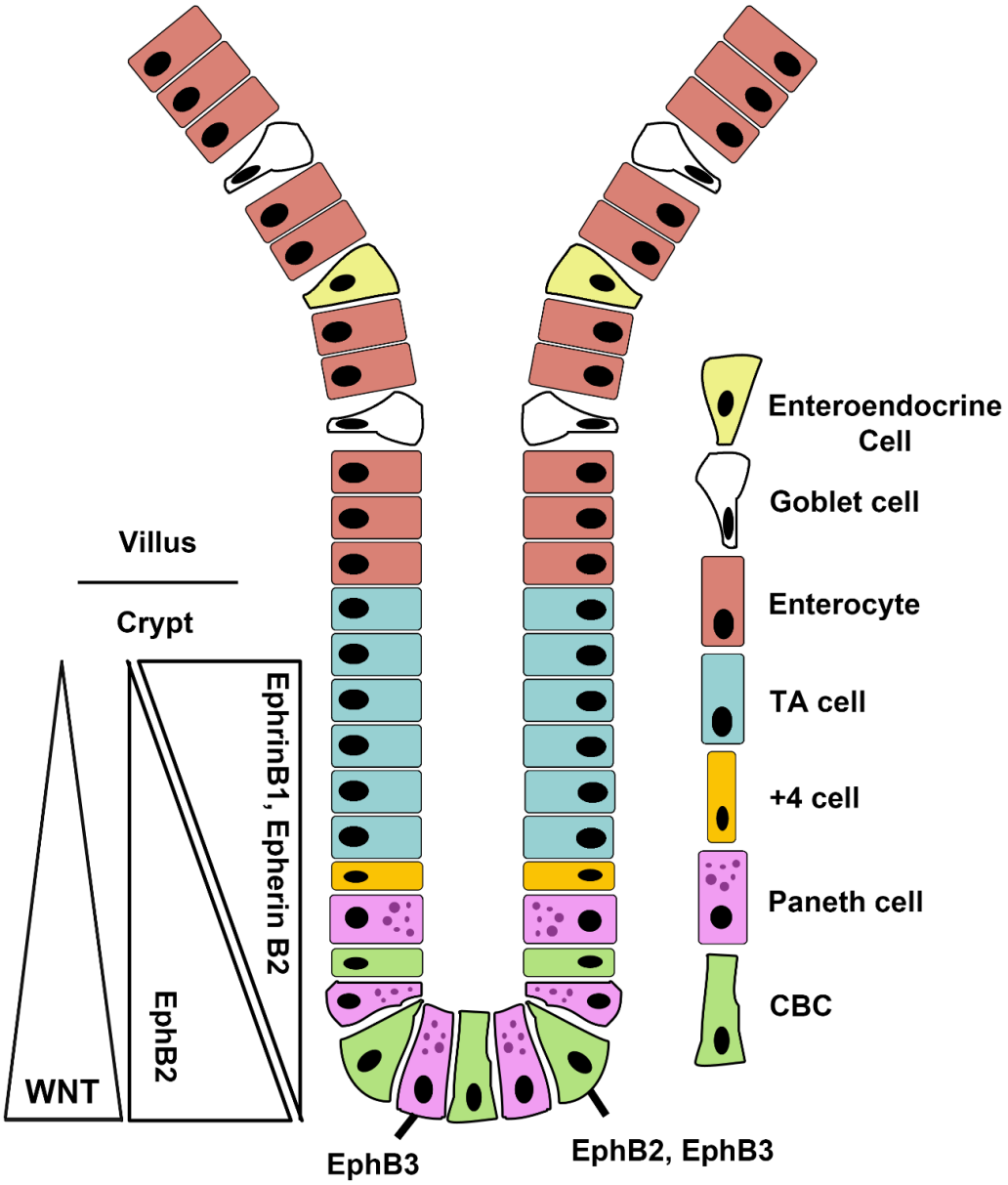

Figure 3.1. EphrinB-EphB gradients within the crypt of the small intestine. Interactions between EpherinB ligands and EphB receptors influence cellualer spatial localization and migration within the crypt. Both WNT and EphrinB ligands within the intestinal epithelium establishes the location and migration of epithelial cells along the crypt-villus axis. The absence of EphrinB ligands in the crypt, despite the presence of the EphB recpetors, anchors both CBC stem cells and Paneth cells to the base of the crypt. Adapted from (Scoville et al., 2008).

A.

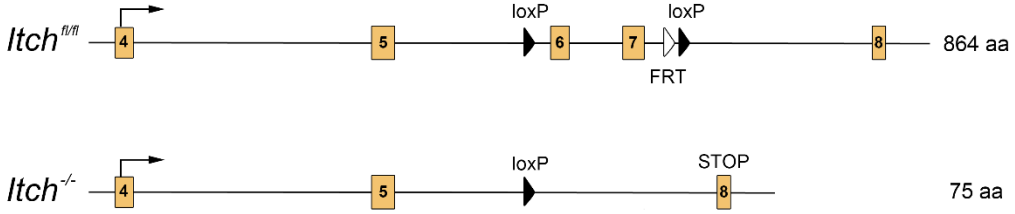

B.

Parental Cross

$Itch^{fl/+}$ X $LysM^{Cre/Cre}$

1st Generation Intercross

$Itch^{fl/+}; LysM^{Cre/+}$ X $Itch^{fl/+}; LysM^{Cre/+}$

2nd Generation Backcross to F1

$Itch^{fl/fl}; LysM^{Cre/+}$ X $Itch^{fl/+}; LysM^{Cre/+}$

3rd Generation Backcross to F2

$Itch^{fl/fl}; LysM^{+/+}$ X $Itch^{+/+}; LysM^{Cre/Cre}$

4th Generation Intercross

$Itch^{fl/+}; LysM^{Cre/+}$ X $Itch^{fl/+}; LysM^{Cre/+}$

5th Generation Intercross

$Itch^{fl/fl}; LysM^{Cre/Cre}$ X $Itch^{fl/fl}; LysM^{Cre/Cre}$

Figure 3.2. Generation of $Itch^{fl/fl}; LysM^{Cre/Cre}$ animals. (**A**) $Itch^{fl/fl}$ aniamls were generated by placing flanked LoxP cite into intron 5 and intron 7 of the *Itch* locus. (**B**) Breeding scheme employed to generate $Itch^{fl/fl}; LysM^{Cre/Cre}$ animals. Due to diffucultes with genotyping, a non-trandiitonal breeding scheme was utilized.

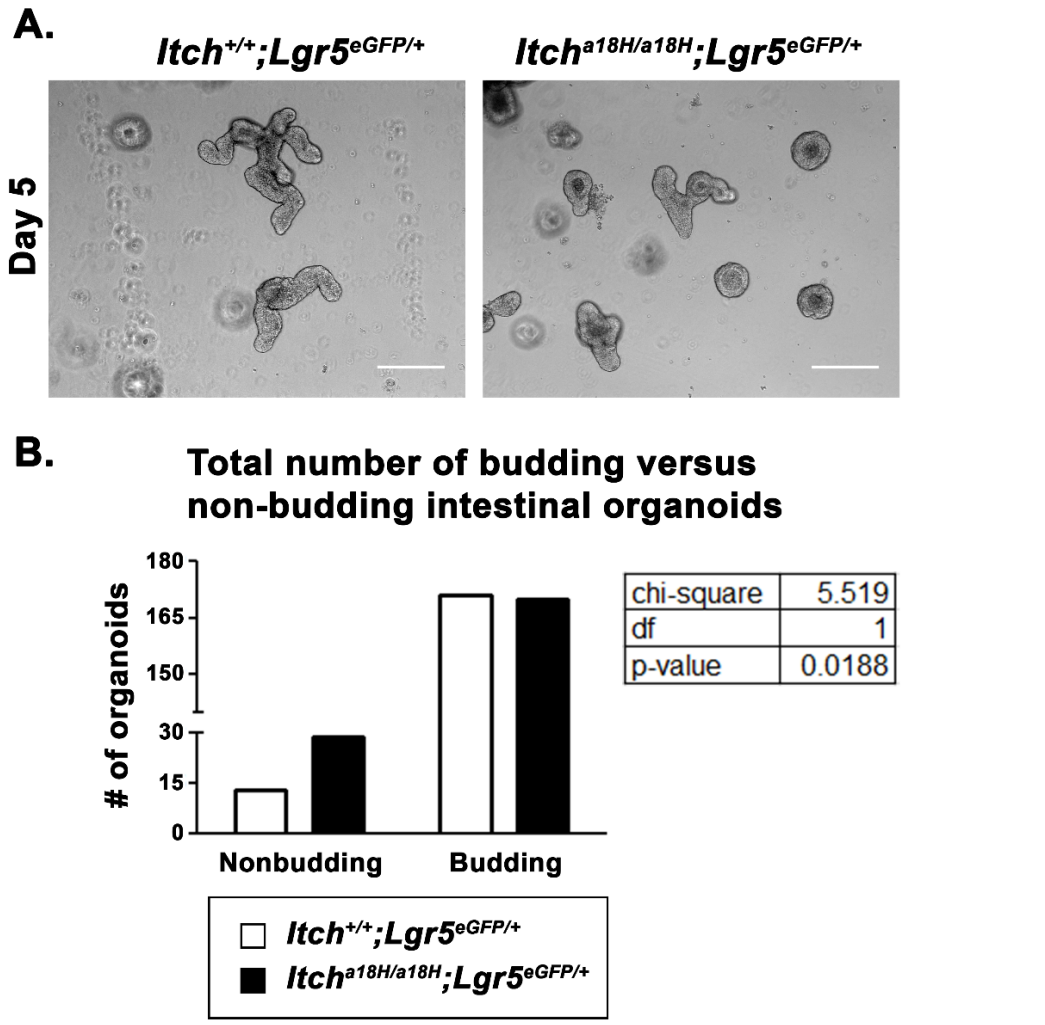
A.
Itch+/+;Lgr5eGFP/+
Itcha18H/a18H;Lgr5eGFP/+
Day 5
B.
Total number of budding versus
non-budding intestinal organoids
# of organoids
180
165
150
30
15
0
Nonbudding
Budding
chi-square 5.519
df 1
p-value 0.0188
Itch+/+;Lgr5eGFP/+
Itcha18H/a18H;Lgr5eGFP/+
C.
Number of buds
per intestinal organoid
Avg. # of Buds
25
20
15
10
5
0
*
Itch+/+;Lgr5eGFP/+
Itcha18H/a18H;Lgr5eGFP/+

Figure 3.3. *Itch* deficient intestinal organoids have alterations in budding initiation and budding fission. (**A**) Representative phase contrast images of *Itch*$^{+/+}$*; Lgr5*$^{eGFP/+}$ and *Itch*$^{a18H/a18H}$*; Lgr5*$^{eGFP/+}$ intestinal organoids at day 5 following plating highlights an increase in the number of nonbudding organoids in *Itch* deficient organoids compared to *Itch* sufficient organoids. Scale bars = 200 μm. (**B**) Graphical representation of a chi-squared analysis of a 2x2 contingency table (chi-square=5.519, df=1) demonstrating a statistically significant difference (p =0.0188) in the number of nonbudding versus budding organoids between *Itch*$^{+/+}$*; Lgr5*$^{eGFP/+}$ (n=184) and *Itch*$^{a18H/a18H}$*; Lgr5*$^{eGFP/+}$ (n=199). Organoids were counted from 3 independent wells per *Itch*$^{+/+}$*; Lgr5*$^{eGFP/+}$ and *Itch*$^{a18H/a18H}$*; Lgr5*$^{eGFP/+}$ intestinal crypt isolate. Data represents a total of 3 isolates per genotype. (**C**) A significant reduction (*p<0.05) in the average number of buds per intestinal organoid was observed when comparing only budding structures in *Itch*$^{+/+}$*; Lgr5*$^{eGFP/+}$ (n=167, median = 7, IQR = 6) to *Itch*$^{a18H/a18H}$*; Lgr5*$^{eGFP/+}$ (n=162, median = 6, IQR = 5) derived enteroids at day 5. Organoids were counted from 3 independent wells per *Itch*$^{+/+}$*; Lgr5*$^{eGFP/+}$ and *Itch*$^{a18H/a18H}$*; Lgr5*$^{eGFP/+}$ intestinal crypt isolate. Data represents a total of 3 isolates per genotype.

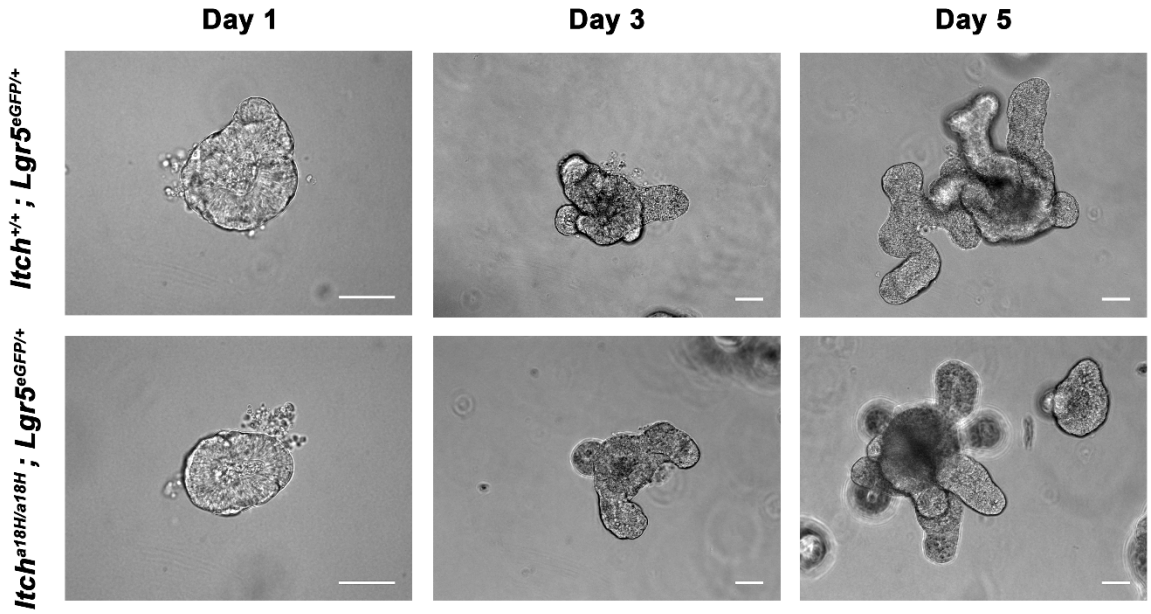

3.4. Loss of ITCH results in more compact and less intricate organoids. Representative phase contrast images of *Itch*$^{+/+}$*; Lgr5*$^{eGFP/+}$ and *Itch*$^{a18H/a18H}$*; Lgr5*$^{eGFP/+}$ intestinal organoids at day 1, day 3, and day 5. No difference in growth kinetics was observed between mature Itch sufficient and Itch deficient organoids. Scale bars = 50 μm.

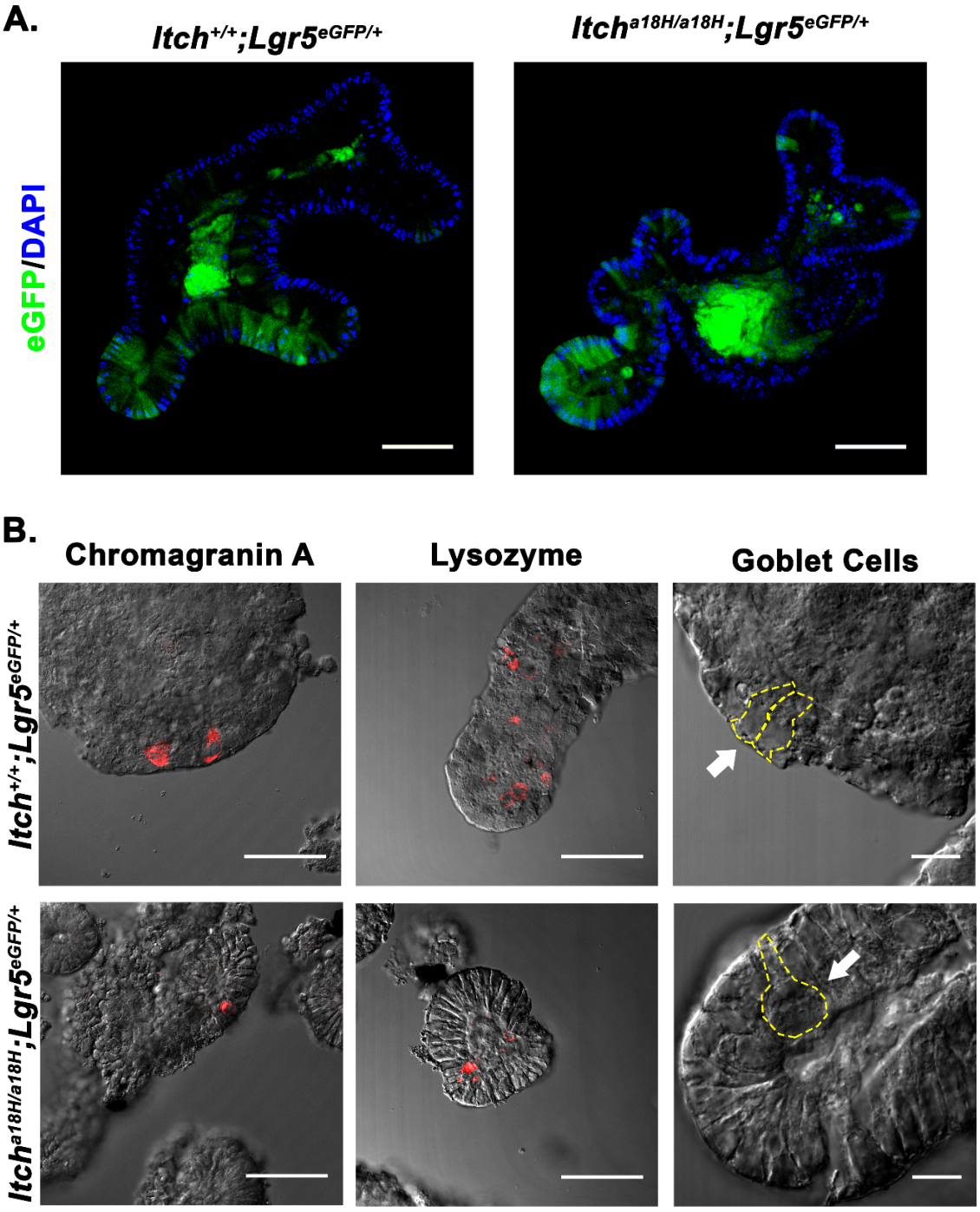
A.
Itch+/+;Lgr5eGFP/+
Itcha18H/a18H;Lgr5eGFP/+
eGFP/DAPI
B.
Chromagranin A
Lysozyme
Goblet Cells
Itch+/+;Lgr5eGFP/+
Itcha18H/a18H;Lgr5eGFP/+

Figure 3.5. *Itch* deficient organoids are capable of producing differentiated cell types from *Lgr5*$^{eGFP/+}$ stem cells. (**A**) Confocal fluorescent imaging of endogenous eGFP expression of whole-mount *Itch*$^{+/+}$*; Lgr5*$^{eGFP/+}$ and *Itch*$^{a18H/a18H}$ *; Lgr5*$^{eGFP/+}$ intestinal organoids fixed in 4% PFA and co-stainined with DAPI. ITCH deficiency does not appear to impact the number or location of intestinal *Lgr5*$^{eGFP+}$ stem cells within the budding structures of the intestinal organoids when compared to ITCH sufficient organoids. Scale bar = 50μm. (**B**) Confocal fluorescent-phase contrast images of 4% PFA-fixed, frozen sections stained with anti-chromagranin A (enteroendocrine cell marker) or anti-lysozyme (Paneth cell marker). Goblet cells were identified by cell morphology using phase-contrast microscopy. No difference was observed in ITCH deficienct organoids compared to ITCH sufficient organoids, suggesting that loss of ITCH in the intestinal epithelium does not markedly impact epithelial cell differentation. Scale bar = 50 μm (Chromagranin A and Lysozyme) and 10 μm for goblet cells.

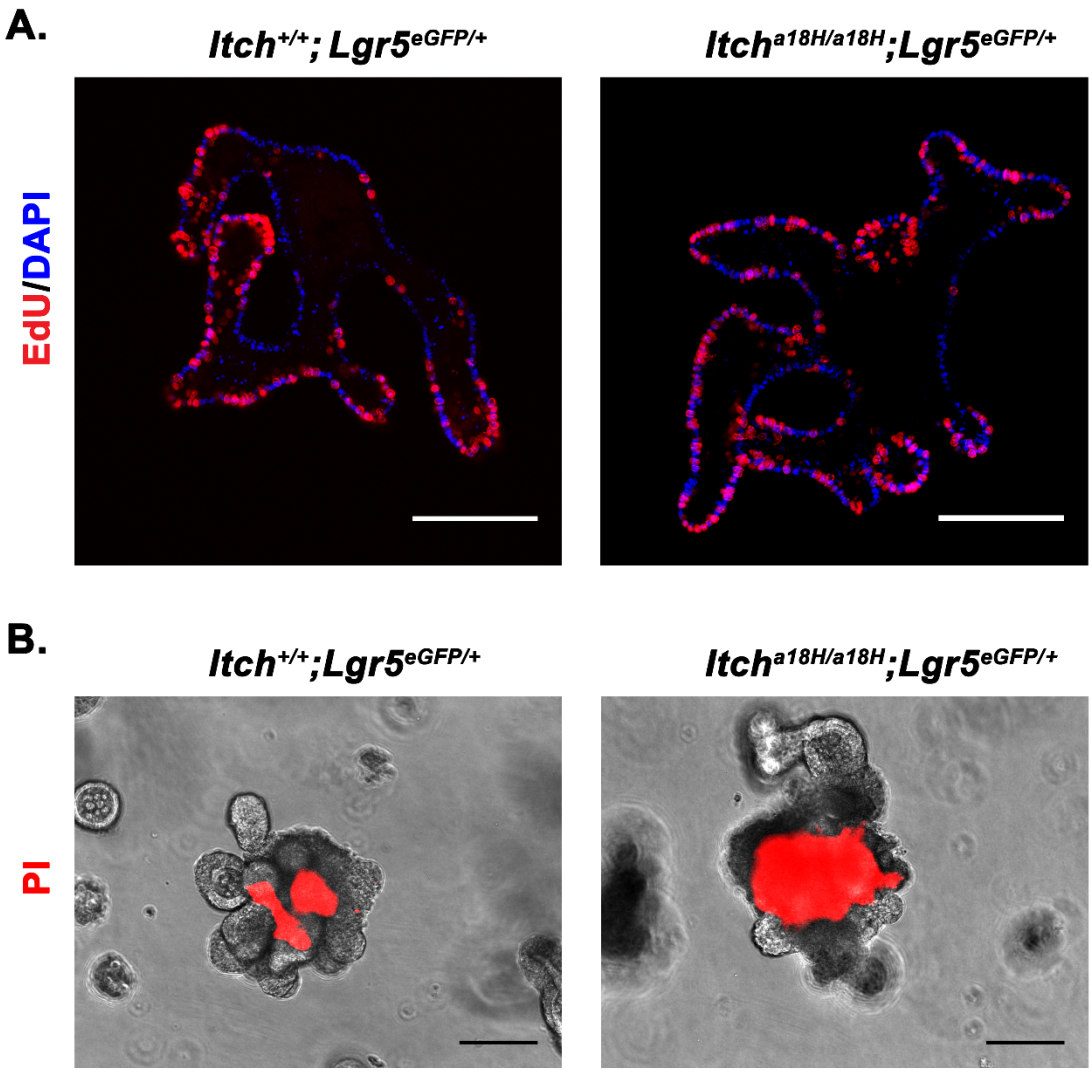
A.
Itch+/+; Lgr5eGFP/+
Itcha18H/a18H;Lgr5eGFP/+
EdU/DAPI
B.
Itch+/+;Lgr5eGFP/+
Itcha18H/a18H;Lgr5eGFP/+
PI
Apopotsis within intestinal organoids
% Surface Area of PI Fluorescence
40
30
20
10
0
*
Itch+/+;Lgr5eGFP/+
Itcha18H/a18H;Lgr5eGFP/+

Figure 3.6. Loss of ITCH in intestinal organoids impacts cell apoptosis in budding organoids. (**A**) Confocal fluorescent imaging of EdU incorporation within proliferating cells from whole-mount *Itch*$^{+/+}$*; Lgr5*$^{eGFP/+}$ and *Itch*$^{a18H/a18H}$*; Lgr5*$^{eGFP/+}$ intestinal organoids fixed in 4% PFA and co-stainined with DAPI. ITCH deficiency does not appear to impact cell proliferation when compared to ITCH sufficient organoids. Scale bar = 100 µm. (**B**) Epifluorescent-phase contrast images of whole mount *Itch*$^{+/+}$ *; Lgr5*$^{eGFP/+}$ and *Itch*$^{a18H/a18H}$ *; Lgr5*$^{eGFP/+}$ intestinal organoids stained with propridium iodide (PI). A 10% statisctically significant increase (*$p<0.05$) in the surface area of PI fluorescence is observed in *Itch*$^{a18H/a18H}$ *; Lgr5*$^{eGFP/+}$ intestinal organoids (n=84) compared to *Itch*$^{+/+}$*; Lgr5*$^{eGFP/+}$ (n=94). Organoids were counted from 2 independent wells per *Itch*$^{+/+}$*; Lgr5*$^{eGFP/+}$ and *Itch*$^{a18H/a18H}$*;Lgr5*$^{eGFP/+}$ intestinal crypt isolate. Data represents a total of 2 isolates per genotype. Scale bar = 100 µm. Error bars represent SEM.

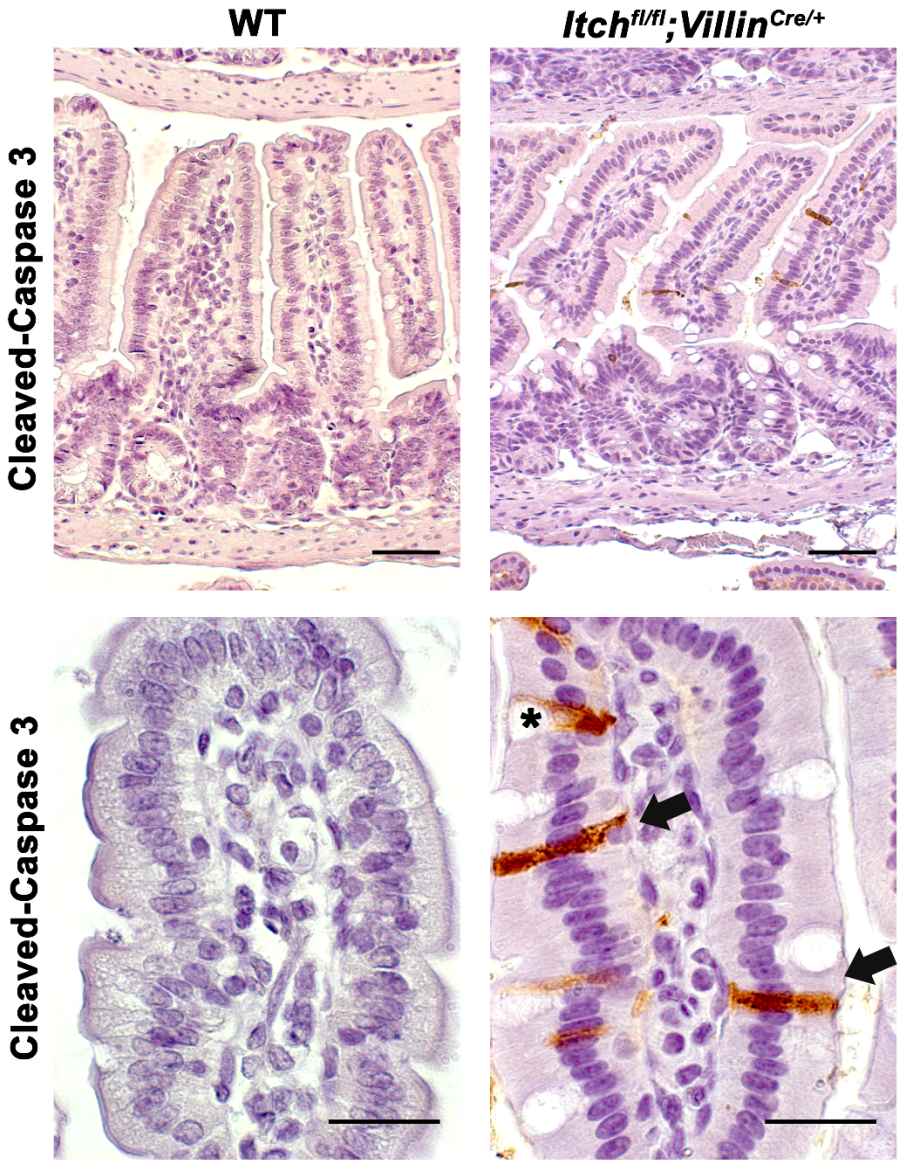

Figure 3.7. Epithelial specific loss of ITCH in the small intestine promotes epithelial apoptosis. Paraffin-embedded sections from the distal small intestine of 3 month old WT and *Itch*$^{fl/fl}$; *Villin*$^{Cre/+}$ animals immunostained for cleaved-caspase 3 and counterstained with hematoxylin. Animals lacking ITCH in the intestinal epithelium have increased apoptosis on the villi of the small intestine compared to WT controls. Higher power magnification (bottom) highlights apoptotic goblet (*) and enterocytes (arrows), indicating that apoptosis is not cell-type dependent. Scale bars = 100 μm (top) and 50 μm (bottom).

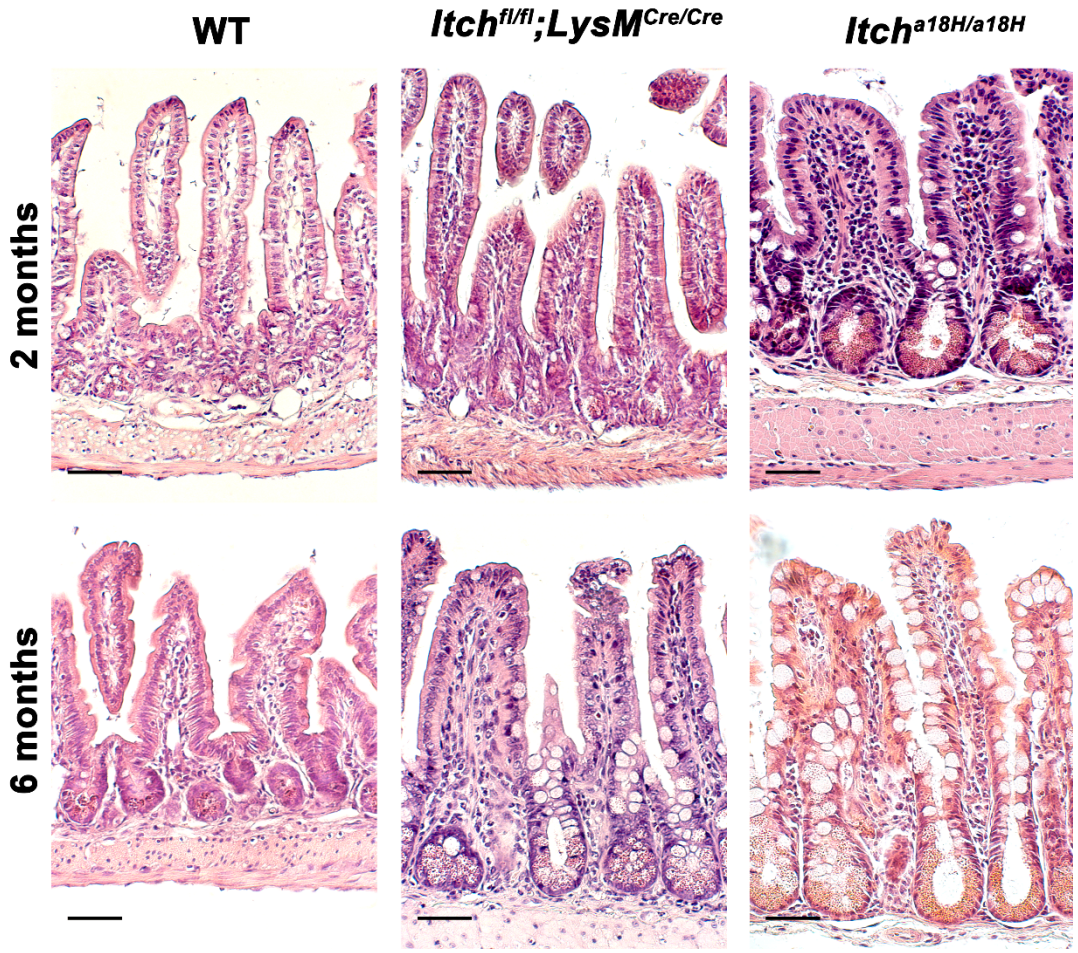

Figure 3.8. Loss of ITCH in the myeloid lineage leads to late-onset alterations in intestinal epithelial morphology that is similar to *Itch*$^{a18H/a18H}$ at 2 months. H&E paraffin-embedded sections from the distal small intestine of 2 month and 6 month old WT, *Itch*$^{fl/fl}$*; LysM*$^{Cre/Cre}$, and *Itch*$^{a18H/a18H}$ animals. At 2 months, no histological abnormalities are observed in the epithelium of the small intestine from *Itch*$^{fl/fl}$*; LysM*$^{Cre/Cre}$ animals. By 6 months, the intestinal epithelium from *Itch*$^{fl/fl}$*; LysM*$^{Cre/Cre}$ looks similar to *Itch*$^{a18H/a18H}$ animals at 2 months of age with an expanded crypt compartment and increased goblet and Paneth cell numbers suggesting that loss of ITCH in the myeloid cell lineage contributes to the epithelial alterations observed in the small intestine of *Itch*$^{a18H/a18H}$ animals. However, a delay in the presentation of altered intestinal morphology suggests that loss of ITCH in additional tissue types (*i.e.,* epithelium) likely accelerates the epithelial defects that are observed in *Itch*$^{a18H/a18H}$ animals at 2 months of age. Scale bars = 100 μm.

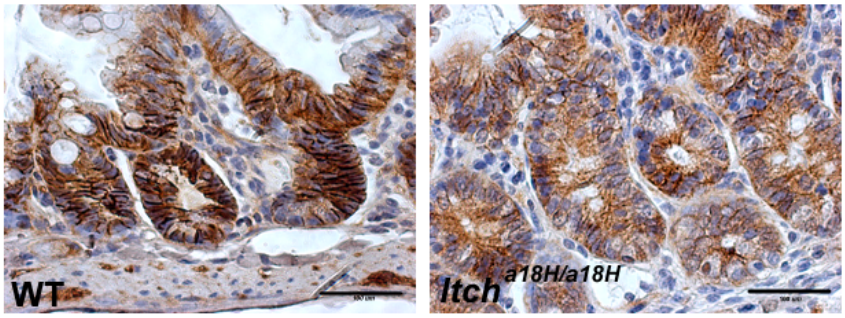

Figure 3.9. β-catenin expression is reduced in *Itch*$^{a18H/a18H}$ animals. Paraffin-embedded sections from the distal small intestine of young adult *Itch*$^{+/+}$ and *Itch*$^{a18H/a18H}$ animals immunostained for β-catenin and counterstained with hematoxylin. Animals lacking ITCH in the intestinal epithelium have reduced levels of β-catenin at the membrane of cells in the crypt of the small intestine compared to WT controls. Scale bars = 50μm.

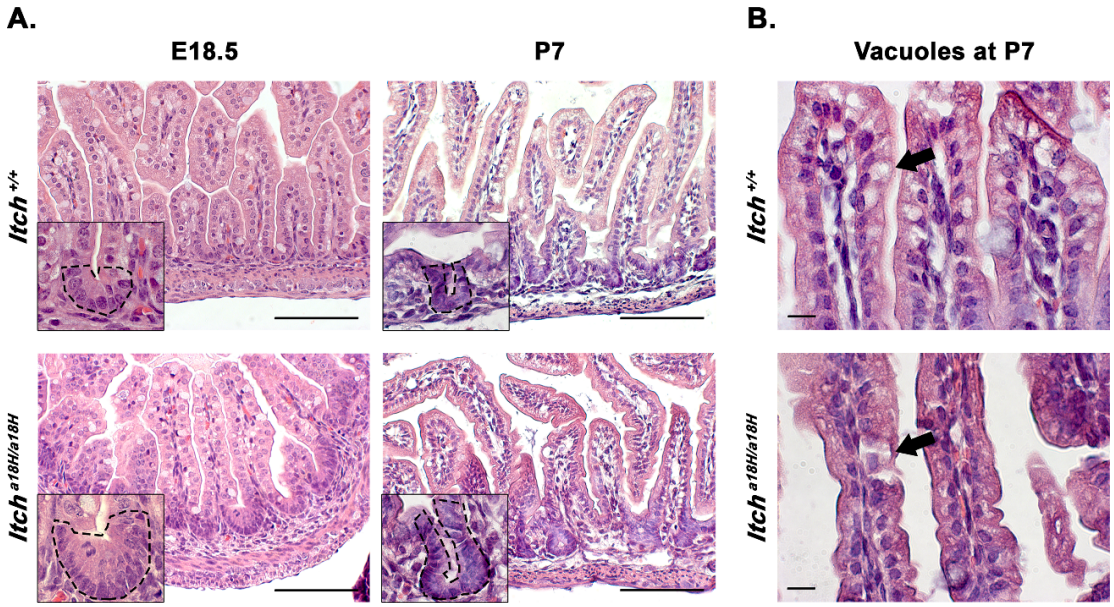

Figure 3.10. Loss of ITCH accelerates epithelial maturation during development. (**A**) Representative H&E stained paraffin-embedded small intestinal sections from E18.5 (left) and P7 (right) *Itch*$^{+/+}$ and *Itch*$^{a18H/a18H}$ animals show precocious crypt emergence in the *Itch*$^{a18H/a18H}$ animals. Black dashed lines in the insets outline crypt borders. Scale bars = 200 μm. Original magnification of insets = 63x. (**B**) Intracellular vacuoles (arrows) located within distal enterocytes from P7 *Itch*$^{+/+}$ and *Itch*$^{a18H/a18H}$ animals highlight a difference in the apical canalicular system in the *Itch*$^{a18H/a18H}$ animals, consistent with accelerated epithelial maturation. Scale bars = 20 μm.

CHAPTER 4

CONCLUDING REMARKS

The small intestine is a highly dynamic tissue that plays a vital role in digestion, nutrient absorption, and water balance while simultaneously preventing the entry of foreign substrates (Bischoff et al., 2014). The mucosal barrier is an integral component of this process, effectively separating the external environment from the body's internal milieu. Preservation of the mucosal barrier is, in part, established by the concerted effort between the epithelium and the immune system (Rescigno, 2011.) Bacteria that colonize the small intestine are constantly challenging the efficacy of the barrier. The epithelium that lines the luminal cavity provides an initial physical barrier that prevents the passage of bacteria into the internal compartment of the host. While this mainstay barrier is typically an effective deterrent, the constant exposure of noxious substances, antigens, and microorganisms to the surface of the epithelium makes a breach in foreign material eventually inevitable (Schenk and Mueller, 2008). In this event, resident intestinal macrophages and dendritic cells that encounter the bacteria will cytotoxically destroy the bacteria without initiating an inflammatory response, which preserves the architecture and function of the epithelium (intestinal epithelial homeostasis). However, if the innate immune cells fail to remain tolerogenic, an inappropriate inflammatory response is generated which can lead to epithelial destruction and compromised small intestinal function.

Here we present evidence of both cell autonomous and non-cell autonomous roles for the ubiquitin ligase ITCH in epithelial homeostasis in the small intestine. Increased cell death was noted in both ITCH deficient organoids and in *Itch*$^{fl/fl}$*; Villin*$^{Cre/+}$ animals, supportive of an epithelial-specific function for ITCH in cell demise. As previously discussed, increased ITCH-mediated epithelial apoptosis could be driven by the disorganization of adherens junctions (Chapter 1) or by the increased expression of the ITCH-targeted substrates LATS1 or TXNIP (Chapter 3). However, an additional role for ITCH in the regulation of apoptosis, most likely associated with inappropriate activation of the immune system, is emphasized by a shift in apoptotic cells from the villus of *Itch*$^{fl/fl}$*; Villin*$^{Cre/+}$ animals towards the upper region of the crypt in the *Itch*$^{a18H/a18H}$ small intestine. TNF-α, a pro-inflammatory cytokine that is produced by both innate and acquired immune responses, enhances epithelial apoptosis in the intestine (Nunes et al., 2014; Watson and Hughes, 2012). We anticipate that the aberrant activation of the immune system within the gastrointestinal tract of the *Itch*$^{a18H/a18H}$ animal will promote TNF-α mediated apoptosis, and, in combination with ITCH's cell autonomous role in epithelial apoptosis, increased stress is placed on the epithelium to initiate apoptosis at an earlier point in the epithelial turnover process. Alternatively, cell death within the crypt has been suggested as a homeostatic mechanism to control the number of terminally differentiated cells that will migrate onto the villus by controlling the number of progenitor cells within the crypt (Hall et al., 1994). The prevalence of apoptotic cells in the

upper crypt of *Itch*$^{a18H/a18H}$ animals may represent an attempt to limit the number of transit-amplifying cells to maintain homeostasis.

It is interesting to note that additional signaling pathways within the epithelium, such as NFκB, can influence the outcome of TNF-α mediated apoptosis (Chang et al., 2006; Wullaert et al., 2011). Active NFκB signaling in the intestinal epithelium is protective against TNF-α mediated apoptosis, and the absence of NFκB signaling in the presence of this cytokine promotes cell death. (Wullaert et al., 2011). Accumulating evidence supports that ITCH is a negative regulator of NFκB signaling (Chang et al., 2006; Shembade et al., 2008; M. Tao et al., 2009). We anticipate that loss of ITCH function promotes NFκB signaling in the epithelium, which could protect the epithelium from TNF-α induced apoptosis. Thus, loss of ITCH in the epithelium in the presence of inflammation might serve as a protective mechanism to counteract inflammation-driven apoptosis in an attempt to preserve barrier function.

The fact that the epithelial-specific loss of ITCH fails to recapitulate the small intestinal epithelial phenotype in the ubiquitous loss of function ITCH animals suggests that ITCH plays an important role in immune tissue to contribute to epithelial homeostasis. Loss of ITCH function in the myeloid cell compartment of 6-month-old animals resulted in crypt hyperplasia as well as increased specification toward goblet and Paneth cells, similar to the young adult *Itch*$^{a18H/a18H}$ small intestinal phenotype. Evidence supports a cell autonomous function for ITCH in macrophages to fine tune the proinflammatory response in macrophages by modulating NFκB signaling (M.

Tao et al., 2009). To prevent an inappropriate response to the luminal bacteria, macrophages in the small intestine are tolerogenic and do not induce pro-inflammatory cytokines in the presence of antigenic substrates (Gross et al., 2015). Due to the aberrant activation of the immune system in the absence of a known pathogen in *Itch*$^{a18H/a18H}$ animals, we suspect ITCH deficient macrophages are less tolerogenic and initiate an NFκB-dependent, pro-inflammatory response that influences epithelial homeostasis. Additionally, the heightened immune response of ITCH deficient macrophages likely activates effector T cells, which, in turn, will feed back onto the epithelium to further influence tissue homeostasis. Consistent with assertion, the delayed development of an epithelial phenotype in *Itch*$^{fl/fl}$*; LysM*$^{Cre/Cre}$ animals as compared to *Itch*$^{a18H/a18H}$ animals supports that additional tissue types contribute to the shift in epithelial homeostasis. While the epithelium is a likely contributor to this phenotype (Chapter 2 Discussion), loss of ITCH in lymphoid tissues might contribute as well, which is evidenced by the lack of epithelial disarray that is observed in *Itch*$^{a18H/a18H}$ animals on a *Rag1*$^{-/-}$ background as compared to *Itch*$^{a18H/a18H}$ animals.

The inability of the tissue-specific losses of ITCH in either the epithelium or in the immune system to recapitulate the global loss of ITCH phenotype characterized by increased cell proliferation and apoptosis within the crypt, enhanced terminal differentiation of goblet and Paneth cells, and accelerated cell migration along the crypt-villus axis, suggests that loss of ITCH in both epithelial and immune tissues contributes to this phenotype. We hypothesize the loss of

ITCH in the epithelium enhances apoptosis, which promotes the translocation of commensal bacteria into the host more readily. The presence of bacteria in the lamina propria prompts a response from the resident innate immune cells. However, due to loss of ITCH function in this tissue as well, this likely decreases the tolerance of the innate immune cells to the bacteria and leads to a heightened inflammatory response, which feeds back onto the epithelium and influences homeostasis. Because the epithelium response by increasing migration, as well as goblet and Paneth cell differentiation, which are considered protective measures against pathogen invasion. This shift in epithelial homeostasis attempts to minimize further bacteria invasion and epithelial destruction. Similar to NFκB signaling in the small intestine, we propose that ITCH has dual functions in regulating small intestinal mucosal homeostasis that is context-dependent. Further elucidation of how ITCH influences mucosal homeostasis in the epithelium and the immune system, as well as the cross-talk between this two tissue types, will provide insight how ITCH impacts a range of gastrointestinal enteropathies, including inflammatory bowel diseases, celiac disease, and cancer.

Interestingly, our data support that loss of ITCH is protective in sporadic colorectal cancer. With the numerous tumor suppressor targets that are substrates for ITCH, it is not surprising that ITCH expression is robustly increased in intestinal adenocarcinomas (Uhlen, 2005). While we have proposed that loss of ITCH function in $Apc^{Min/+}$ tumorigenesis significantly reduces tumor burden by driving cells toward a differentiated state and leads to a reduction in

anchorage dependent growth of transformed cells (Chapter 2), it is tempting the speculate that apoptosis contributes as well. We anticipate that loss of ITCH would enhance apoptosis in *Apc*$^{Min/+}$ small intestinal adenomas. Alternatively, the altered inflammatory state that is present in the small intestine of the *Itch*$^{a18H/a18H}$ animals could also contribute to decreased tumor burden. In colorectal cancer, the activation of the immune system establishes a pro-inflammatory environment which promotes tumor growth (Ellyard et al., 2007). Thus, we anticipate that loss of ITCH function either does not produce a pro-inflammatory environment or the immune system's response is modified. γδ T-cells are subset of specialized T-cells that primarily localize to the lamina propria of the intestine and contribute to innate immunity by destroying epithelial cells that have been invaded or damaged by pathogenic material as well as by producing multifunctional memory T-cells that rapidly response if re-exposure occurs (Sheridan et al., 2013; van Wijk and Cheroutre, 2010). In *Itch*$^{a18H/a18H}$ animals, elevated levels of serum IgE, an immunoglobulin that promotes allergic reactions, is secreted by the γδ T cell population (Parravicini et al., 2008). However, accumulating evidence also suggests a role for IgE in anti-tumor immunity (Leoh et al., 2015). Thus, it is tempting to speculate that loss if ITCH promotes antibody-dependent cell-mediated cytotoxicity toward intestinal adenomas by generating IgEs targeted against a tumor-associated antigen. Further, the aberrant activation of the immune system in ITCH deficient animals may provide a more robust inflammatory response to effectively destroy the tumor. IgE induces a robust inflammatory response by recruiting key effector mediator cells, such as

eosinophils, basophils, and mast cells, to destroy the target. The increased presence of eosinophils is a hallmark of the IgE inflammatory response, and the degranulation of these cells contributes to cytotoxic destruction of their targets (Leoh et al., 2015). In 5-month-old *Itch*$^{a18H/a18H}$ animals, an increased number of eosinophils are present in the small intestine (Ramon et al., 2011), potentially providing support for IgE-mediated destruction of *Apc*$^{Min/+}$ intestinal adenomas.

The activation of the host's immune system has proven extremely effective in the adjuvant treatment of cancer. Since 2013, the FDA has approved 15 monoclonal immunotherapies for the treatment of cancer (Farkona et al., 2016). The potential ability of ITCH deficient γδ T-cells to secrete IgE antibodies targeted against tumor-specific antigens could be of therapeutic interest in the treatment of colorectal cancer. While passive immunotherapy has proven extremely effective, endogenous activation of the immune system to induce immunoglobulins that are specifically directed at tumor-associated antigens will provide a more personalized approach in the treatment of colorectal cancer. Furthermore, the endogenous activation of the immune system will likely generate memory effectors cells that can induce a more rapid immune response if subsequent exposure occurs. Thus, the continued examination of ITCH in epithelial and immune tissues in the intestine, as well as how these tissue interact to maintain mucosal homeostasis, will likely identify novel therapeutic avenues that will provide personalized treatment in a range of gastrointestinal enteropathies.

REFERENCES

Agace, W.W., McCoy, K.D., 2017. Regionalized Development and Maintenance of the Intestinal Adaptive Immune Landscape. Immunity. doi:10.1016/j.immuni.2017.04.004

Ahern, P.P., Schiering, C., Buonocore, S., McGeachy, M.J., Cua, D.J., Maloy, K.J., Powrie, F., 2010. Interleukin-23 Drives Intestinal Inflammation through Direct Activity on T Cells. Immunity 33, 279–288. doi:10.1016/j.immuni.2010.08.010

Aki, D., Zhang, W., Liu, Y.C., 2015. The E3 ligase Itch in immune regulation and beyond. Immunol. Rev. 266, 6–26. doi:10.1111/imr.12301

Al-Sadi, R., Khatib, K., Guo, S., Ye, D., Youssef, M., Ma, T., 2011. Occludin regulates macromolecule flux across the intestinal epithelial tight junction barrier. Am. J. Physiol. Gastrointest. Liver Physiol. 300, G1054–G1064. doi:10.1152/ajpgi.00055.2011

Armbruster, N.S., Stange, E.F., Wehkamp, J., 2017. In the Wnt of Paneth cells: Immune-epithelial crosstalk in small intestinal Crohn's disease. Front. Immunol. doi:10.3389/fimmu.2017.01204

Bain, C.C., Mowat, A.M., 2014. Macrophages in intestinal homeostasis and inflammation. Immunol. Rev. doi:10.1111/imr.12192

Baker, A.M., Cereser, B., Melton, S., Fletcher, A.G., Rodriguez-Justo, M., Tadrous, P.J., Humphries, A., Elia, G., McDonald, S.A.C., Wright, N.A.,

Simons, B.D., Jansen, M., Graham, T.A., 2014. Quantification of crypt and stem cell evolution in the normal and neoplastic human colon. Cell Rep. 8, 940–947. doi:10.1016/j.celrep.2014.07.019

Barker, N., 2013. Adult intestinal stem cells: critical drivers of epithelial homeostasis and regeneration. Nat. Rev. Mol. Cell Biol. 15, 19–33. doi:10.1038/nrm3721

Barker, N., Ridgway, R.A., van Es, J.H., van de Wetering, M., Begthel, H., van den Born, M., Danenberg, E., Clarke, A.R., Sansom, O.J., Clevers, H., 2009. Crypt stem cells as the cells-of-origin of intestinal cancer. Nature 457, 608–611. doi:10.1038/nature07602

Barker, N., Van De Wetering, M., Clevers, H., 2008. The intestinal stem cell. Genes Dev 22, 1856–1864.

Barker, N., van Es, J.H., Kuipers, J., Kujala, P., van den Born, M., Cozijnsen, M., Haegebarth, A., Korving, J., Begthel, H., Peters, P.J., Clevers, H., 2007a. Identification of stem cells in small intestine and colon by marker gene Lgr5. Nature. doi:10.1038/nature06196

Barker, N., Van Es, J.H., Kuipers, J., Kujala, P., Van Den Born, M., Cozijnsen, M., Haegebarth, A., Korving, J., Begthel, H., Peters, P.J., Clevers, H., 2007b. Identification of stem cells in small intestine and colon by marker gene Lgr5. Nature 449, 1003–1007.

Barker, N., Van Oudenaarden, A., Clevers, H., 2012. Identifying the stem cell of the intestinal crypt: Strategies and pitfalls. Cell Stem Cell. doi:10.1016/j.stem.2012.09.009

Basak, O., Beumer, J., Wiebrands, K., Seno, H., van Oudenaarden, A., Clevers, H., 2017. Induced Quiescence of Lgr5+ Stem Cells in Intestinal Organoids Enables Differentiation of Hormone-Producing Enteroendocrine Cells. Cell Stem Cell. doi:10.1016/j.stem.2016.11.001

Basheer, W.A., Harris, B.S., Mentrup, H.L., Abreha, M., Thames, E.L., Lea, J.B., Swing, D.A., Copeland, N.G., Jenkins, N.A., Price, R.L., Matesic, L.E., 2015. Cardiomyocyte-specific overexpression of the ubiquitin ligase Wwp1 contributes to reduction in Connexin 43 and arrhythmogenesis. J. Mol. Cell. Cardiol. 88. doi:10.1016/j.yjmcc.2015.09.004

Batlle, E., Henderson, J.T., Beghtel, H., Van den Born, M.M.W., Sancho, E., Huls, G., Meeldijk, J., Robertson, J., Van de Wetering, M., Pawson, T., Clevers, H., 2002a. β-catenin and TCF mediate cell positioning in the intestinal epithelium by controlling the expression of EphB/EphrinB. Cell. doi:10.1016/S0092-8674(02)01015-2

Batlle, E., Henderson, J.T., Beghtel, H., Van den Born, M.M.W., Sancho, E., Huls, G., Meeldijk, J., Robertson, J., Van de Wetering, M., Pawson, T., Clevers, H., 2002b. β-catenin and TCF mediate cell positioning in the intestinal epithelium by controlling the expression of EphB/EphrinB. Cell 111, 251–263. doi:10.1016/S0092-8674(02)01015-2

Berer, K., Mues, M., Koutrolos, M., Rasbi, Z. Al, Boziki, M., Johner, C., Wekerle, H., Krishnamoorthy, G., 2011. Commensal microbiota and myelin autoantigen cooperate to trigger autoimmune demyelination. Nature 479, 538–541. doi:10.1038/nature10554

Bernassola, F., Karin, M., Ciechanover, A., Melino, G., 2008. The HECT Family of E3 Ubiquitin Ligases: Multiple Players in Cancer Development. Cancer Cell. doi:10.1016/j.ccr.2008.06.001

Birchenough, G.M.H., Johansson, M.E., Gustafsson, J.K., Bergström, J.H., Hansson, G.C., 2015. New developments in goblet cell mucus secretion and function. Mucosal Immunol. 8, 712–719. doi:10.1038/mi.2015.32

Bischoff, S.C., Barbara, G., Buurman, W., Ockhuizen, T., Schulzke, J.-D., Serino, M., Tilg, H., Watson, A., Wells, J.M., 2014. Intestinal permeability – a new target for disease prevention and therapy. BMC Gastroenterol. 14, 189. doi:10.1186/s12876-014-0189-7

Bondow, B.J., Faber, M.L., Wojta, K.J., Walker, E.M., Battle, M.A., 2012. E-cadherin is required for intestinal morphogenesis in the mouse. Dev. Biol. 371, 1–12. doi:10.1016/j.ydbio.2012.06.005

Brand, S., Beigel, F., Olszak, T., Zitzmann, K., Eichhorst, T., Otte, J., Diepolder, H., Marquardt, A., Jagla, W., Popp, A., Herrmann, K., Seiderer, J., Ochsenku, T., Auernhammer, C.J., Dambacher, J., Mar-, A., Herr-, K., Go, B., 2006. IL-22 is increased in active Crohn's disease and promotes proinflammatory gene expression and intestinal epithelial cell migration. Am J Physiol Gastrointest Liver Physiol 290, G827-838. doi:10.1152/ajpgi.00513.2005.

Brenchley, J.M., Price, D. a, Schacker, T.W., Asher, T.E., Silvestri, G., Rao, S., Kazzaz, Z., Bornstein, E., Lambotte, O., Altmann, D., Blazar, B.R., Rodriguez, B., Teixeira-Johnson, L., Landay, A., Martin, J.N., Hecht, F.M.,

Picker, L.J., Lederman, M.M., Deeks, S.G., Douek, D.C., 2006. Microbial translocation is a cause of systemic immune activation in chronic HIV infection. Nat. Med. 12, 1365–71. doi:10.1038/nm1511

Buller, N.V.J.A., Rosekrans, S.L., Westerlund, J., van den Brink, G.R., 2012. Hedgehog Signaling and Maintenance of Homeostasis in the Intestinal Epithelium. Physiology 27, 148–155. doi:10.1152/physiol.00003.2012

Burstone, M.S., 1958. Histochemical demonstration of acid phosphatases with naphthol as-phosphates. J. Natl. Cancer Inst. 21, 523–538. doi:10.1093/jnci/21.3.523

Carothers, A.M., Melstrom, K.A., Mueller, J.D., Weyant, M.J., Bertagnolli, M.M., 2001. Progressive Changes in Adherens Junction Structure during Intestinal Adenoma Formation in Apc Mutant Mice. J. Biol. Chem. 276, 39094–39102. doi:10.1074/jbc.M103450200

Caruso, R., Warner, N., Inohara, N., Núñez, G., 2014. NOD1 and NOD2: Signaling, host defense, and inflammatory disease. Immunity. doi:10.1016/j.immuni.2014.12.010

Catalioto, R.-M., Maggi, C.A., Giuliani, S., 2011. Intestinal epithelial barrier dysfunction in disease and possible therapeutical interventions. Curr. Med. Chem. 18, 398–426. doi:10.2174/092986711794839179

Chang, L., Kamata, H., Solinas, G., Luo, J.L., Maeda, S., Venuprasad, K., Liu, Y.C., Karin, M., 2006. The E3 ubiquitin ligase itch couples JNK activation to TNFα-induced cell death by inducing c-FLIPL turnover. Cell 124, 601–613. doi:10.1016/j.cell.2006.01.021

Chastagner, P., Israël, A., Brou, C., 2008. AIP4/Itch regulates notch receptor degradation in the absence of ligand. PLoS One 3. doi:10.1371/journal.pone.0002735

Chen, C., Matesic, L.E., 2007. The Nedd4-like family of E3 ubiquitin ligases and cancer. Cancer Metastasis Rev. 26, 587–604.

Cheng, H., Leblond, C.P., 1974. Origin, differentiation and renewal of the four main epithelial cell types in the mouse small intestine V. Unitarian theory of the origin of the four epithelial cell types. Am. J. Anat. 141, 537–561. doi:10.1002/aja.1001410407

Cho, K.R., Vogelstein, B., 1992. Genetic alterations in the adenoma–carcinoma sequence. Cancer 70, 1727–1731. doi:10.1002/1097-0142(19920915)70:4+<1727::AID-CNCR2820701613>3.0.CO;2-P

Chwalinski, S., Potten, C.S., Evans, G., 1988. Double labelling with bromodeoxyuridine and [3H]-thymidine of proliferative cells in small intestinal epithelium in steady state and after irradiation. Cell Tissue Kinet. 21, 317–329.

Clevers, H., 2009. Searching for adult stem cells in the intestine. EMBO Mol. Med. 1, 255–259. doi:10.1002/emmm.200900034

Clevers, H.C., Bevins, C.L., 2013. Paneth Cells: Maestros of the Small Intestinal Crypts. Annu. Rev. Physiol. 75, 289–311. doi:10.1146/annurev-physiol-030212-183744

Cornell, M., Evans, D.A.P., Mann, R., Fostier, M., Flasza, M., Monthatong, M., Artavanis-Tsakonas, S., Baron, M., 1999. The Drosophila melanogaster

Suppressor of deltex gene, a regulator of the Notch receptor signaling pathway, is an E3 class ubiquitin ligase. Genetics 152, 567–576.

De Mey, J.R., Freund, J., 2013. Understanding epithelial homeostasis in the intestine: An old battlefield of ideas, recent breakthroughs and remaining controversies. Tissue barriers 1, e24965. doi:10.4161/tisb.24965

Dehmer, J.J., Garrison, A.P., Speck, K.E., Dekaney, C.M., Van Landeghem, L., Sun, X., Henning, S.J., Helmrath, M.A., 2011. Expansion of Intestinal Epithelial Stem Cells during Murine Development. PLoS One 6, e27070. doi:10.1371/journal.pone.0027070

Delgado, M.E., Grabinger, T., Brunner, T., 2016. Cell death at the intestinal epithelial front line. FEBS J. doi:10.1111/febs.13575

Di Marcotullio, L., Greco, A., Mazzà, D., Canettieri, G., Pietrosanti, L., Infante, P., Coni, S., Moretti, M., De Smaele, E., Ferretti, E., Screpanti, I., Gulino, A., 2011. Numb activates the E3 ligase Itch to control Gli1 function through a novel degradation signal. Oncogene 30, 65–76. doi:10.1038/onc.2010.394

Donaldson, G.P., Lee, S.M., Mazmanian, S.K., 2015. Gut biogeography of the bacterial microbiota. Nat. Rev. Microbiol. 14, 20–32. doi:10.1038/nrmicro3552

Durand, A., Donahue, B., Peignon, G., Letourneur, F., Cagnard, N., Slomianny, C., Perret, C., Shroyer, N.F., Romagnolo, B., 2012. Functional intestinal stem cells after Paneth cell ablation induced by the loss of transcription factor Math1 (Atoh1). Proc. Natl. Acad. Sci. 109, 8965–8970. doi:10.1073/pnas.1201652109

Eisenstein, E.M., Williams, C.B., 2009. The Treg/Th17 cell balance: A new paradigm for autoimmunity. Pediatr. Res. doi:10.1203/PDR.0b013e31819e76c7

Ellyard, J.I., Simson, L., Parish, C.R., 2007. Th2-mediated anti-tumour immunity: Friend or foe? Tissue Antigens. doi:10.1111/j.1399-0039.2007.00869.x

Elphick, D.A., Mahida, Y.R., 2005. Paneth cells: their role in innate immunity and inflammatory disease. Gut 54, 1802–9. doi:10.1136/gut.2005.068601

Etienne-Manneville, S., 2012. Adherens junctions during cell migration. Subcell. Biochem. 60, 225–249. doi:10.1007/978-94-007-4186-7_10

Fang, D., Elly, C., Gao, B., Fang, N., Altman, Y., Joazeiro, C., Hunter, T., Copeland, N., Jenkins, N., Liu, Y.-C., 2002a. Dysregulation of T lymphocyte function in itchy mice: a role for Itch in TH2 differentiation. Nat. Immunol. 3, 281–287. doi:10.1038/ni763

Fang, D., Elly, C., Gao, B., Fang, N., Altman, Y., Joazeiro, C., Hunter, T., Copeland, N., Jenkins, N., Liu, Y.-C., 2002b. Dysregulation of T lymphocyte function in itchy mice: a role for Itch in TH2 differentiation. Nat. Immunol. doi:10.1038/ni763

Fang, D., Elly, C., Gao, B., Fang, N., Altman, Y., Joazeiro, C., Hunter, T., Copeland, N., Jenkins, N., Liu, Y.-C., 2002c. Dysregulation of T lymphocyte function in itchy mice: a role for Itch in TH2 differentiation. Nat. Immunol. 3, 281–287. doi:10.1038/ni763

Fanning, A.S., Jameson, B.J., Jesaitis, L.A., Anderson, J.M., 1998. The tight junction protein ZO-1 establishes a link between the transmembrane protein

occludin and the actin cytoskeleton. J. Biol. Chem. 273, 29745–29753. doi:10.1074/jbc.273.45.29745

Farkona, S., Diamandis, E.P., Blasutig, I.M., 2016. Cancer immunotherapy: the beginning of the end of cancer? BMC Med. 14, 73. doi:10.1186/s12916-016-0623-5

Fevr, T., Robine, S., Louvard, D., Huelsken, J., 2007. Wnt/β-Catenin Is Essential for Intestinal Homeostasis and Maintenance of Intestinal Stem Cells. Mol. Cell. Biol. 27, 7551–7559. doi:10.1128/MCB.01034-07

Flier, L.G. Van Der, Clevers, H., 2009. Stem Cells , Self-Renewal , and Differentiation in the Intestinal Epithelium. Annu. Rev. Physiol. 71, 241–260. doi:10.1146/annurev.physiol.010908.163145

Foersch, S., Neurath, M.F., 2014. Colitis-associated neoplasia: Molecular basis and clinical translation. Cell. Mol. Life Sci. doi:10.1007/s00018-014-1636-x

Fre, S., Pallavi, S.K., Huyghe, M., Laé, M., Janssen, K.-P., Robine, S., Artavanis-Tsakonas, S., Louvard, D., 2009. Notch and Wnt signals cooperatively control cell proliferation and tumorigenesis in the intestine. Proc. Natl. Acad. Sci. U. S. A. 106, 6309–6314. doi:10.1073/pnas.0900427106

Garcia, M.A., Nelson, W.J., Chavez, N., 2017. Cell–Cell Junctions Organize Structural and Signaling Networks. Cold Spring Harb. Perspect. Biol. a029181. doi:10.1101/cshperspect.a029181

Garrett, W.S., Gordon, J.I., Glimcher, L.H., 2010. Homeostasis and Inflammation in the Intestine. Cell. doi:10.1016/j.cell.2010.01.023

Geissmann, F., Manz, M.G., Jung, S., Sieweke, M.H., Merad, M., Ley, K., 2010.

Development of monocytes, macrophages, and dendritic cells. Science 327, 656–61. doi:10.1126/science.1178331

Gerbe, F., Van Es, J.H., Makrini, L., Brulin, B., Mellitzer, G., Robine, S., Romagnolo, B., Shroyer, N.F., Bourgaux, J.F., Pignodel, C., Clevers, H., Jay, P., 2011. Distinct ATOH1 and Neurog3 requirements define tuft cells as a new secretory cell type in the intestinal epithelium. J. Cell Biol. 192, 767–780. doi:10.1083/jcb.201010127

Germann, M., Xu, H., Malaterre, J., Sampurno, S., Huyghe, M., Cheasley, D., Fre, S., Ramsay, R.G., 2014. Tripartite interactions between Wnt signaling, Notch and Myb for stem/progenitor cell functions during intestinal tumorigenesis. Stem Cell Res. doi:10.1016/j.scr.2014.08.002

Gersemann, M., Becker, S., Kübler, I., Koslowski, M., Wang, G., Herrlinger, K.R., Griger, J., Fritz, P., Fellermann, K., Schwab, M., Wehkamp, J., Stange, E.F., 2009. Differences in goblet cell differentiation between Crohn's disease and ulcerative colitis. Differentiation 77, 84–94. doi:10.1016/j.diff.2008.09.008

Grabinger, T., Luks, L., Kostadinova, F., Zimberlin, C., Medema, J.P., Leist, M., Brunner, T., 2014. Ex vivo culture of intestinal crypt organoids as a model system for assessing cell death induction in intestinal epithelial cells and enteropathy. Cell Death Dis. 5, e1228. doi:10.1038/cddis.2014.183

Gregorieff, A., Stange, D.E., Kujala, P., Begthel, H., van den Born, M., Korving, J., Peters, P.J., Clevers, H., 2009. The Ets-Domain Transcription Factor Spdef Promotes Maturation of Goblet and Paneth Cells in the Intestinal Epithelium. Gastroenterology 137. doi:10.1053/j.gastro.2009.06.044

Grimelius, L., 2004. Silver stains demonstrating neuroendocrine cells. Biotech. Histochem. 79, 37–44. doi:10.1080/10520290410001715264

Groschwitz, K.R., Hogan, S.P., 2009. Intestinal barrier function: molecular regulation and disease pathogenesis. J. Allergy Clin. Immunol. 124, 3-20–2. doi:10.1016/j.jaci.2009.05.038

Gross, M., Salame, T.M., Jung, S., 2015. Guardians of the gut - murine intestinal macrophages and dendritic cells. Front. Immunol. doi:10.3389/fimmu.2015.00254

Guan, Y., Watson, A.J.M., Marchiando, A.M., Bradford, E., Shen, L., Turner, J.R., Montrose, M.H., 2011. Redistribution of the tight junction protein ZO-1 during physiological shedding of mouse intestinal epithelial cells. AJP Cell Physiol. 300, C1404-14. doi:10.1152/ajpcell.00270.2010

Günther, C., Martini, E., Wittkopf, N., Amann, K., Weigmann, B., Neumann, H., Waldner, M.J., Hedrick, S.M., Tenzer, S., Neurath, M.F., Becker, C., 2011. Caspase-8 regulates TNF-α-induced epithelial necroptosis and terminal ileitis. Nature 477, 335–339. doi:10.1038/nature10400

Halbleib, J.M., Nelson, W.J., 2006. Cadherins in development: Cell adhesion, sorting, and tissue morphogenesis. Genes Dev. doi:10.1101/gad.1486806

Hall, P. a, Coates, P.J., Ansari, B., Hopwood, D., 1994. Regulation of cell number in the mammalian gastrointestinal tract: the importance of apoptosis. J. Cell Sci. doi:10.1002/path.1711670106

Hanahan, D., Weinberg, R. a, Francisco, S., 2000. The Hallmarks of Cancer. Cell 100, 57–70. doi:10.1016/S0092-8674(00)81683-9

Hartsock, A., Nelson, W.J., 2008. Adherens and tight junctions: Structure, function and connections to the actin cytoskeleton. Biochim. Biophys. Acta - Biomembr. doi:10.1016/j.bbamem.2007.07.012

Hausmann, M., 2010. How Bacteria-Induced Apoptosis of Intestinal Epithelial Cells Contributes to Mucosal Inflammation. Int. J. Inflam. 2010, 1–9. doi:10.4061/2010/574568

Heller, F., Florian, P., Bojarski, C., Richter, J., Christ, M., Hillenbrand, B., Mankertz, J., Gitter, A.H., Bürgel, N., Fromm, M., Zeitz, M., Fuss, I., Strober, W., Schulzke, J.D., 2005. Interleukin-13 is the key effector Th2 cytokine in ulcerative colitis that affects epithelial tight junctions, apoptosis, and cell restitution. Gastroenterology 129, 550–564. doi:10.1016/j.gastro.2005.05.002

Henriksson, J.T., Coursey, T.G., Corry, D.B., De Paiva, C.S., Pflugfelder, S.C., 2015. IL-13 stimulates proliferation and expression of mucin and immunomodulatory genes in cultured conjunctival goblet cells. Investig. Ophthalmol. Vis. Sci. 56, 4186–4197. doi:10.1167/iovs.14-15496

Hermiston, M.L., Gordon, J.I., 1995. Inflammatory bowel disease and adenomas in mice expressing a dominant negative N-cadherin. Science 270, 1203–7. doi:10.1126/science.270.5239.1203

Hermiston, M.L., Wong, M.H., Gordon, J.I., 1996. Forced expression of E-cadherin in the mouse intestinal epithelium slows cell migration and provides evidence for nonautonomous regulation of cell fate in a self-renewing system. Genes Dev. 10, 985–996. doi:10.1101/gad.10.8.985

Ho, K.C., Zhou, Z., She, Y.-M., Chun, A., Cyr, T.D., Yang, X., 2011. Itch E3 ubiquitin ligase regulates large tumor suppressor 1 stability [corrected]. Proc. Natl. Acad. Sci. doi:10.1073/pnas.1101273108

Huang, Y., Chen, Z., 2016. Inflammatory bowel disease related innate immunity and adaptive immunity. Am. J. Transl. Res.

Huh, J.R., Littman, D.R., 2012. Small molecule inhibitors of RORγt: Targeting Th17 cells and other applications. Eur. J. Immunol. doi:10.1002/eji.201242740

Hustad, C.M., Perry, W.L., Siracusa, L.D., Rasberry, C., Cobb, L., Cattanach, B.M., Kovatch, R., Copeland, N.G., Jenkins, N.A., 1995. Molecular genetic characterization of six recessive viable alleles of the mouse agouti locus. Genetics 140, 255–265.

Hustad, C.M., Perry, W.L., Siracusa, L.D., Rasberry, C., Cobb, L., Cattanach, B.M., Kovatch, R., Copeland, N.G., Jenkins, N.A., 1995. Molecular genetic characterization of six recessive viable alleles of the mouse agouti locus. Genetics 140, 255–265.

Izcue, A., Hue, S., Buonocore, S., Arancibia-Cárcamo, C. V., Ahern, P.P., Iwakura, Y., Maloy, K.J., Powrie, F., 2008. Interleukin-23 Restrains Regulatory T Cell Activity to Drive T Cell-Dependent Colitis. Immunity 28, 559–570. doi:10.1016/j.immuni.2008.02.019

Jin, H., Park, Y., Elly, C., Liu, Y.-C., 2013. Itch expression by Treg cells controls Th2 inflammatory responses. J. Clin. Invest. 123, 4923–34. doi:10.1172/JCI69355

Jin, H.S., Park, Y., Elly, C., Liu, Y.C., 2013. Itch expression by Treg cells controls Th2 inflammatory responses. J. Clin. Invest. 123, 4923–4934. doi:10.1172/JCI69355

Johansson, M.E. V., Hansson, G.C., 2016. Immunological aspects of intestinal mucus and mucins. Nat. Rev. Immunol. 16, 639–649. doi:10.1038/nri.2016.88

K.A., M., M., J., S., D., C., S., K.Y., K., 2015. Chronic infection drives hematopoietic stem cell exhaustion through differentiation and a lowered threshold for apoptosis. Blood 126, 2406.

Kathania, M., Khare, P., Zeng, M., Cantarel, B., Zhang, H., Ueno, H., Venuprasad, K., 2016. Itch inhibits IL-17-mediated colon inflammation and tumorigenesis by ROR-γt ubiquitination. Nat. Immunol. 17, 997–1004. doi:10.1038/ni.3488

Korinek, V., Barker, N., Moerer, P., Van Donselaar, E., Huls, G., Peters, P.J., Clevers, H., 1998. Depletion of epithelial stem-cell compartments in the small intestine of mice lacking Tcf-4. Nat Genet 19, 379–383.

Kosiewicz, M.M., Nast, C.C., Krishnan, A., Rivera-Nieves, J., Moskaluk, C.A., Matsumoto, S., Kozaiwa, K., Cominelli, F., 2001. Th1-type responses mediate spontaneous ileitis in a novel murine model of Crohn's disease. J. Clin. Invest. 107, 695–702. doi:10.1172/JCI10956

Kretzschmar, K., Clevers, H., 2016. Organoids: Modeling Development and the Stem Cell Niche in a Dish. Dev. Cell. doi:10.1016/j.devcel.2016.08.014

Kühn, R., Löhler, J., Rennick, D., Rajewsky, K., Müller, W., 1993. Interleukin-10-

deficient mice develop chronic enterocolitis. Cell 75, 263–274. doi:10.1016/0092-8674(93)80068-P

Langlands, A.J., Almet, A.A., Appleton, P.L., Newton, I.P., Osborne, J.M., Näthke, I.S., 2016. Paneth Cell-Rich Regions Separated by a Cluster of Lgr5+ Cells Initiate Crypt Fission in the Intestinal Stem Cell Niche. PLoS Biol. 14. doi:10.1371/journal.pbio.1002491

Langrish, C.L., Chen, Y., Blumenschein, W.M., Mattson, J., Basham, B., Sedgwick, J.D., McClanahan, T., Kastelein, R.A., Cua, D.J., 2005. IL-23 drives a pathogenic T cell population that induces autoimmune inflammation. J. Exp. Med. 201, 233–240. doi:10.1084/jem.20041257

Leaphart, C.L., Cavallo, J., Gribar, S.C., Cetin, S., Li, J., Branca, M.F., Dubowski, T.D., Sodhi, C.P., Hackam, D.J., 2007. A Critical Role for TLR4 in the Pathogenesis of Necrotizing Enterocolitis by Modulating Intestinal Injury and Repair. J. Immunol. 179, 4808–4820. doi:10.4049/jimmunol.179.7.4808

Lee, Y.K., Menezes, J.S., Umesaki, Y., Mazmanian, S.K., 2011. Proinflammatory T-cell responses to gut microbiota promote experimental autoimmune encephalomyelitis. Proc. Natl. Acad. Sci. 108, 4615–4622. doi:10.1073/pnas.1000082107

Leoh, L.S., Daniels-Wells, T.R., Penichet, M.L., 2015. Ige immunotherapy against cancer. Curr. Top. Microbiol. Immunol. 388, 109–149. doi:10.1007/978-3-319-13725-4_6

Li, N., Yousefi, M., Nakauka-Ddamba, A., Jain, R., Tobias, J., Epstein, J.A., Jensen, S.T., Lengner, C.J., 2014. Single-cell analysis of proxy reporter

allele-marked epithelial cells establishes intestinal stem cell hierarchy. Stem Cell Reports 3, 876–891. doi:10.1016/j.stemcr.2014.09.011

Li, W., Bengtson, M.H., Ulbrich, A., Matsuda, A., Reddy, V.A., Orth, A., Chanda, S.K., Batalov, S., Joazeiro, C.A.P., 2008. Genome-wide and functional annotation of human E3 ubiquitin ligases identifies MULAN, a mitochondrial E3 that regulates the organelle's dynamics and signaling. PLoS One 3. doi:10.1371/journal.pone.0001487

Liao, B., Zhong, X., Xu, H., Xiao, F., Fang, Z., Gu, J., Chen, Y., Zhao, Y., Jin, Y., 2013. Itch, an E3 ligase of Oct4, is required for embryonic stem cell self-renewal and pluripotency induction. J. Cell. Physiol. 228, 1443–1451. doi:10.1002/jcp.24297

Liu, Y.C., 2007. The E3 ubiquitin ligase Itch in T cell activation, differentiation, and tolerance. Semin. Immunol. doi:10.1016/j.smim.2007.02.003

Lohr, N.J., Molleston, J.P., Strauss, K.A., Torres-Martinez, W., Sherman, E.A., Squires, R.H., Rider, N.L., Chikwava, K.R., Cummings, O.W., Morton, D.H., Puffenberger, E.G., 2010. Human ITCH E3 Ubiquitin Ligase Deficiency Causes Syndromic Multisystem Autoimmune Disease. Am. J. Hum. Genet. 86, 447–453. doi:10.1016/j.ajhg.2010.01.028

Macpherson, A.J., Harris, N.L., 2004. Opinion: Interactions between commensal intestinal bacteria and the immune system. Nat. Rev. Immunol. 4, 478–485. doi:10.1038/nri1373

Maloy, K.J., Powrie, F., 2011. Intestinal homeostasis and its breakdown in inflammatory bowel disease. Nature 474, 298–306. doi:10.1038/nature10208

Mankertz, J., Schulzke, J.-D., 2007. Altered permeability in inflammatory bowel disease: pathophysiology and clinical implications. Curr. Opin. Gastroenterol. 23, 379–383. doi:10.1097/MOG.0b013e32816aa392

Mantovani, A., Marchesi, F., 2014. IL-10 and macrophages orchestrate gut homeostasis. Immunity. doi:10.1016/j.immuni.2014.04.015

Marchiando, A.M., Graham, W.V., Turner, J.R., 2010. Epithelial Barriers in Homeostasis and Disease. Annu. Rev. Pathol. Mech. Dis. 5, 119–144. doi:10.1146/annurev.pathol.4.110807.092135

Marchiando, A.M., Shen, L., Graham, W.V., Edelblum, K.L., Duckworth, C.A., Guan, Y., Montrose, M.H., Turner, J.R., Watson, A.J.M., 2011. The epithelial barrier is maintained by in vivo tight junction expansion during pathologic intestinal epithelial shedding. Gastroenterology 140, 1208–1218. doi:10.1053/j.gastro.2011.01.004

Marino, A., Menghini, R., Fabrizi, M., Casagrande, V., Mavilio, M., Stoehr, R., Candi, E., Mauriello, A., Moreno-Navarrete, J.M., Gómez-Serrano, M., Peral, B., Melino, G., Lauro, R., Fernandez Real, J.M., Federici, M., 2014. ITCH deficiency protects from diet-induced obesity. Diabetes 63, 550–61. doi:10.2337/db13-0802

Matesic, L.E., Haines, D.C., Copeland, N.G., Jenkins, N.A., 2006. Itch genetically interacts with Notch1 in a mouse autoimmune disease model. Hum. Mol. Genet. 15, 3485–3497. doi:10.1093/hmg/ddl425

McGee, D.W., Vitkus, S.J., 1996. IL-4 enhances IEC-6 intestinal epithelial cell proliferation yet has no effect on IL-6 secretion. Clin. Exp. Immunol. 105,

274–277. doi:10.1046/j.1365-2249.1996.d01-750.x

Merritt, A.J., Potten, C.S., Watson, A.J., Loh, D.Y., Nakayama, K., Nakayama, K., Hickman, J.A., 1995. Differential expression of bcl-2 in intestinal epithelia. Correlation with attenuation of apoptosis in colonic crypts and the incidence of colonic neoplasia. J. Cell Sci. 108 (Pt 6, 2261–71.

Metzger, M.B., Hristova, V.A., Weissman, A.M., 2012. HECT and RING finger families of E3 ubiquitin ligases at a glance. J. Cell Sci. 125, 531–537. doi:10.1242/jcs.091777

Miki, T., Yasuda, S., Kahn, M., 2011. Wnt/β-catenin signaling in embryonic stem cell self-renewal and somatic cell reprogramming. Stem Cell Rev. 7, 836–46. doi:10.1007/s12015-011-9275-1

Moran, G.W., Leslie, F.C., Levison, S.E., McLaughlin, J.T., 2008. Review: Enteroendocrine cells: Neglected players in gastrointestinal disorders? Therap. Adv. Gastroenterol. doi:10.1177/1756283X08093943

Mucida, D., Park, Y., Kim, G., Turovskaya, O., Scott, I., Kronenberg, M., Cheroutre, H., 2007. Reciprocal TH17 and Regulatory T Cell Differentiation Mediated by Retinoic Acid. Science (80-.). 317, 256–260. doi:10.1126/science.1145697

Mukherjee, S., Vaishnava, S., Hooper, L. V., 2008. Multi-layered regulation of intestinal antimicrobial defense. Cell. Mol. Life Sci. doi:10.1007/s00018-008-8182-3

Murray-Zmijewski, F., Lane, D.P., Bourdon, J.-C., 2006. p53/p63/p73 isoforms: an orchestra of isoforms to harmonise cell differentiation and response to

stress. Cell Death Differ. 13, 962–972. doi:10.1038/sj.cdd.4401914

Nalbantoglu, Ilk., Blanc, V., Davidson, N.O., 2016. Characterization of Colorectal Cancer Development in Apc (min/+) Mice. Methods Mol. Biol. 1422, 309–27. doi:10.1007/978-1-4939-3603-8_27

Nenci, A., Becker, C., Wullaert, A., Gareus, R., van Loo, G., Danese, S., Huth, M., Nikolaev, A., Neufert, C., Madison, B., Gumucio, D., Neurath, M.F., Pasparakis, M., 2007. Epithelial NEMO links innate immunity to chronic intestinal inflammation. Nature 446, 557–561. doi:10.1038/nature05698

Noah, T.K., Shroyer, N.F., 2012. Notch in the Intestine: Regulation of Homeostasis and Pathogenesis. Annu. Rev. Physiol. 1–26. doi:10.1146/annurev-physiol-030212-183741

Nunes, T., Bernardazzi, C., De Souza, H.S., 2014. Cell death and inflammatory bowel diseases: Apoptosis, necrosis, and autophagy in the intestinal epithelium. Biomed Res. Int. doi:10.1155/2014/218493

OKUMURA, R., TAKEDA, K., 2016. Maintenance of gut homeostasis by the mucosal immune system. Proc. Japan Acad. Ser. B 92, 423–435. doi:10.2183/pjab.92.423

Omenetti, S., Pizarro, T.T., 2015. The Treg/Th17 axis: A dynamic balance regulated by the gut microbiome. Front. Immunol. doi:10.3389/fimmu.2015.00639

Oniscu, a, Sphyris, N., Morris, R.G., Bader, S., Harrison, D.J., 2004. P73Alpha Is a Candidate Effector in the P53 Independent Apoptosis Pathway of Cisplatin Damaged Primary Murine Colonocytes. J. Clin. Pathol. 57, 492–

498. doi:10.1136/jcp.2003.012559

Paoli, P., Giannoni, E., Chiarugi, P., 2013. Anoikis molecular pathways and its role in cancer progression. Biochim. Biophys. Acta - Mol. Cell Res. 1833, 3481–3498. doi:10.1016/j.bbamcr.2013.06.026

Parker, A., Maclaren, O.J., Fletcher, A.G., Muraro, D., Kreuzaler, P.A., Byrne, H.M., Maini, P.K., Watson, A.J.M., Pin, C., 2017. Cell proliferation within small intestinal crypts is the principal driving force for cell migration on villi. FASEB J. 31, 636–649. doi:10.1096/fj.201601002

Parravicini, V., Field, A.C., Tomlinson, P.D., Basson, M.A., Zamoyska, R., 2008. Itch-/- αβ and γδ T cells independently contribute to autoimmunity in Itchy mice. Blood 111, 4273–4282. doi:10.1182/blood-2007-10-115667

Pastorelli, L., De Salvo, C., Mercado, J., Vecchi, M., Pizarro, T., 2013. Central Role of the Gut Epithelial Barrier in the Pathogenesis of Chronic Intestinal Inflammation: Lessons Learned from Animal Models and Human Genetics . Front. Immunol. .

Peglion, F., Llense, F., Etienne-Manneville, S., 2014. Adherens junction treadmilling during collective migration. Nat. Cell Biol. 16, 639–51. doi:10.1038/ncb2985

Pelaseyed, T., Bergstr??m, J.H., Gustafsson, J.K., Ermund, A., Birchenough, G.M.H., Sch??tte, A., van der Post, S., Svensson, F., Rodr??guez-Pi??eiro, A.M., Nystr??m, E.E.L., Wising, C., Johansson, M.E. V, Hansson, G.C., 2014. The mucus and mucins of the goblet cells and enterocytes provide the first defense line of the gastrointestinal tract and interact with the immune

system. Immunol. Rev. doi:10.1111/imr.12182

Pellegrinet, L., Rodilla, V., Liu, Z., Chen, S., Koch, U., Espinosa, L., Kaestner, K.H., Kopan, R., Lewis, J., Radtke, F., 2011. Dll1- and Dll4-mediated notch signaling are required for homeostasis of intestinal stem cells. Gastroenterology 140, 1230–1240. doi:10.1053/j.gastro.2011.01.005

Perez, J.M., Chirieleison, S.M., Abbott, D.W., 2015. An IκB Kinase-Regulated Feedforward Circuit Prolongs Inflammation. Cell Rep. 12, 537–544. doi:10.1016/j.celrep.2015.06.050

Perry, W.L., Hustad, C.M., Swing, D.A., O'Sullivan, T.N., Jenkins, N.A., Copeland, N.G., 1998. The itchy locus encodes a novel ubiquitin protein ligase that is disrupted in a18H mice. Nat. Genet. 18, 143–146.

Perry, W.L., Hustad, C.M., Swing, D.A., O'Sullivan, T.N., Jenkins, N.A., Copeland, N.G., 1998. The itchy locus encodes a novel ubiquitin protein ligase that is disrupted in a 18H mice. Nat. Genet. 18, 143–146. doi:10.1038/ng0298-143

Peterson, L.W., Artis, D., 2014. Intestinal epithelial cells: regulators of barrier function and immune homeostasis. Nat. Rev. Immunol. 14, 141–153. doi:10.1038/nri3608

Pin, C., Parker, A., Gunning, A.P., Ohta, Y., Johnson, I.T., Carding, S.R., Sato, T., 2015. An individual based computational model of intestinal crypt fission and its application to predicting unrestrictive growth of the intestinal epithelium. Integr. Biol. 7, 213–228. doi:10.1039/C4IB00236A

Popovic, D., Vucic, D., Dikic, I., 2014. Ubiquitination in disease pathogenesis and

treatment. Nat. Med. 20, 1242–1253. doi:10.1038/nm.3739

Potten, C.S., 1998. Stem cells in gastrointestinal epithelium: numbers, characteristics and death. Philos. Trans. R. Soc. Lond. B. Biol. Sci. 353, 821–830. doi:10.1098/rstb.1998.0246

Potten, C.S., 1990. A comprehensive study of the radiobiological response of the murine (BDF1) small intestine. Int. J. Radiat. Biol. doi:10.1080/09553009014552281

POTTEN, C.S., 1977. Extreme sensitivity of some intestinal crypt cells to X and γ irradiation. Nature 269, 518–521. doi:10.1038/269518a0

Potten, C.S., Booth, C., Pritchard, D.M., 1997. The intestinal epithelial stem cell: the mucosal governor. Int. J. Exp. Pathol. 78, 219–43. doi:10.1046/j.1365-2613.1997.280362.x

Powell, D.W., Pinchuk, I. V, Saada, J.I., Chen, X., Mifflin, R.C., 2011. Mesenchymal cells of the intestinal lamina propria. Annu. Rev. Physiol. 73, 213–37. doi:10.1146/annurev.physiol.70.113006.100646

Powrie, F., Leach, M.W., Mauze, S., Caddle, L.B., Coffman, R.L., 1993. Phenotypically distinct subsets of CD4+ T cells induce or protect from chronic intestinal inflammation in C. B-17 scid mice. Int. Immunol. 5, 1461–1471. doi:10.1093/intimm/5.11.1461

Ramon, H.E., Riling, C.R., Bradfield, J., Yang, B., Hakonarson, H., Oliver, P.M., 2011. The ubiquitin ligase adaptor Ndfip1 regulates T cell-mediated gastrointestinal inflammation and inflammatory bowel disease susceptibility. Mucosal Immunol. 4, 314–324. doi:10.1038/mi.2010.69

Rathinam, C., Matesic, L.E., Flavell, R.A., 2011. The E3 ligase Itch is a negative regulator of the homeostasis and function of hematopoietic stem cells. Nat. Immunol. 12, 399–407. doi:10.1038/ni.2021

Renehan, A.G., Bach, S.P., Potten, C.S., 2001. The relevance of apoptosis for cellular homeostasis and tumorigenesis in the intestine. Can. J. Gastroenterol.

Rescigno, M., 2011. The intestinal epithelial barrier in the control of homeostasis and immunity. Trends Immunol. doi:10.1016/j.it.2011.04.003

Roda, G., Jharap, B., Neeraj, N., Colombel, J.-F., 2016. Loss of Response to Anti-TNFs: Definition, Epidemiology, and Management. Clin. Transl. Gastroenterol. 7, e135. doi:10.1038/ctg.2015.63

Roda, G., Sartini, A., Zambon, E., Calafiore, A., Marocchi, M., Caponi, A., Belluzzi, A., Roda, E., 2010. Intestinal epithelial cells in inflammatory bowel diseases. World J. Gastroenterol. 16, 4264–4271. doi:10.3748/wjg.v16.i34.4264

Rossi, M., Aqeilan, R.I., Neale, M., Candi, E., Salomoni, P., Knight, R. a, Croce, C.M., Melino, G., 2006. The E3 ubiquitin ligase Itch controls the protein stability of p63. Proc. Natl. Acad. Sci. U. S. A. 103, 12753–12758. doi:10.1073/pnas.0603449103

Rossi, M., De Laurenzi, V., Munarriz, E., Green, D.R., Liu, Y.-C., Vousden, K.H., Cesareni, G., Melino, G., 2005. The ubiquitin–protein ligase Itch regulates p73 stability. EMBO J. 24, 836–848. doi:10.1038/sj.emboj.7600444

Rotin, D., Kumar, S., 2009. Physiological functions of the HECT family of

ubiquitin ligases. Nat. Rev. Mol. Cell Biol. 10, 398–409. doi:10.1038/nrm2690

Sabates-Bellver, J., Van der Flier, L.G., de Palo, M., Cattaneo, E., Maake, C., Rehrauer, H., Laczko, E., Kurowski, M. a, Bujnicki, J.M., Menigatti, M., Luz, J., Ranalli, T. V, Gomes, V., Pastorelli, A., Faggiani, R., Anti, M., Jiricny, J., Clevers, H., Marra, G., 2007. Transcriptome profile of human colorectal adenomas. Mol. Cancer Res. 5, 1263–1275. doi:10.1158/1541-7786.MCR-07-0267

Sandler, N.G., Koh, C., Roque, A., Eccleston, J.L., Siegel, R.B., Demino, M., Kleiner, D.E., Deeks, S.G., Liang, T.J., Heller, T., Douek, D.C., 2011. Host response to translocated microbial products predicts outcomes of patients with HBV or HCV infection. Gastroenterology 141. doi:10.1053/j.gastro.2011.06.063

Sangiorgi, E., Capecchi, M.R., 2008. Bmi1 is expressed in vivo in intestinal stem cells. Nat. Genet. 40, 915–920.

Sansom, O.J., Mansergh, F.C., Evans, M.J., Wilkins, J.A., Clarke, A.R., 2007. Deficiency of SPARC suppresses intestinal tumorigenesis in APCMin/+ mice. Gut 56, 1410–4. doi:10.1136/gut.2006.116921

Sato, T., Clevers, H., 2013. Growing Self-Organizing Mini-Guts from a Single Intestinal Stem Cell: Mechanism and Applications. Science (80-.). doi:10.1126/science.1234852

Sato, T., Clevers, H., 2013. Growing Self-Organizing Mini-Guts. Science (80-.). 340, 1190–1195. doi:10.1126/science.1234852

Sato, T., van Es, J.H., Snippert, H.J., Stange, D.E., Vries, R.G., van den Born, M., Barker, N., Shroyer, N.F., van de Wetering, M., Clevers, H., 2011. Paneth cells constitute the niche for Lgr5 stem cells in intestinal crypts. Nature 469, 415–418. doi:10.1038/nature09637

Sato, T., Vries, R.G., Snippert, H.J., van de Wetering, M., Barker, N., Stange, D.E., van Es, J.H., Abo, A., Kujala, P., Peters, P.J., Clevers, H., 2009. Single Lgr5 stem cells build crypt–villus structures in vitro without a mesenchymal niche. Nature 459, 262–265. doi:10.1038/nature07935

Schenk, M., Mueller, C., 2008. The mucosal immune system at the gastrointestinal barrier. Best Pract. Res. Clin. Gastroenterol. 22, 391–409. doi:10.1016/j.bpg.2007.11.002

Schneider, M.R., Dahlhoff, M., Horst, D., Hirschi, B., Trülzsch, K., Müller-Höcker, J., Vogelmann, R., Allgäuer, M., Gerhard, M., Steininger, S., Wolf, E., Kolligs, F.T., 2010. A key role for E-cadherin in intestinal homeostasis and paneth cell maturation. PLoS One 5. doi:10.1371/journal.pone.0014325

Scoville, D.H., Sato, T., He, X.C., Li, L., 2008. Current View: Intestinal Stem Cells and Signaling. Gastroenterology 134, 849–864. doi:10.1053/j.gastro.2008.01.079

Shembade, N., Harhaj, N.S., Parvatiyar, K., Copeland, N.G., Jenkins, N.A., Matesic, L.E., Harhaj, E.W., 2008. The E3 ligase Itch negatively regulates inflammatory signaling pathways by controlling the function of the ubiquitin-editing enzyme A20. Nat. Immunol. 9, 254–262. doi:10.1038/ni1563

Sheridan, B.S., Romagnoli, P.A., Pham, Q.M., Fu, H.H., Alonzo, F., Schubert,

W.D., Freitag, N.E., Lefrançois, L., 2013. γδ T Cells Exhibit Multifunctional and Protective Memory in Intestinal Tissues. Immunity 39, 184–195. doi:10.1016/j.immuni.2013.06.015

Shroyer, N.F., Wallis, D., Venken, K.J.T., Bellen, H.J., Zoghbi, H.Y., 2005. Gfi1 functions downstream of Math1 to control intestinal secretory cell subtype allocation and differentiation. Genes Dev 19, 2412–2417.

Ślebioda, T.J., Kmieć, Z., 2014. Tumour necrosis factor superfamily members in the pathogenesis of inflammatory bowel disease. Mediators Inflamm. doi:10.1155/2014/325129

Smalley-Freed, W.G., Efimov, A., Burnett, P.E., Short, S.P., Davis, M.A., Gumucio, D.L., Washington, M.K., Coffey, R.J., Reynolds, A.B., 2010. p120-catenin is essential for maintenance of barrier function and intestinal homeostasis in mice. J. Clin. Invest. 120, 1824–1835. doi:10.1172/JCI41414

Smythies, L.E., Sellers, M., Clements, R.H., Mosteller-Barnum, M., Meng, G., Benjamin, W.H., Orenstein, J.M., Smith, P.D., 2005. Human intestinal macrophages display profound inflammatory anergy despite avid phagocytic and bacteriocidal activity. J. Clin. Invest. 115, 66–75. doi:10.1172/JCI200519229

Steele, S.P., Melchor, S.J., Petri, W.A., 2016. Tuft Cells: New Players in Colitis. Trends Mol. Med. doi:10.1016/j.molmed.2016.09.005

Stockwin, L.H., McGonagle, D., Martin, I.G., Blair, G.E., 2000. Dendritic cells: immunological sentinels with a central role in health and disease. Immunol. Cell Biol. 78, 91–102. doi:10.1046/j.1440-1711.2000.00888.x

Strikoudis, A., Guillamot, M., Aifantis, I., 2014. Regulation of stem cell function by protein ubiquitylation. EMBO Rep. doi:10.1002/embr.201338373

Sun, C.-M., Hall, J.A., Blank, R.B., Bouladoux, N., Oukka, M., Mora, J.R., Belkaid, Y., 2007. Small intestine lamina propria dendritic cells promote de novo generation of Foxp3 T reg cells via retinoic acid. J. Exp. Med. 204, 1775–1785. doi:10.1084/jem.20070602

Symons, A., Budelsky, A.L., Towne, J.E., 2012. Are Th17 cells in the gut pathogenic or protective? Mucosal Immunol. 5, 4–6. doi:10.1038/mi.2011.51

Tan, D.W.M., Barker, N., 2014. Intestinal Stem Cells and Their Defining Niche. Curr. Top. Dev. Biol. 107, 77–107. doi:10.1016/B978-0-12-416022-4.00003-2

Tao, M., Scacheri, P.C., Marinis, J.M., Harhaj, E.W., Matesic, L.E., Abbott, D.W., 2009. ITCH K63-Ubiquitinates the NOD2 Binding Protein, RIP2, to Influence Inflammatory Signaling Pathways. Curr. Biol. 19, 1255–1263. doi:10.1016/j.cub.2009.06.038

Tao, M.F., Scacheri, P.C., Marinis, J.M., Harhaj, E.W., Matesic, L.E., Abbott, D.W., 2009. ITCH K63-Ubiquitinates the NOD2 Binding Protein, RIP2, to Influence Inflammatory Signaling Pathways. Curr. Biol. 19, 1255–1263. doi:10.1016/j.cub.2009.06.038

Tetteh, P.W., Farin, H.F., Clevers, H., 2015. Plasticity within stem cell hierarchies in mammalian epithelia. Trends Cell Biol. doi:10.1016/j.tcb.2014.09.003

Theivanthiran, B., Kathania, M., Zeng, M., Anguiano, E., Basrur, V., Vandergriff, T., Pascual, V., Wei, W., Massoumi, R., Venuprasad, K., 2015. The E3

ubiquitin ligase Itch inhibits p38 a signaling and skin inflammation through the ubiquitylation of Tab1. Sci. Signal. 8, 1–14. doi:10.1126/scisignal.2005903

Tian, H., Biehs, B., Warming, S., Leong, K.G., Rangell, L., Klein, O.D., De Sauvage, F.J., 2011. A reserve stem cell population in small intestine renders Lgr5-positive cells dispensable. Nature 478, 1–6. doi:10.1038/nature10408

Traweger, A., Fang, D., Liu, Y.C., Stelzhammer, W., Krizbai, I.A., Fresser, F., Bauer, H.C., Bauer, H., 2002. The tight junction-specific protein occludin is a functional target of the E3 ubiquitin-protein ligase itch. J. Biol. Chem. 277, 10201–10208. doi:10.1074/jbc.M111384200

Tsui, Y.-M., Sze, K.M.-F., Tung, E.K.-K., Ho, D.W.-H., Lee, T.K.-W., Ng, I.O.-L., 2017. Dishevelled-3 phosphorylation is governed by HIPK2/PP1Cα/ITCH axis and the non-phosphorylated form promotes cancer stemness via LGR5 in hepatocellular carcinoma. Oncotarget 8, 39430–39442. doi:10.18632/oncotarget.17049

Tucker, J.M., Davis, C., Kitchens, M.E., Bunni, M.A., Priest, D.G., Spencer, H.T., Berger, F.G., 2002. Response to 5-fluorouracil chemotherapy is modified by dietary folic acid deficiency in ApcMin/+ mice. Cancer Lett. 187, 153–162. doi:10.1016/S0304-3835(02)00402-0

Tucker, J.M., Murphy, J.T., Kisiel, N., Diegelman, P., Barbour, K.W., Davis, C., Medda, M., Alhonen, L., Jänne, J., Kramer, D.L., Porter, C.W., Berger, F.G., 2005. Potent modulation of intestinal tumorigenesis in Apcmin/+ mice by the

polyamine catabolic enzyme spermidine/spermine N1- acetyltransferase. Cancer Res. 65, 5390–5398. doi:10.1158/0008-5472.CAN-05-0229

Turner, J.R., 2009. Intestinal mucosal barrier function in health and disease. Nat. Rev. Immunol. 9, 799–809. doi:10.1038/nri2653

Uhlen, M., 2005. A Human Protein Atlas for Normal and Cancer Tissues Based on Antibody Proteomics. Mol. Cell. Proteomics 4, 1920–1932. doi:10.1074/mcp.M500279-MCP200

Ulluwishewa, D., Anderson, R.C., McNabb, W.C., Moughan, P.J., Wells, J.M., Roy, N.C., 2011. Regulation of tight junction permeability by intestinal bacteria and dietary components. J. Nutr. 141, 769–776. doi:10.3945/jn.110.135657

Vaishnava, S., Behrendt, C.L., Ismail, A.S., Eckmann, L., Hooper, L. V., 2008. Paneth cells directly sense gut commensals and maintain homeostasis at the intestinal host-microbial interface. Proc. Natl. Acad. Sci. 105, 20858–20863. doi:10.1073/pnas.0808723105

van der Flier, L.G., Clevers, H., 2009. Stem Cells, Self-Renewal, and Differentiation in the Intestinal Epithelium. Annu. Rev. Physiol. 71, 241–260. doi:10.1146/annurev.physiol.010908.163145

Van Der Gracht, E., Zahner, S., Kronenberg, M., 2016. When Insult Is Added to Injury: Cross Talk between ILCs and Intestinal Epithelium in IBD. Mediators Inflamm. doi:10.1155/2016/9765238

Van Es, J.H., Clevers, H., 2014. Paneth cells. Curr. Biol. doi:10.1016/j.cub.2014.04.049

van Es, J.H., Sato, T., van de Wetering, M., Lyubimova, A., Yee Nee, A.N., Gregorieff, A., Sasaki, N., Zeinstra, L., van den Born, M., Korving, J., Martens, A.C.M., Barker, N., van Oudenaarden, A., Clevers, H., 2012. Dll1+ secretory progenitor cells revert to stem cells upon crypt damage. Nat. Cell Biol. 14, 1099–1104. doi:10.1038/ncb2581

van Wijk, F., Cheroutre, H., 2010. Mucosal T cells in gut homeostasis and inflammation. Expert Rev. Clin. Immunol. 6, 559–566. doi:10.1586/eci.10.34

VanDussen, K.L., Carulli, A.J., Keeley, T.M., Patel, S.R., Puthoff, B.J., Magness, S.T., Tran, I.T., Maillard, I., Siebel, C., Kolterud, A., Grosse, A.S., Gumucio, D.L., Ernst, S.A., Tsai, Y.-H., Dempsey, P.J., Samuelson, L.C., 2012. Notch signaling modulates proliferation and differentiation of intestinal crypt base columnar stem cells. Development 139, 488–497. doi:10.1242/dev.070763

Vijayakumar, S., Liu, G., Wen, H., Abu, Y., Chong, R., 2017. Extracellular LDLR repeats modulate Wnt signaling activity by promoting LRP6 receptor endocytosis mediated by the Itch E3 ubiquitin ligase 8.

Vilgelm, A., El-Rifai, W., Zaika, A., 2008. Therapeutic prospects for p73 and p63: Rising from the shadow of p53. Drug Resist. Updat. 11, 152–163. doi:10.1016/j.drup.2008.08.001

Vindigni, S.M., Zisman, T.L., Suskind, D.L., Damman, C.J., 2016. The intestinal microbiome, barrier function, and immune system in inflammatory bowel disease: a tripartite pathophysiological circuit with implications for new therapeutic directions. Therap. Adv. Gastroenterol. 9, 606–625. doi:10.1177/1756283X16644242

Visvader, J.E., Clevers, H., 2016. Tissue-specific designs of stem cell hierarchies. Nat Cell Biol 18, 349–355. doi:10.1038/ncb3332

Vlantis, K., Wullaert, A., Sasaki, Y., Schmidt-Supprian, M., Rajewsky, K., Roskams, T., Pasparakis, M., 2011. Constitutive IKK2 activation in intestinal epithelial cells induces intestinal tumors in mice. J. Clin. Invest. 121, 2781–2793. doi:10.1172/JCI45349

Vooijs, M., Liu, Z., Kopan, R., 2011. Notch: Architect, landscaper, and guardian of the intestine. Gastroenterology 141, 448–459. doi:10.1053/j.gastro.2011.06.003

Watson, A.J., Hughes, K.R., 2012. TNF-alpha-induced intestinal epithelial cell shedding: implications for intestinal barrier function. Ann N Y Acad Sci 1258, 1–8. doi:10.1111/j.1749-6632.2012.06523.x

Wehkamp, J., Koslowski, M., Wang, G., Stange, E.F., 2008. Barrier dysfunction due to distinct defensin deficiencies in small intestinal and colonic Crohn's disease. Mucosal Immunol. 1, S67–S74. doi:10.1038/mi.2008.48

Wei, W., Li, M., Wang, J., Nie, F., Li, L., 2012. The E3 Ubiquitin Ligase ITCH Negatively Regulates Canonical Wnt Signaling by Targeting Dishevelled Protein. Mol. Cell. Biol. 32, 3903–3912. doi:10.1128/MCB.00251-12

Welz, P.-S., Wullaert, A., Vlantis, K., Kondylis, V., Fernández-Majada, V., Ermolaeva, M., Kirsch, P., Sterner-Kock, A., van Loo, G., Pasparakis, M., 2011. FADD prevents RIP3-mediated epithelial cell necrosis and chronic intestinal inflammation. Nature 477, 330–334. doi:10.1038/nature10273

Wen, L., Ley, R.E., Volchkov, P.Y., Stranges, P.B., Avanesyan, L., Stonebraker,

A.C., Hu, C., Wong, F.S., Szot, G.L., Bluestone, J.A., Gordon, J.I., Chervonsky, A. V., 2008. Innate immunity and intestinal microbiota in the development of Type 1 diabetes. Nature 455, 1109–1113. doi:10.1038/nature07336

Wenzel, U.A., Magnusson, M.K., Rydström, A., Jonstrand, C., Hengst, J., Johansson, M.E. V, Velcich, A., Öhman, L., Strid, H., Sjövall, H., Hansson, G.C., Wick, M.J., 2014. Spontaneous colitis in Muc2-deficient mice reflects clinical and cellular features of active ulcerative colitis. PLoS One 9. doi:10.1371/journal.pone.0100217

Williams, J.M., Duckworth, C.A., Burkitt, M.D., Watson, A.J.M., Campbell, B.J., Pritchard, D.M., 2015. Epithelial Cell Shedding and Barrier Function. Vet. Pathol. 52, 445–455. doi:10.1177/0300985814559404

Williams, J.M., Duckworth, C.A., Burkitt, M.D., Watson, A.J.M., Campbell, B.J., Pritchard, D.M., 2015. Epithelial cell shedding and barrier function: a matter of life and death at the small intestinal villus tip. Vet. Pathol. 52, 445–55. doi:10.1177/0300985814559404

Wong, M.H., Hermiston, M.L., Syder, A.J., Gordon, J.I., 1996. Forced expression of the tumor suppressor adenomatosis polyposis coli protein induces disordered cell migration in the intestinal epithelium. Proc. Natl. Acad. Sci. 93, 9588–9593. doi:10.1073/pnas.93.18.9588

Wu, H.J., Ivanov, I.I., Darce, J., Hattori, K., Shima, T., Umesaki, Y., Littman, D.R., Benoist, C., Mathis, D., 2010. Gut-residing segmented filamentous bacteria drive autoimmune arthritis via T helper 17 cells. Immunity 32, 815–

827. doi:10.1016/j.immuni.2010.06.001

Wullaert, A., Bonnet, M.C., Pasparakis, M., 2011. NFκB in the regulation of epithelial homeostasis and inflammation. Cell Res. 21, 146–158. doi:10.1038/cr.2010.175

Yousefi, M., Li, L., Lengner, C.J., 2017. Hierarchy and Plasticity in the Intestinal Stem Cell Compartment. Trends Cell Biol. doi:10.1016/j.tcb.2017.06.006

Yu, H., Yuan, Y., Shen, H., Cheng, T., 2006. Hematopoietic stem cell exhaustion impacted by p18INK4C and p21Cip1/Waf1 in opposite manners. Blood 107, 1200–1206. doi:10.1182/blood-2005-02-0685

Zaika, a I., El-Rifai, W., 2006. The role of p53 protein family in gastrointestinal malignancies. Cell Death Differ. 13, 935–940. doi:10.1038/sj.cdd.4401897

Zhang, P., Wang, C., Gao, K., Wang, D., Mao, J., An, J., Xu, C., Wu, D., Yu, H., Liu, J.O., Yu, L., 2010. The ubiquitin ligase itch regulates apoptosis by targeting thioredoxin-interacting protein for ubiquitin-dependent degradation. J. Biol. Chem. 285, 8869–8879. doi:10.1074/jbc.M109.063321

Zihni, C., Mills, C., Matter, K., Balda, M.S., 2016. Tight junctions: from simple barriers to multifunctional molecular gates. Nat. Rev. Mol. Cell Biol. 17, 564–580. doi:10.1038/nrm.2016.80